

The Chemical Evolution of the Draco Dwarf Spheroidal Galaxy¹

Judith G. Cohen² and Wenjin Huang³

ABSTRACT

We present an abundance analysis based on high resolution spectra of 8 stars selected to span the full range in metallicity in the Draco dwarf spheroidal galaxy. We find $[\text{Fe}/\text{H}]$ for the sample stars ranges from -1.5 to -3.0 dex. Combining our sample with previously published work for a total of 14 luminous Draco giants, we show that the abundance ratios $[\text{Na}/\text{Fe}]$, $[\text{Mg}/\text{Fe}]$ and $[\text{Si}/\text{Fe}]$ for the Draco giants overlap those of Galactic halo giants at the lowest $[\text{Fe}/\text{H}]$ probed, but are significantly lower for the higher Fe-metallicity Draco stars. For the explosive α -elements Ca and Ti, the abundance ratios for Draco giants with $[\text{Fe}/\text{H}] > -2.4$ dex are approximately constant and slightly sub-solar, well below values characteristic of Galactic halo stars. The s -process contribution to the production of heavy elements begins at significantly lower Fe-metallicity than in the Galactic halo.

Using a toy model we compare the behavior of the abundance ratios within the sample of Draco giants with those from the literature of Galactic globular clusters, and the Carina and Sgr dSph galaxies. The differences appear to be related to the timescale for buildup of the heavy elements, with Draco having the slowest rate.

We note the presence of a Draco giant with $[\text{Fe}/\text{H}] < -3.0$ dex in our sample, and reaffirm that the inner Galactic halo could have been formed by early accretion of Galactic satellite galaxies and dissolution of young globular clusters, while the outer halo could have formed from those satellite galaxies accreted later.

Subject headings: galaxies: individual (Draco), galaxies: abundances, galaxies: dwarf

1. Introduction

The Draco dwarf spheroidal (dSph) galaxy is a nearby satellite of the Milky Way. It was extensively studied by Baade & Swope (1961), who constructed a CMD and searched for variable stars. HST imaging by Grillmair et al (1998) suggested that the bulk of the stars are old,

¹Based on observations obtained at the W.M. Keck Observatory, which is operated jointly by the California Institute of Technology, the University of California and the National Aeronautics and Space Administration

²Palomar Observatory, Mail Stop 105-24, California Institute of Technology, Pasadena, California 91125 (jlc@astro.caltech.edu)

³Palomar Observatory, current address: University of Washington, Astronomy, Box 351580, Seattle, Washington, 98195 (hwenjin@astro.washington.edu)

with a luminosity function similar to that of old, metal-poor Galactic globular clusters. Although Hernandez, Gilmore & Valls-Gabaud (2000) find a median age for Draco stars of 7 Gyr from HST archival images, the recent HST study by Orban et al (2006), which provides coarse age distributions for Draco and several other Galactic satellites, yields a somewhat older mean age for this stellar population. There is no evidence for multiple main sequences nor any sign of ongoing star formation. A very low upper limit for neutral hydrogen gas in Draco was established by Young (1999).

Many radial velocity surveys of large samples of stars have been carried out to confirm membership and measure the stellar velocity dispersion as a function of radius in Draco as well as in the other Milky Way satellites; Armandroff, Olszewski & Pryor (1995) is an early example of such for Draco, while Walker et al (2008) highlights the very large v_r datasets that can be assembled today. The observed σ_v in Draco is unexpectedly high, given the low luminosity of the system, and remains flat to large radii, which according to Munoz et al (2005) (see also the references therein) requires the presence of large amounts of dark matter. These studies generally ignore the issue of potential ongoing tidal disruption affecting the internal kinematics of the Milky Way satellite, which does not appear to be a concern in the case of Draco (Segall *et al.* 2007).

There is great current interest in the detailed properties of satellites of the Galaxy in light of our greatly improved hierarchical cold dark matter cosmological models, which gave rise to the the missing satellite problem (Klypin et al 1999). This is only enhanced by the discovery that the dSph galaxies appear to be dark matter dominated systems, unlike globular clusters of similar total stellar mass. With the advent of efficient high dispersion spectrographs, large area CCD detectors, and 10-m class telescopes, studying stars in at least the nearer Galactic satellites at high spectral dispersion has become feasible.

Early moderate resolution spectroscopic studies of Draco by Zinn (1978) and by Lehnert et al (1992) established the presence of an abundance spread of ~ 1 dex within Draco. In this paper we present detailed abundance analyses of a sample of 8 luminous Draco stars near the RGB tip, which more than doubles the sample of Draco stars from the earlier work of Shetrone, Bolte & Stetson (1998) and of Shetrone, Côté & Sargent (2001). Our goal is understanding the chemical evolution of Draco, and how this and other dSph galaxies may be related to the population of Galactic halo field stars and to Galactic globular clusters. The sample is presented in §2 where the procedure for determining their stellar parameters is described. The next section describes the observations, while §4 gives the details of the abundance analysis. We compare our results to those for Galactic halo field stars in §5 and introduce our toy model for abundance ratios in §6. A comparison with the predictions of nucleosynthesis is given in §6.2 and with chemical evolution models in §7. This is followed by a discussion of role the dSph satellite galaxies might have played the formation of the Galactic halo in §8. After a brief summary we discuss in an appendix the Fe-metallicity calibration for the infrared Ca triplet, and compare our derived metallicities for Draco giants with those inferred from CaT measurements and from Stromgren photometry.

2. Stellar Sample and Stellar Parameters

Our sample in the Draco dSph galaxy contains 8 stars; details are given in Table 1. It was selected from Table 2.9 of Winnick (2003) to include stars which are known radial velocity members of this satellite to the Galaxy at or near the RGB tip spanning the full range in color and in metallicity and not previously observed at high spectral resolution. Winnick measured the infrared Ca triplet in moderate resolution spectra of Draco stars obtained using the multi-fiber Hydra spectrograph at the WIYN telescope. Her sample was chosen from the photometric survey of Piatek *et al.* (2001) and previous radial velocity surveys (see, e.g. Armandroff, Olszewski & Pryor 1995). Only confirmed radial velocity members are listed in her table; carbon stars known to be members of Draco were excluded. She developed her own calibration of the relationship between Ca triplet indices and Fe or Ca metallicity based on data for Galactic globular clusters. Details of the calibration and related issues are discussed in the appendix.

We adopt the procedures described in Cohen *et al.* (2002) and used in all subsequent work by the first author published to date to determine the stellar parameters for our sample of luminous Draco giants. Our T_{eff} determinations are based on the broad band colors $V - J$ and $V - K$. The optical photometry (we use V only, the $V - I$ color supports the deduced T_{eff} in most cases, but is not used) is from the SDSS (York *et al.* 2000) using the transformation equations of Smith *et al.* (2002). The IR photometry is taken from 2MASS (Skrutskie *et al.* 1997; Cutri *et al.* 2003), and is transformed from the 2MASS system to the Johnson-Bessell system using the results of Carpenter (2001). The galactic extinction is from the map of Schlegel, Finkbeiner & Davis (1998); $E(B - V)$ does not exceed 0.03 mag for any star in the Draco sample.

We derive surface gravities by combining these T_{eff} with an appropriate theoretical isochrone from the grid of Yi *et al.* (2002) assuming a fixed age of 12 Gyr. We use the $[Fe/H]$ values of Winnick (2003) from the infrared Ca triplet as an initial guess. We iterate as necessary given the metallicity we derive here through analysis of our high resolution spectra.

We calculate the dereddened M_V for each sample star (ignoring the thickness of Draco itself along the line of sight), adopting 76 kpc as its distance based on the RR Lyrae study in this dSph by Bonanos *et al.* (2004). We use the M_V , which are independent of the adopted stellar parameters, to check for overall consistency with the adopted isochrones. We find the position along the RGB in the adopted isochrone appropriate for the initial estimate of metallicity for each star that has that M_V and compare the corresponding T_{eff} with our adopted value inferred from the photometry for each star. The two independently determined values of T_{eff} are reasonably consistent given the uncertainty in our adopted T_{eff} of 100 K. Achieving this agreement is made easier since the slope of the upper RGB in the CMD is quite steep; we find for $\Delta T_{eff} = 100$ K that $\Delta M_V \sim 0.45$ mag and $\Delta \log(g) \sim 0.25$ dex from the adopted isochrones.

The resulting stellar parameters, which have been derived with no reference to the spectra themselves, are given in the second and third columns of Table 2, as are their heliocentric radial velocities. The random uncertainties in the adopted T_{eff} from photometric errors are 100 K. This

ignores systematic errors which may be present. The adopted uncertainties in $\log(g)$ based on the evolutionary tracks of Yi *et al.* (2002) for stars on the upper RGB are 0.25 dex.

Fig. 1 shows our sample of 8 luminous giants in Draco in a plot of $g' - i'$ versus g' corrected for interstellar reddening; the previously studied sample of 6 giants from Shetrone, Bolte & Stetson (1998) and by Shetrone, Côté & Sargent (2001) is shown as well. Members of Draco from the list of Winnick (2003), which excludes the known carbon stars, were cross indexed with the CFHT Megacam photometry of Segall *et al.* (2007)¹ and are also displayed. The positional tolerance was 1.0 arcsec; a few spurious identifications may have occurred. Superposed in this figure are isochrones from the Dartmouth Stellar Evolution Database (Dotter *et al.* 2008) for $[\text{Fe}/\text{H}] -2.5$ dex with $[\alpha/\text{Fe}] = +0.2$ dex (solid lines) and for $[\text{Fe}/\text{H}] -1.5$ dex with $[\alpha/\text{Fe}]$ Solar (dashed lines) for ages 9 and 12.5 Gyr.

Our HIRES sample of luminous Draco giants was selected to span the full range in metallicity as inferred from the Ca triplet indices (Winnick 2003). Fig. 1 shows it does cover the full range in $g' - i'$ color of the upper RGB of Draco members. The luminosity of the brightest Draco giants is in good agreement with that predicted from the isochrones for the RGB tip as a function of metallicity in the g', i' colors. The deduced ages will be described later in §7.1.

3. Observations

The Draco stars in our sample were observed with HIRES (Vogt *et al.* 1994) at the Keck I telescope during two runs, in June 2005 and in Sep. 2006. Sky conditions during the 2006 run were better than in the 2005 run; one star from the earlier run was re-observed at that time. Total exposure times were two hours per star, broken up into 1800 or 2400 sec segments to expedite removal of cosmic rays. The instrument configuration yielded complete spectral coverage in a single exposure from 3810 to 6700 Å, and extends to 8350 Å with small gaps between orders. The slit width was 1.1 arcsec, which corresponds to a spectral resolution of 35,000 for all exposures. The signal-to-noise ratio per spectral resolution element ranges from 40 to 85 (with 5 of the sample stars having at least 65) in the continuum in the central order of the spectrum (at ~ 6050 Å), depending on the brightness of the star and the sky conditions during the exposure, most importantly on the seeing. The SNR at the bluest end of these spectra is poor, only 30 to 40 per spectral resolution element. This SNR calculation utilizes only Poisson statistics, ignoring issues of cosmic ray removal, night sky subtraction, flattening, etc. The observations were carried out with the slit length aligned to the parallactic angle.

¹The four brightest Draco giants do not appear in their Megacam database (presumably they were saturated); their photometry is from the SDSS (York *et al.* 2000) DR5 release (Adelman-McCarthy et al 2007), as is the i' mag of the brightest Draco giant with a HIRES spectrum.

The processing of the spectra was done with MAKEE² and Figaro (Shortridge 1993) scripts, and follows closely that described by Cohen *et al.* (2006). The equivalent widths were measured as described in Cohen *et al.* (2004). Due to the lower SNR in the blue, lines bluer than 4400 Å were ignored if the species had sufficient other detected lines. Lines with $W_\lambda > 175$ mÅ were discarded except for two lines from the Mg triplet, the Na D lines and Ba II lines in some of the stars; for these key elements no or only a few weaker features could be detected in most of the stars. Sometimes only one line of the Na D doublet could be measured; the v_r of some of the Draco stars was such that the other component of the doublet was mangled by NaD line emission from the Earth’s atmosphere. Table 3 lists the atomic parameters adopted for each line and their equivalent widths measured in the spectra of each of the Draco dSph stars.

The very luminous giant Draco XI-2 shows strong emission in the red wing of H α in its spectrum, with even stronger emission seen in the blue wing. No other star in the sample shows any detectable emission in H α .

4. Analysis

The analysis is identical to that of Cohen *et al.* (2008) and earlier references therein. In particular we use the model stellar atmosphere grid of Kurucz (1993) and a current version of the LTE spectral synthesis program MOOG (Snedden 1973), which treats scattering as LTE absorption.

Our analysis assumes classical plane parallel stellar atmospheres and LTE, both for atomic and for molecular features. We adopt a Solar Fe abundance of $\log[\epsilon(\text{Fe})] = 7.45$ dex, which is somewhat lower (by up to 0.10 dex) than that used by many groups. This leads directly to our [Fe/H] values for a given star being somewhat higher and to our abundance ratios [X/Fe] being somewhat lower than those which would be inferred by most other teams. Our gf values are generally taken from Version 3.1.0 of the NIST Atomic Spectra Database (physics.nist.gov/PhysRefData/ASD/index.html, NIST Standard Reference Database 78). A comparison of gf values for Fe we adopt with those of the First Stars Project at the VLT (Cayrel et al 2004) shows that the mean difference in Fe transition probabilities between these us is $|\Delta| < 0.01$ dex for Fe I and 0.04 dex for Fe II. Corrections for hyperfine structure for Sc II, V I, Mn I, Co I, Cu I, Ba II, and Eu II, when necessary, were used; the majority of the HFS patterns were adopted from Prochaska et al (2000).

Our abundances for C are from the 4320 Å region of the G band of CH, where the absorption is less than in the main part of the G band at 4300 Å. O abundances are from the forbidden line at 6300 Å; sometimes the weaker 6363 Å line is also detected. Our nominal Solar C and O abundances are 8.59 and 8.83 dex respectively. We adopt a dissociation potential of 3.47 eV (Huber & Herzberg

²MAKEE was developed by T.A. Barlow specifically for reduction of Keck HIRES data. It is freely available on the world wide web at the Keck Observatory home page, http://www2.keck.hawaii.edu/inst/hires/data_reduction.html.

1979) for CH. We have checked that with our adopted molecular parameters we can reproduce the Solar spectrum of the G band of CH, taken from Wallace, Hinkle & Livingston (1998). The adopted Solar abundances of C and of O are close to those of Grevesse & Sauval (1998), but somewhat larger than the values obtained using 3D model atmospheres by Asplund *et al.* (2004) and Asplund *et al.* (2005). We use 1D model atmospheres to synthesize the molecular features, ignoring any 3D effects, although Collet, Asplund & Trampedach (2006) suggest that these may be very large at $[\text{Fe}/\text{H}] \sim -3$ dex, becoming less important at higher metallicities. They claim that CNO abundances may be overestimated by ~ 0.8 dex as compared to a 1D analysis when molecular bands are used in extremely metal-poor stars. However, we prefer not to attempt 3D corrections until a full grid of 3D model atmospheres or of corrections to CNO abundances derived from the molecular bands from 3D to 1D models becomes available.

Since the Draco stars are rather faint for 2MASS, the uncertainties in the J and particularly in the K_s magnitudes are large. We therefore feel free to slightly adjust T_{eff} and $\log(g)$ after the first pass through the analysis to improve the ionization equilibrium and slope of the abundances determined from the set of Fe I lines as a function of χ (the excitation potential of the lower level). These spectroscopic stellar parameters are given in the fourth and fifth column of Table 2 and are the ones used subsequently. With these values we were able to achieve good ionization equilibrium for Ti and Fe as well reasonable excitation equilibrium of Fe I. Table 4 gives the slope of a linear fit to the abundances determined from the set of Fe I lines as a function of χ , W_λ , and λ , which are most sensitive to T_{eff} , v_t , and the wavelength dependence of any problems in establishing the correct location of the continuum (perhaps arising from the more severe crowding towards bluer wavelengths) or of a missing major source of continuous opacity, respectively. There are ~ 55 to 150 Fe I lines detected in each star, with χ ranging from 0 to ~ 4.5 eV. The only slope which is large enough to be of concern and which tends to have the most significant correlation coefficient is that with χ ($|cc(\chi)| > 0.4$ for some of the sample giants), which depends largely on T_{eff} . In our final adopted solutions, the Fe I slope as a function of χ tends to be slightly negative, with values ranging from -0.03 to -0.10 dex/eV. However, since this slope decreases by ~ 0.2 dex/eV/ $(\Delta T_{eff} = 250 \text{ K})$, a decrease in T_{eff} of a maximum of 125 K, consistent with our adopted T_{eff} uncertainty, would make all these slopes zero, and would decrease the $[\text{Fe}/\text{H}]$ derived from Fe I lines by ~ 0.2 dex.

One potential concern is the possibility of non-LTE in Fe affecting the determination of stellar parameters using ionization equilibrium. In particular Fe overionization has been observed in M dwarfs in the Hyades open cluster, where the true Fe abundance can be established from a detailed abundance analysis of the hotter members, by Schuler et al (2005). They find that the overionization, in the sense of the deduced abundance from Fe II lines being higher than that from Fe I lines, is considerably smaller in the Hyades giants. A similar problem in the same open cluster was found earlier by Yong et al (2003), who demonstrate that the Fe I abundance in the coolest Hyades dwarfs they studied is much closer to the cluster mean Fe-metallicity. Similarly, in resonance scattering (e.g. see Asplund 2005) the source function, S_ν , is reduced to below the local Planck function, thus leading to a stronger line in non-LTE. Resonance scattering is seen in the

Na D lines of metal-poor stars (e.g. Andrievsky *et al.* 2007), the OI triplet at 7774 Å in the Sun and may have affected the abundances from the Ca I 4226 Å resonance line of McWilliam *et al.* (1995a).

The slightly negative Fe I slope with excitation potential mentioned above may be a sign that overionization of Fe is occurring. If this were the case, to compensate we would then have been driven to adopt a higher T_{eff} than the actual value; our derived [Fe/H] values would be too high as indicated above, but the deduced abundance ratios would not be significantly affected by such a decrease in T_{eff} . With this in mind, we adopt asymmetrical uncertainties for T_{eff} of +100 K, –150 K. Since we have been able to achieve satisfactory ionization equilibrium for Fe and for Ti and at the same time reasonably good excitation equilibrium for Fe with a single value of T_{eff} which differs from that set solely from broad band photometry by 50 K or less for 6 of the 8 Draco giants, we regard our choices for stellar parameters as satisfactory. However, we could not find a consistent set of stellar parameters for one of the most luminous and coolest Draco giants, Draco XI-2, that would simultaneously satisfy the above conditions. In particular we could not achieve Ti and Fe ionization equilibrium simultaneously, and had to adopt compromise values. Ideally, of course, one would like to have a full non-LTE 3D analysis including both convection and spherical (as distinct from plane parallel) layers for all species, but at the present time this is not practical.

5. Comparison with Galactic Halo Field Stars

In this section we study the behavior of abundance ratios within Draco and compare them to those of Galactic halo field stars in detail. The sample of Draco stars with detailed abundance analyses based on high dispersion spectra is now 14, including the 8 we present here. Shetrone, Bolte & Stetson (1998) and Shetrone, Côté & Sargent (2001) presented an analysis for 6 Draco members. They used 1 hour exposures per star and observed with HIRES prior to the major detector upgrade in 2004. The most metal-poor star they observed, Draco 119, was re-observed with much longer HIRES exposures by Fulbright, Rich & Castro (2004) as the earlier study only found an upper limit for Ba II; they too could only set upper limits for all elements heavier than Ni³. Both studies adopted essentially the same T_{eff} for this star, but the recent work has $\log(g)$ 0.6 dex larger. Although they derive essentially the same [Fe/H] for this star, there are substantial differences in abundance ratios between these two works, presumably largely due to the much higher SNR of the Fulbright, Rich & Castro (2004) spectra. In the following we always replace the Shetrone, Côté & Sargent (2001) abundances for Draco 119 with those of Fulbright, Rich & Castro (2004) and we refer to this collective data set for six Draco giants as

³Koch et al (2008b) recently found two stars with very low upper limits for [Ba/Fe] yet very high [Mg/Fe] in the faint Hercules dSph galaxy. These are reminiscent of Draco 119, which until now was believed to be unique in that no element heavier than Ni could be detected in its spectrum in spite of a major effort at Keck with HIRES by Fulbright, Rich & Castro (2004).

Shetrone, Côté & Sargent (2001). Our spectra of luminous stars in the Draco dSph are not as deep as that of the single star observed by Fulbright, Rich & Castro (2004), but are substantially better than those of Shetrone, Bolte & Stetson (1998) and Shetrone, Côté & Sargent (2001).

We proceed by examining a series of plots (Figs. 2 to 16) in which we show the Draco sample, both our 8 stars (indicated by large filled circles) and the 6 observed previously from Shetrone, Côté & Sargent (2001) (denoted by open circles, and less accurate than subsequent Draco studies), with the more accurate revisiting of the star Draco 119 by Fulbright, Rich & Castro (2004) (the large open circle) used in preference to the earlier less accurate values. These figures also display results from the 0Z project led by J. Cohen to datamine the Hamburg/ESO Survey for extremely metal-poor stars. Many of the most metal-poor candidates from this work have been observed with HIRES at the Keck Observatory and analyzed in a manner very similar to the present study as described in Cohen *et al.* (2004) and Cohen *et al.* (2008), with the difference that most of the spectra for the 0Z project were taken further towards the blue than those of the Draco stars, a move necessary because of the low density of lines in the red in the spectra such low metallicity stars. Only the metal-rich end of the 0Z project database, much of which is not yet published (J. Cohen, N. Christlieb *et al.*, in preparation), is shown in these figures. A number of other halo field star surveys, the most important of which at the lower metallicities probed here is the First Stars Project (Cayrel *et al.* 2004), are shown as well as those stars from McWilliam *et al.* (1995a) not re-observed by Cayrel *et al.* (2004). Fulbright (2002), Johnson (2002) and other sources noted in the symbol key shown on each figure provide coverage at the higher metallicities reached by the Draco stars. Nissen *et al.* (2000) add higher metallicity information for Sc and Mn.

We examine plots of $[X/Fe]$ vs $[Fe/H]$ for each element and use them to look for differences in the chemical inventory between Galactic halo field stars and the Draco sample, which may be a function of Fe-metallicity. We will see that the differences are small, not larger than ~ 0.3 dex in most cases. This means that some care is required to ensure that all the abundances from the various sources are homogeneous. While we have not done a full check of this, we have taken a few steps the first of which is to adjust each survey to our set of Solar abundances, particularly to our adopted value of $[Fe/H]$, whenever possible. Specific cases where there are clear problems related to issues of homogeneity between the various analyses are discussed individually below. It should be noted that the analyses for our Draco sample, including the methods used to determine stellar parameters, are essentially identical to those of the 0Z Project.

The trend of $[C/Fe]$ versus $[Fe/H]$ is shown in Fig. 2, based for the majority of these stars on the strength of the G band of CH. The solid lines represent the mean behavior of thick disk dwarfs from the survey by Reddy, Lambert & Allende Prieto (2006). The C abundance in luminous giants is lowered substantially from an initial $[C/Fe] \approx 0.0$ dex due to intrinsic nucleosynthesis (the CN cycle of H burning) followed by dredge-up to the stellar surface of processed material within which C has burned to N (see e.g. Cohen, Briley & Stetson 2005). Thus the initial C abundance of the Draco giants cannot be determined. Note that in Fig. 2 and those that follow the asymmetric uncertainties we adopted in §2 are shown for $[Fe/H]$, but not for abundance ratios $[X/Fe]$; for the

latter the larger uncertainty is plotted.

It is quite difficult to measure O abundances in metal-poor giants. The set of features that can be used is very limited and each has problems. This has resulted in considerable controversy about O abundances in metal-poor stars in recent years, see e.g. the discussion in Melendez et al (2004). The forbidden OI lines at 6300 and 6363 Å line are very weak, and the 7770 Å triplet, which has substantial non-LTE effects, is not detectable. [O/Fe] ratios for the Draco giants and for a compilation of surveys in the literature are shown in Fig. 3.

The arrow in Fig. 3 indicates the probable correction for 1D to 3D effects required for luminous giants given by Cayrel et al (2004), which has not been implemented, but which would bring the plateau in [O/Fe] down to a mean level of $\sim +0.5$ dex. The lines are linear fits from Ramirez, Allende Prieto & Lambert (2007) to their samples of thick disk and halo dwarfs (solid line) and to thin disk dwarfs (dashed line). They use only the 7770 Å triplet, with appropriate non-LTE corrections; these lines become detectable in dwarf stars. The net result is that the Draco giants appear low in [O/Fe] when compared to samples of field halo giants which rely on the same 6300 Å forbidden line. The more metal-rich thick disk and halo dwarfs can be made consistent in [O/Fe] with the metal-poor luminous giants in the halo and in the Draco giants once the 3D to 1D correction suggested by Cayrel et al (2004) is implemented.

Fig. 4 suggests that there is a separation of ~ 0.2 dex for [Na/Fe] at a fixed [Fe/H] between the two large surveys of very metal-poor halo field stars, i.e. the First Stars Survey led by R. Cayrel and the 0Z Survey led by J. Cohen. Cayrel et al (2004) use only the two NaD lines to determine the Na abundance, as was the case for most of the stars from the 0Z project; only few of the more metal-rich giants in the 0Z database had detectable 5682, 5688 Na I lines. The origin of this offset is not clear. It could result from differences in the samples. The 0Z sample is ~ 3 mag fainter on average than is the First Stars sample, and so is picking up many relatively nearby lower luminosity RGB giants, as well as a few very distant giants near the RGB tip; the distribution in distance and in luminosity might be somewhat different within the much brighter First Stars sample. [Na/Fe] ratios vary enormously from star to star among very metal-poor stars, perhaps as a function of Galactocentric radius, or perhaps as a result of deep mixing, symptoms of which have been found among very metal-poor halo giants by Spite et al (2005), or contamination from a former AGB companion.

Non-LTE corrections for the NaD doublet for metal-poor giants calculated by Takeda et al (2003) are ~ -0.2 dex, but no non-LTE corrections for Na were applied to any of the Draco stars nor to those from the 0Z or First Stars projects. In spite of these concerns, the Draco giants clearly have [Na/Fe] somewhat lower than the Galactic halo field stars, with Draco XI-2, a high luminosity giant in our sample, having an extremely low [Na/Fe]. At the lowest metallicities, the Draco sample appears to overlap the Galactic halo field stars.

Fig. 5 shows the important α -element Mg, another element with only a few accessible features in our Draco spectra. The published values from Cayrel et al (2004) for the First Stars project

have been increased by 0.15 dex. This was done in accordance with Bonifacio *et al.* (2009), who state in §6.1 of their paper that an error was made by the First Stars group in the measurement of W_λ for the strong Mg triplet lines in the more metal-rich giants in their sample such that $[\text{Mg}/\text{Fe}]$ was underestimated by this amount for these stars in the tables of Cayrel et al (2004). The gf values for Mg I lines are uncertain, and systematic differences of ~ 0.05 dex may arise between surveys from the choice of gf values for the Mg lines, depending on the specific Mg lines measured in a particular star, as discussed in §7.4 of Cohen *et al.* (2004). We also note that the sample from Johnson (2002) is systematically high in $[\text{Mg}/\text{Fe}]$ across more than 1 dex in $[\text{Fe}/\text{H}]$ compared to both the 0Z project and the First Stars Project. She took her Mg I gf values from three sources; only those taken from the most recent of the three (Fuhrmann, Axer & Gehren 1995) agree well with the values we adopt. We find that $[\text{Mg}/\text{Fe}]$ definitely is low in the Draco stars at $[\text{Fe}/\text{H}] > -2$ dex, but at the lowest metallicities the Draco giants overlap with the 0Z Survey and First Stars Survey giants, once the correction suggested by Bonifacio *et al.* (2009) is implemented.

The behavior of the α -element Si is shown in Fig. 6 with the mean relation for thick disk stars from Reddy, Lambert & Allende Prieto (2006) indicated. The figure shows good agreement between the 0Z and First Stars Project abundance ratios for this element; $[\text{Si}/\text{Fe}]$ from Johnson (2002) is again slightly high. The behavior of $[\text{Si}/\text{Fe}]$ in the Draco giants is similar to that described above for $[\text{Mg}/\text{Fe}]$, i.e. the lowest metallicity Draco giants overlap the Galactic halo stars, while at somewhat higher metallicities, where the Galactic halo field stars still have elevated $[\text{Si}/\text{Fe}]$, $\sim +0.5$ dex, the Draco stars have fallen to the Solar value.

The explosive α -element Ca also has problems with inconsistencies between the two large surveys of very metal-poor halo stars, the First Stars Project and the 0Z Project. An offset of ~ 0.2 dex is required for agreement between them. This problem appears to originate in our 0Z database, as the mean $[\text{Ca}/\text{Fe}]$ for dwarfs given in Cohen *et al.* (2004), which is ~ 0.15 dex higher than that found here, agrees well with that of the First Stars Survey (Cayrel et al 2004 for halo giants, Bonifacio et al 2009 for halo dwarfs, their two means for $[\text{Ca}/\text{Fe}]$ in Galactic halo field stars are identical). The gf values adopted are essentially identical for the two large extremely metal-poor halo field star surveys, and are those of NIST. Many of the older analyses use those from Smith & Raggett (1981), which scatter widely around the recent values. Thus, as is also the case for Mg I, ideally one must correct each star individually, checking which specific Mg I and Ca I lines were used and what gf values were adopted. Irrespective of this issue, the luminous Draco giants have $[\text{Ca}/\text{Fe}]$ lower than that of the Galactic halo stars over the full range of $[\text{Fe}/\text{H}]$ found in Draco. At the lowest Fe-metallicities probed, they come close to the abundance ratios for Ca from the 0Z project, but don't quite reach as high in $[\text{Ca}/\text{Fe}]$.

Figs. 8 and 9 show the behavior for $[\text{Sc}/\text{Fe}]$ and $[\text{Ti}/\text{Fe}]$ respectively. The mean relation for thick disk stars from Reddy, Lambert & Allende Prieto (2006) is shown for the latter. In both cases there is good agreement between the abundance ratios deduced by the 0Z Project and the First Stars Project. For the explosive α -element Ti as well as for Sc the metal-rich Draco stars fall well below the halo field. $[\text{Ti}/\text{Fe}]$ is slightly sub-solar in this regime; $[\text{Sc}/\text{Fe}]$ is definitely sub-solar.

Among the lowest metallicity Draco giants [Sc/Fe] overlaps the halo field star samples, while for [Ti/Fe] the Draco stars still appear ~ 0.2 dex low compared to the Galactic halo field stars.

At high metallicities, [Cr/Fe] (Fig. 10) appears lower among the Draco stars than among the Galactic halo field stars. The difference, if it exists at all, is smaller for the lowest metallicity Draco stars. [Mn/Fe] (Fig. 11) declines rapidly from Solar to about -0.4 dex as [Fe/H] decreases in Galactic halo field stars. A known problem discussed in Cohen *et al.* (2004) requires that the Mn abundance be increased by 0.2 dex for stars where the 4030 resonance triplet lines are used. These are the strongest Mn I lines in the optical and the only ones accessible for extremely metal-poor stars, but are too blue to be included in our Draco analyses. This offset has been applied to the 0Z Project analyses; the First Stars Project values already contain this offset. The Draco giants overlap the Galactic halo field stars at all Fe-metallicities.

Fig. 12 displays the [Co/Fe] ratios which for Galactic halo stars rise rapidly from near the Solar ratio as [Fe/H] decreases below -2 dex. It appears that the lowest Fe-metallicity Draco giants follow this trend, with the higher metallicity Draco giants perhaps lying slightly lower than do Galactic halo field stars. However, there is only one Co I line detected in most of these stars; only a few have measurements for the stronger line at 4121 \AA , which is uncomfortably far in the blue, as confirmation of the deduced abundance ratio. Thus any conclusion regarding the behavior of [Co/Fe] in Draco is still uncertain.

The nickel abundance relative to Fe (Fig. 13) appears to fall below that of the halo field (which has [Ni/Fe] at the Solar ratio over the entire range of Fe-metallicity) among the higher metallicity Draco stars. The [Ni/Fe] ratios for the lowest metallicity Draco stars overlap in Fig. 13 those of Galactic field halo stars.

The Galactic halo field samples from the 0Z Project and the First Stars Project overlap well for the abundance ratio [Zn/Fe]. Among field halo stars, [Zn/Fe] is close to the Solar ratio but rises rapidly below [Fe/H] ~ -2 dex, as shown most recently for halo dwarfs by Nissen et al (2008). In the Draco giants, [Zn/Fe] behaves similarly to the Co and Ni abundance ratios for intermediate metallicities, where the Draco stars fall below those in the Galactic halo. At the lowest metallicities, [Zn/Fe] may rise above the Solar value, but there are not enough detections among the lowest metallicity stars in the Draco sample to be certain.

The Galactic halo field samples from the 0Z Project and the First Stars Project (data for Sr and Ba is from Francois et al 2007) overlap well for the abundance ratio [Sr/Fe] versus Fe-metallicity shown in Fig. 15. The Draco stars over the full range of Fe-metallicity have [Sr/Fe] ratios that fall below the bulk of the Galactic sample, although, except for Draco 119, which only has an upper limit to [Sr/Fe] from Fulbright, Rich & Castro (2004), they are not outside the range of the low outliers in the much larger Galactic sample. The Sr II lines used are the resonance lines at 4077 and 4215 \AA ; they are uncomfortably far in the blue, where the SNR of our Draco spectra is rather low. In addition, the Draco stars are right at the tip of the RGB, and hence are cooler and more luminous than almost all of the stars in the Galactic halo surveys of the 0Z Survey and most of

those in First Stars Project, as well as essentially all in the surveys of somewhat higher metallicity field halo stars used here. One might be concerned that some differential error, for example, the magnitude of the non-LTE corrections, might affect our comparisons shown in Fig. 3 to 16. This might be an issue for $[\text{Sr}/\text{Fe}]$ in view of the large positive non-LTE corrections for low metallicity stars calculated by Mashonkina & Gehren (2001) and by Short & Hauschildt (2006) which appear from the limited number of cases studied to be highly variable with T_{eff} and $\log(g)$. However, the sample of luminous giants in the Galactic globular cluster NGC 7099 of J. Cohen (unpublished) are closer in T_{eff} to the Draco giants. These GC giants with $[\text{Fe}/\text{H}] \sim -2.4$ dex show Solar $[\text{Sr}/\text{Fe}]$ and $[\text{Co}/\text{Fe}]$ as well, suggesting that any such differential effect is probably not very large.

Fig. 16 shows the abundance ratios $[\text{Ba}/\text{Fe}]$, with the mean for the Galactic thick disk from Reddy, Lambert & Allende Prieto (2006) indicated as a solid line. The Draco stars as well as the Galactic halo field stars display a very large range in $[\text{Ba}/\text{Fe}]$ at low metallicities (see Fig. 16). Most of the Draco stars lie within the regime occupied by the majority of the Galactic halo stars from the OZ Project and the First Stars project. There are however two Draco giants that are moderately low, though still within the range of the Galactic giants, while Draco 119 (Fulbright 2002), which only has an upper limit for $[\text{Ba}/\text{Fe}]$, is an extremely low outlier and lies below any known Galactic star.

5.1. The Outer Galactic Halo

The SDSS (York *et al.* 2000; Adelman-McCarthy *et al.* 2007) has obtained moderate resolution spectra and multi-color photometry of very large samples of Galactic halo stars. Their database is large enough and uniform enough to determine the properties (spatial, kinematic, and chemical) of such stars as a function of their Galactocentric distance, which program was carried out by Carollo *et al.* (2007). They demonstrate in a definitive way that the outer halo with $R_{GC} > 15$ kpc contains in the mean stars which have a more spherical spatial distribution with low retrograde net rotation about the center of the Galaxy and with lower metallicity in the mean than does the stellar population of the inner halo. However, their discussion is restricted to Fe-metallicities.

Much smaller samples of outer halo stars in the local neighborhood have been isolated and their chemical inventory analyzed in detail in several previous studies, in particular by Nissen & Schuster (1997) and by Stephens (1999), who searched for local dwarfs with retrograde motions. They comment on some peculiarities unearthed in their abundance analyses of such retrograde dwarfs, which they consider as outer halo stars, as compared to metal-poor dwarfs with normal orbital characteristics. Such anomalous dwarfs tend to have low α -ratios and perhaps have $[\text{Ni}/\text{Fe}]$ somewhat below the Solar value; Stephens (1999) found $\langle [\text{Ni}/\text{Fe}] \rangle = -0.09 \pm 0.07$ dex. These are reminiscent of some of the differences noted earlier between the Galactic halo field stars and the giants from the Draco dSph galaxy.

Roederer (2008) has recently compiled a sample of halo stars with published detailed abundance

analyses and with parallaxes so that their orbits within the Galaxy can be derived. He classifies his sample on the basis of kinematics into inner halo and outer halo stars, and has again found a small deficit in $[\text{Mg}/\text{Fe}]$ in outer halo stars as compared to inner halo ones shown by the dotted and dashed lines in Fig. 5, but he does not find any difference for the other α -elements he could study, Ca and Ti. He also finds a somewhat larger scatter in abundance ratios in outer halo stars than in inner halo stars for $[\text{Ni}/\text{Fe}]$ and for $[\text{Ba}/\text{Fe}]$. Much more work remains to be done along these lines, but these tantalizing hints suggest that to find stars with the chemical inventory of the Draco dSph one must look far out in the halo rather than at the closer in samples that have been well studied over the past decade by the First Stars Project of Cayrel et al (2004). A fraction of the OZ Survey resides in the outer halo (in situ, not stars moving with retrograde velocities through the Solar neighborhood, see Schörck et al 2009) but the necessary parallaxes for most of these stars are not available, or are so uncertain and close to zero to be useless.

The many abundance analyses for giants in Galactic globular clusters, reviewed by Gratton, Sneden & Carretta (2004), reveal abundance ratios that follow those seen in the inner halo, so that the stellar population in the inner halo could easily be composed of globular clusters that dissolved before the correlations among the light elements C,N,O, Na, Mg and Al (widely believed to result from contributions from intermediate mass AGB stars) were imprinted. However, there are a few exceptions such as Pal 12, which according to Cohen *et al.* (2004) has a chemical inventory similar to that of intermediate metallicity dSph stars. Specifically $[\text{Ca}/\text{Fe}]$ is almost Solar, as is $[\text{Ti}/\text{Fe}]$, and Na is very deficient. This provides evidence, also supported by kinematic data and calculation of Galactic orbits, that Pal 12 originally was a cluster in the Sgr dSph galaxy, which is currently being accreted by the Milky Way. During the process of accretion Pal 12 was presumably stripped from the Sgr dSph to become part of the extended Sgr stream; Layden & Sarajedini (2000) suggest several other Milky Way globular clusters were also stripped from the Sgr dSph, one of which is Terzan 7. An abundance analysis of this globular cluster by Sbordone et al (2005) shows the same anomalies as noted above for Pal 12. The globular cluster M54 is at the location of the nucleus of the Sgr dSph galaxy, but Siegel et al (2007) suggest that it is not the nucleus itself, but rather was pulled in very close to it by dynamical friction. Many of the most distant Galactic GCs, which tend to show somewhat younger ages than the inner halo GCs (see, e.g. Marin-Franch et al 2009), are now believed to have been accreted by the Milky Way.

6. A Toy Model for the Draco Abundances

The 8 Draco giants in our sample have $[\text{Fe}/\text{H}]$ between -1.45 and -3.05 dex. To provide a context for the understanding of our results we develop a toy model for the behavior of abundance ratios $[\text{X}/\text{Fe}]$ vs $[\text{Fe}/\text{H}]$ to apply to the Draco sample. We look for guidance to the behavior of abundance ratios in Galactic populations, the thin disk, thick disk, and Galactic halo field stars since the same nucleosynthetic processes are involved, although they may contribute different relative fractions to the chemical inventory in different environments. Fig. 17 shows a plot of $[\text{Mg}/\text{Fe}]$

vs $[\text{Fe}/\text{H}]$ for thin and thick disk F and G dwarfs based on the detailed abundance analyses of Reddy et al (2003) and of Reddy, Lambert & Allende Prieto (2006) respectively. We note, as have many others, that at low metallicities, the $[\text{Mg}/\text{Fe}]$ ratios for thick disk stars appear to reach a plateau level. Both thin and thick disk stars reach the Solar ratio at approximately the Solar Fe-metallicity. Galactic halo field stars show a similar behavior with $[\text{Mg}/\text{Fe}]$ reaching a comparable low Fe-metallicity plateau level (see, e.g. Cohen *et al.* 2004).

We characterize the data for the abundance ratios for each element X detected by first finding $A(X)$, the value of $[\text{X}/\text{Fe}]$ at the lowest $[\text{Fe}/\text{H}]$ found in the sample and $B(X)$, a value for stars at the high end of the Fe-metallicity of the sample. We assume that the set of values of $[\text{X}/\text{Fe}]$ for the sample can be modeled by constant $[\text{X}/\text{Fe}] \equiv A(X)$ over the metallicity range $[\text{Fe}/\text{H}](A) < [\text{Fe}/\text{H}] < [\text{Fe}/\text{H}](\text{low},X)$, and $B(X)$ over the range $[\text{Fe}/\text{H}](\text{high},X) < [\text{Fe}/\text{H}] < [\text{Fe}/\text{H}](B)$. Between $[\text{Fe}/\text{H}](\text{low},X)$ (the knee of the distribution) and $[\text{Fe}/\text{H}](\text{high},X)$ the values of $[\text{X}/\text{Fe}]$ are assumed to change linearly with $[\text{Fe}/\text{H}]$. We thus have a plateau in $[\text{X}/\text{Fe}]$ over the range $[\text{Fe}/\text{H}](A)$ to $[\text{Fe}/\text{H}](\text{low},X)$ and another plateau at a value of $[\text{X}/\text{Fe}]$ which may be different at the high metallicity end from $[\text{Fe}/\text{H}](\text{high},X)$ to $[\text{Fe}/\text{H}](B)$, with a straight line connecting the two plateaus. We solve for the two parameters in this toy model $[\text{Fe}/\text{H}](\text{low},X)$ and $[\text{Fe}/\text{H}](\text{high},X)$ by minimizing the variance around the fit. Thus our model has four variables whose values are determined directly from the dataset of $[\text{X}/\text{Fe}]$ as a function of $[\text{Fe}/\text{H}]$, with two additional fit parameters.

Our toy model is based on the behavior of abundance ratios in the Galactic disk and halo as exemplified by Fig 17. Our model fits to the $[\text{Mg}/\text{Fe}]$ ratios for thin and thick disk Solar neighborhood F and G dwarfs from Reddy et al (2003) and Reddy, Lambert & Allende Prieto (2006) are given in Table 8; the latter is shown in this figure. These fits are a good representation of the behavior of the data for abundance ratios of Mg and of other elements as a function of $[\text{Fe}/\text{H}]$ for Galactic stellar populations.

Our toy model fits offer important clues for the importance of various nucleosynthesis processes in Draco as compared to in the Galactic thick disk and halo stellar populations. The parameters of the toy model depend on the nucleosynthetic yields for the production channels for each of the elements X and Fe, the IMF, the rate of star formation, accretion, loss of gas via galactic winds, interaction between the dSph and the Milky Way via tides, ram pressure stripping, etc. as will be discussed in §6.2.

We apply this toy model to the sample of 14 Draco giants. We use the two lowest metallicity and three highest metallicity stars in the Draco sample to determine the plateau values for $[\text{X}/\text{Fe}]$, $A(X)$ and $B(X)$, as well as the minimum and maximum $[\text{Fe}/\text{H}]$ values over which the model is fit, $[\text{Fe}/\text{H}](A)$ and $[\text{Fe}/\text{H}](B)$. Weights are halved for the 5 stars with lower accuracy spectra. Note that these four values are calculated directly from the data. We solve for the two parameters in this toy model $[\text{Fe}/\text{H}](\text{low},X)$ and $[\text{Fe}/\text{H}](\text{high},X)$ by minimizing the variance around the fit using our sample of Draco giants described above.

We have applied this model to 10 elements for which sufficient accurate data is available for

Draco members. The resulting parameters for each element are listed in Table 8 and the fits are shown when available in Figs. 4 to 16. The uncertainties in $A(X)$ and in $B(X)$ are approximately those of $\sigma[X/Fe]$ for a single Draco star from our sample. The latter values are given in Table 6. Thus, for example, for $[Mg/Fe]$ they are ± 0.14 dex, while $A(Mg)$ is 0.50 dex larger than $B(Mg)$. The decline in $[Mg/Fe]$ as $[Fe/H]$ increases is highly significant, as is the increase in $[Cr/Fe]$, $[Sr/Fe]$ and $[Ba/Fe]$ as $[Fe/H]$ increases, while $[Ca/Fe]$ and $[Ti/Fe]$ are constant at approximately the Solar value to within the uncertainties.

Even when the change between the low and high metallicity abundance ratio is clearly statistically significant, as is the case for Mg, the values for the knees of the distribution, $[Fe/H](low)$ and $[Fe/H](high)$ are quite uncertain due to the small sample of Draco giants coupled with the uncertainty of the individual $[Mg/Fe]$ determinations for each Draco giant. However, the possibility of a straight line connecting $A(X)$ to $B(X)$ without any plateau at either low or high metallicities is included as part of the search for the best knee values. This straight line without any plateau has a variance which is $\sim 50\%$ larger than the minimum found here for the knee values (listed in Table 8) for the $[Mg/Fe]$ abundance ratios.

We consider whether our simple toy model provides an adequate fit to the Draco abundance ratios. We assume that the minimum $\sigma[X/Fe]$ for all elements is 0.15 dex, which is for some elements somewhat larger than the value given in Table 6. We then calculate χ^2 for the the 14 Draco giants between their observed abundance ratios and the values from the toy model fits. We find that six of the 10 elements with such fits have $\chi^2 \leq 22$ for all 14 stars. The same is true for two additional cases of the 10 when one highly discrepant giant (Draco XI-2), which is a low outlier, is ignored. This suggests that the uncertainties in $[X/Fe]$ have been slightly underestimated by perhaps 20% or that the adopted toy model is somewhat too simple to describe the full range of behavior seen in Figs. 4 to 16. However, as an initial approach towards a simple model, our toy model seems to represent the data regarding abundance ratios for the Draco giants reasonably well.

There are a number of elements for which the toy model could not be applied due to the low number of stars with measured $[X/Fe]$ or to our judgement, based on issues discussed in §5, that the abundance ratios are not reliable enough. Table 9 provides means, extreme values and dispersions for all species detected in the Draco sample.

6.1. Summary of the Comparison of the Toy Model Parameters Between Draco and Galactic Populations

Using the toy model described above we compare the behavior of the abundance ratios within the sample of Draco giants with those of Galactic stellar populations in the thin disk, the thick disk, and the halo. The $[X/Fe]$ values at low metallicity, $A(X)$, for the elements Na, Mg, Si, Cr, Mn, and Ni and perhaps Sc and Ti are identical to those of the thick disk to within the uncertainties. $[Ca/Fe]$ is approximately constant at a slightly sub-solar values over the full range of $[Fe/H]$ spanned

by the Draco giants. It falls somewhat below the halo values even at the lowest Fe-metallicities probed. The uncertainties are still large, and for Ca the systematic differences between the two large scale surveys of Galactic halo field stars (our OZ survey and the First Stars survey at the VLT led by R. Cayrel) remain to be resolved. [Cr/Fe] and [Mn/Fe] both increase as [Fe/H] increases in Draco and in Milky Way halo stars. For the heavy neutron capture elements Sr and Ba, the abundance ratios at the lowest metallicity are at or below the most extreme stars in the much larger halo samples; [Sr/Fe] and [Ba/Fe] both also increase towards the Solar ratio as [Fe/H] increases in Draco and in the halo field. Intermediate [Fe/H] Draco stars in general have lower abundance ratios than do the Galactic halo field stars.

The Galactic populations all approach $[X/Fe] = 0$ close to or at the Solar Fe-metallicity, i.e. $B(X)$ and $[Fe/H](\text{high}, X) \sim 0$. A comparison of Fig. 5, [Mg/Fe] vs. [Fe/H] for the Draco stars, with Fig. 17, the same for the thick and thin disk stars in the Milky Way, suggests that the toy model can adequately represent both the Galactic and Draco data, and that that the shape of the mean relation is similar. But in the Galactic populations, as is shown in Table 8, the approach toward Solar ratios for many elements begins at a considerably higher [Fe/H]. For example. $[Fe/H](\text{low}, \text{Mg})$ is -0.53 dex for the Milky Way thick disk and less than -2 dex for Draco.

6.2. Comparison with Nucleosynthesis Predictions

The parameters of our toy model have close ties with nucleosynthesis. The dependencies on star formation rates, yields of various nuclear reactions, etc. of the various parameters in the toy model are most clear in the case of elements which are produced largely by sources different from those of Fe. The plateau value $A(X)$ at low [Fe/H] presumably represents the abundance ratio $[X/Fe]$ from only those sources of material processed through the nucleosynthesis channels that were active at very early times, i.e. SNII from core collapse of massive stars, events characteristic of the earliest epochs of star formation. The plateau level $B(X)$ represents the abundance ratio for element X at late times when all relevant sources, SNIa, SNII, AGB, novae, etc are contributing. These abundance ratios are independent of accretion of primordial material and, for a well mixed ISM, of galactic winds.

The abundance ratios for the α -elements, produced strongly in SNII, but not much in SNIa, and for the heavy neutron capture elements fall into this category. On the other hand, when the nucleosynthesis channels for element X are approximately the same as those for Fe, we expect that the abundance ratio will be approximately constant, with $A(X) \approx B(X) \approx 0$, ignoring issues of metallicity dependent yields.

There is overall agreement of the plateau values at both high and low [Fe/H] for the α -elements between the Draco giants and field halo stars in the Milky Way. [Mg/Fe] has the largest range, as might be expected since Mg, unlike Ca or Si, is produced only in SNII, while Ca and Si are produced in both SNII and SNIa (Woosley & Weaver 1995). $A(\text{Ca})$ is 2σ low compared to the

Galactic halo field stars; all other α -element plateau values are close to those of the halo field stars. This suggests that the relative contributions to $[X/Fe]$ of SNII at early times and of a mixture of various sources, dominated by SNIa, at later times are similar in the cases being compared. The yields depend both on the rates of various nuclear reactions (which are mass dependent) and on the initial mass function for star formation. The former is fixed by physics, so this implies that there cannot be much variation in the latter, i.e. in the initial mass function (and in the mass loss during the course of evolution of massive stars). The agreement at high $[Fe/H]$ suggests that the relative contributions of at least the dominant sources must also be the same in the two environments, constraining SNIa production.

The major differences appear to be confined to the fit parameters $[Fe/H](low)$ and $[Fe/H](high)$ which define the point at which $[X/Fe]$ drops off the low-metallicity plateau and where it approaches the Solar value respectively. These parameters are measures of the delay between when the contribution of SNII is dominant and when SNIa contribute at full strength. SNIa are believed to arise from thermonuclear explosion of a white dwarf whose mass increases, presumably through mass transfer in a binary system, until explosive carbon burning is ignited. Thus $[Fe/H](low)$ measures how much $[Fe/H]$ builds up over the timescale required for the binaries responsible for SNIa to form, to explode, and to begin to contribute significantly to the chemical inventory of the ISM in the dSph, while $[Fe/H](high,X)$ refers to the time when the SNIa reach the full level of their contribution.

Greggio, Renzini & Daddi (2008) offer a recent determination of the distribution of delay times between an episode of star formation and the resulting SNIa events. This delay pattern for a specific burst of star formation is to first order fixed by the IMF. The Fe-metallicity built up in Draco over this fixed timescale, corresponding to $[Fe/H](low)$, is lower in Draco than it is in the Galactic halo. Given that we have already offered some evidence that the IMFs are similar, this must constrain some combination of the star formation efficiency, the rate of loss of gas processed through stars and hence enhanced in both X and Fe, and the rate of accretion of primordial gas consisting mostly of H, each of which affect the relationship between $\langle [Fe/H] \rangle$ in the stellar system and time. More detailed models for chemical evolution incorporating the full dependence of these factors are required to further disentangle and evaluate the contributions of each of these.

The light elements C, O, Na and Mg show abundances relative to Fe in luminous Draco giants at similar Fe-metallicity which have a range far larger than can be ascribed to observational error. These elements are believed to have been formed largely in the interiors of massive stars through nuclear fusion reactions, then dispersed into the interstellar medium by SNII explosions, all of which happens quite rapidly after the initiation of star formation. The rates of production of the various elements depend on the initial mass of the SNII progenitor and its subsequent mass loss history, and these dependencies differ not just in amplitude but even in sign among the light elements (Woosley & Weaver 1995). Deep mixing similar to that seen in luminous Galactic globular cluster giants may also be important for these elements.

Draco has $M_V \sim -10$ mag, brighter than all Galactic globular clusters except ω Cen and NGC 6715. Most of Draco’s stars are old, but we cannot be sure that the entire population formed in a single burst. The stellar population may be small enough that stochastic effects of the formation of the very rare most massive stars discussed by Carigi & Hernandez (2008) may become significant especially among the most metal-poor stars in Draco. This may be the source of some or all of the variations among the light elements, although why such stochastic effects are not seen in even low mass globular clusters is an interesting question.

Arnett (1971) (see also Clayton 2003) discusses the production of Na, which is believed to occur in the interiors of massive stars and to depend on the neutron excess, which in turn depends on the initial heavy element abundance in the star. Na thus has both a primary and a secondary nucleosynthesis channel. This presumably gives rise to the very low [Na/Fe] abundances seen among the Draco giants. Sc production in SNII is highly dependent on the details of the explosion, including both the metallicity and mass of the progenitor (Woosley & Weaver 1995; Limongi & Chieffi 2003). Stronger odd-even effects are found for lower metallicity and, in the case of Sc, for lower mass progenitors (Limongi & Chieffi 2003). Thus a relative absence of the higher mass SNII with $M > 35M_\odot$ might give rise to the low [Sc/Fe] in the Draco sample.

The Fe-peak elements Cr through Zn are the highly stable end products of nucleosynthesis via fusion. In the Draco stars, these elements mimic the behavior of the Galactic halo field stars, except that [Ni/Fe] is somewhat lower than expected in the range $-2 < \text{Fe/H} < -1.5$ dex. In the Solar neighborhood and inner Galactic halo, Ni closely follows Fe so that [Ni/Fe] = 0.0 dex, the Solar ratio. The calculations of Woosley & Weaver (1995) suggested that the nucleosynthetic yield for Ni in SNII is metallicity dependent, increasing at higher metallicity. Ohkubo, Umeda, Nomoto & Yoshida (2006) recently showed that the same for SNIa, which may explain the somewhat low [Ni/Fe] in intermediate metallicity Draco giants, but their result is sensitive to the details of the model for the SNIa explosion. [Cr/Fe], [Zn/Fe] and perhaps [Co/Fe] are also lower in intermediate metallicity Draco giants than in Galactic halo field stars. Timmes, Woosley & Weaver (1995) found that the production of Zn in SNII depends on the neutron excess, hence depends on the initial metallicity, and thus should mimic the behavior of Na and Ni.

6.3. The Heavy Neutron Capture Elements

Neutron-capture reactions require both a supply of neutrons and the presence of seeds, presumed to be Fe-peak nuclei. It is widely believed that the *s*-process occurs in the interiors (but well outside the cores) of intermediate mass AGB stars, dredge up to the stellar surface follows. Processed material is then disseminated into the interstellar medium through slow stellar winds. Models of the *s*-process, including the effect of the initial stellar metallicity on the resulting products, are summarized by Busso, Gallino & Wasserburg (1999). Among the expected metallicity effects is a shift in the relative abundance of elements among the various “peaks” where the neutron-capture cross sections are small due to filled shells in the nucleus; the abundance of these specific elements

at the end of neutron-capture are relatively high compared to their close neighbors in the periodic table, thus producing “peaks”. Metallicity effects in r -process nucleosynthesis, whose site is not yet fully identified, are not as clearly understood at present. Suggested sites include SNII, hypernovae (Qian & Wasserburg 2008), accretion-induced collapse of a white dwarf into a neutron star in a binary system (Qian & Wasserburg 2003), and neutrino-driven winds from a nascent neutron star as reviewed by Qian & Wasserburg (2007).

We compare the predicted behavior of the heavy neutron capture elements with that observed in Draco to determine which neutron capture process dominates. In very metal-poor stars in the Galactic halo the chemical inventory of the heavy elements is from the r -process only. There was not enough time for the formation and evolution of any intermediate mass AGB stars, hence no s -process contribution to the ISM prior to the formation of these stars, although subsequent mass transfer across a binary system can alter the surface abundances in the former secondary star and produce large s -process enhancements (Cohen *et al.* 2006). Such cases can be identified by the accompanying large enhancements of C as well. The best diagnostic abundance ratios are Eu/Ba or Eu/La, where Eu is formed almost entirely by the r -process, while Ba and La are formed mostly via the s -process, at least in the Sun. (Ba, La, and Eu all belong to the same neutron-capture peak.) No La features have been detected in any Draco dSph star.

The upper panel of Fig. 18 shows [Ba/Eu] as a function of [Fe/H] for the four Draco giants from the present sample and the two from Shetrone, Côté & Sargent (2001) with detectable Eu II lines. The r -process ratio shown in the top panel is taken from Simmerer *et al* (2004); the solar ratio is a mixture of r and s -process material, while the pure s -process ratio for [Ba/Eu] lies higher than the top of the figure. They suggest that in the Galactic halo, signs of the s -process begin only at [Fe/H] > -2.6 dex, and a mean [Eu/La] ratio halfway between the pure r -process value and the Solar ratio is reached only at [Fe/H] ~ -1.4 dex. The survey of cool metal-poor local dwarfs of Mashonkina *et al* (2003) reaches the halfway point in [Eu/Ba] from pure r -process to the Solar mixture only at [Fe/H] ~ -0.5 dex. Thus the result from Fig. 18 is clear; the lowest [Fe/H] Draco stars have r -process dominated heavy neutron capture elements, but the s -process becomes important at a Fe-metallicity significantly lower than is characteristic of the Galactic halo.

Fig. 19 shows [Ba/Sr] as a function of [Fe/H] for our Draco sample, together with the s and r -process ratios from Simmerer *et al* (2004). Only the lowest metallicity star lies close to the pure r -process ratio. The others deviate from both the pure r and the pure s -process predictions in the sense that production of additional Sr by some other mechanism is required. Travaglio *et al* (2003) discuss the origin of Sr (and Y and Zr, all part of the same peak) in very metal-poor stars and suggest a new additional process of neutron capture, which they call the “lighter element primary process”, while Qian & Wasserburg (2008) suggest a different origin for additional Sr in very metal poor stars.

7. Chemical Evolution of the Draco dSph Galaxy

Recent models of chemical evolution for the disk, bulge, and halo of the Milky Way based on the precepts first established by Tinsley (1973) have been presented by several groups, including Timmes, Woosley & Weaver (1995), Kobayashi et al (2006), Prantzos (2008), and Matteucci (2008). These models assume an initial mass function, a star formation history, a mass infall history, outflow from Galactic winds, all as functions of time. They generally assume complete and uniform mixing of the gas over the total volume considered at all times with the exception of the sophisticated model of Marcolini et al (2006), which includes 3D hydrodynamic simulations of the ISM and the spatial variation of its properties. Such models combine networks of nuclear reactions from SNII with yields from Woosley & Weaver (1995) or Limongi & Chieffi (2003), from SNIa with yields generally from Iwamoto et al (1999); some also add in the contributions to the light elements from AGB winds and novae. They have been reasonably successful in reproducing the chemical evolution of the major components of the Milky Way overall, although failing in some (minor) details.

The evolution of the dSph galaxies differs in principle from that of the Milky Way or its halo. Their binding energies are lower, so the importance of gas loss may be higher, particularly material from SNII, for which the ejection velocity is significantly larger than the escape velocity so that a considerable fraction of the enriched gas may be lost from the galaxy; evidence for this happening today in small starburst galaxies is given by Martin, Kobulnicky & Heckman (2002). Marcolini et al (2006) suggest that if the dark matter halo is sufficiently massive, SNII ejecta may be pushed far out into the halo, away from the central region where stars form, but remain confined within the halo. Furthermore since Draco at present shows no evidence for the presence of gas, gas loss via a galactic wind or through interactions between the dSph satellite and its host, the Milky Way, must have been important in the past. These galaxies also show the consequences of lower star formation efficiency which leads to slower star formation overall without the large initial burst that dominates nucleosynthesis in most of the Milky Way components. In a system where the star formation rate is more constant with time, SNIa ejecta can become important contributors before $[\text{Fe}/\text{H}]$ just from SNII production builds up to high values near ~ -1 dex. It is this time delay between the SNII and SNIa contributions that dominates discussion of the chemical evolution of dSph galaxies. Note that once substantial gas loss begins, either through a wind or an interaction with the Milky Way, the star formation rate drops, the SNII rate drops precipitously, and thus the injection of α -elements into the ISM drops, while SNIa continue unaffected, so the Fe content of the ISM continues to rise. This then causes the drop in $[\alpha/\text{Fe}]$ ratios seen in Draco and in the other dSph galaxies.

7.1. Age – Metallicity Relation for Draco

A very useful diagnostic of the star formation rate as a function of time is the age – metallicity relationship. We construct this for Draco using the $[\text{Fe}/\text{H}]$ available from detailed abundance analyses for our sample and that of Shetrone, Côté & Sargent (2001). We take the remaining members of Draco listed by Winnick (2003) (the 6 known carbon stars in Draco are excluded), adopt her $[\text{Ca}/\text{H}]$ values, and convert them to $[\text{Fe}/\text{H}]$ values (see the appendix). Photometry is taken from Segall *et al.* (2007), who used the Megacam camera on the CFHT to image Draco in the g' , r' , and i' bands. We use the isochrones of Dotter *et al.* (2008) which are available for the SDSS colors. We adopt a relation between $[\alpha/\text{Fe}]$ and $[\text{Fe}/\text{H}]$ based on our results described above. Given $[\text{Fe}/\text{H}]$, $[\alpha/\text{Fe}]$, the colors, the distance of Draco and the adopted reddening, we can determine the age of each Draco giant.

We do this for each star with $M_V < -2.0$ mag. The isochrones along the RGB converge too much in the $(g' - i')$ color to attempt this for stars less luminous than this. The results are shown in Fig. 20. The median age for the luminous Draco giants is 7 Gyr. The uncertainty for each individual star is large as an uncertainty in $[\text{Fe}/\text{H}]$ of 0.3 dex, typical of that values derived from the Ca triplet (see the appendix), introduces an age error of ~ 5 Gyr. At a fixed $[\text{Fe}/\text{H}]$, the $(g' - i')$ color changes by ~ 0.015 mag/Gyr, thus requiring extremely accurate and well calibrated photometry. The random photometric measurement errors are not important compared to those arising from the uncertainty in $[\text{Fe}/\text{H}]$, but systematic errors of only a few hundredths of a mag due to problems in the calibration of the photometry could be serious. Also systematic errors in the transformation between the theoretical T_{eff}, L plane and the g', i' system adopted by the grid of isochrones, if present, could seriously bias the derived ages. HST studies of Draco (see, e.g. Orban et al 2006) reach the main sequence region, have much more accurate photometry for the giants, and perhaps more carefully calibrated isochrones, but they lack metallicity information for individual stars. They too have difficulty distinguishing small age differences at age ~ 10 Gyr.

Fig. 20 suggests a rough age-metallicity relation, with star formation extending over perhaps 5 Gyr beginning about 10 Gyr ago over which the mean $[\text{Fe}/\text{H}]$ decreased by a factor of ~ 5 , although the large uncertainties in age introduce considerable scatter. The apparently youngest stars could be AGB stars as they are bluer at a given luminosity than are first ascent RGB giants of the same luminosity.

7.2. Comparison With Other dSph Galaxies

In recent years there has been a tremendous improvement in abundance data for dSph satellites of the Milky Way due largely to technical improvements and the construction of 8 to 10 m telescopes. The situation prior to 2008 is reviewed by Geisler et al (2008). As of today, although there is a large ongoing project to study dwarf galaxies (the DART project, Tolstoy et al 2003) at the VLT, there are only two other dSph galaxies with published detailed abundance analyses from high dispersion

spectra for 14 or more stars to which we can compare our Draco results. These are the Sgr dSph (the main core, not the stream) (Monaco et al 2005; Sbordone et al 2007) and the Carina dSph galaxy, for which Koch et al (2008a) combines his analysis of 10 giants with 5 from the earlier study by Shetrone et al (2003).

We apply our toy model to the recent data for the Carina and the Sgr dSph galaxies. Fig. 21 for [Mg/Fe] and for [Ti/Fe] show the fits for these two galaxies, for Draco, and for the Milky Way thin and thick disk. This figure clearly demonstrates that to first order the form of the [X/Fe] vs [Fe/H] relations, at least for Mg and for Ti, are identical to within the uncertainties, but what is changing is the Fe-metallicity range, and the knee values [Fe/H](X,low) and [Fe/H](X,high) for these two elements.

This reinforces our previous comparison between the Draco abundance ratios and those of the stellar population of the Milky Way. While the initial low metallicity abundance ratios and the final high metallicity ones are identical to within the uncertainties for most elements, the key differences lie in the [Fe/H] values corresponding to the knee values, i.e. in the timescale at which the overall metallicity of the system increases. The Draco system has the slowest evolution of metallicity in its stars of the three, as well as the lowest mean [Fe/H] for its giants, Carina is intermediate, and Sgr is closest to the Milky Way. In addition, each dSph that has sufficient data for the heavy neutron capture elements appears to have contributions from the *s*-process that begin at somewhat lower [Fe/H] than that characteristic of the Milky Way.

Matteucci (2008) reviews models for the chemical evolution of the dSph galactic satellites of the Milky Way that reproduce the behavior of the α -elements. Presumably the agreement at the lowest [Fe/H] values probed here, where the Galactic halo stars overlap the Draco giants, is a consequence of a chemical inventory to which only SNII contributed. Lanfranchi & Matteucci (2004) present detailed models for the evolution of 6 of the dSph Milky Way satellites, including Draco, which try to reproduce not only the chemical evolution but also the total stellar mass and their individual star formation histories as derived from CMD studies. They vary the star formation efficiency and galactic wind rate to reproduce the dSph characteristics inferred from available data as of that time. Their model for Draco has the lowest star formation efficiency and the weakest galactic wind of these 6 dSph galaxies, with a single burst lasting 4 Gyr which occurred 6 Gyr ago. To within the uncertainties of the measurements and the models, they succeed in reproducing the almost flat [Ca/Fe] relation with [Fe/H] of Fig. 7 as well as the steep decline in [Mg/Fe] vs [Fe/H] of Fig. 5. Carigi, Hernandez & Gilmore (2002) present chemical evolution models for four dSph satellites of the Milky Way, but Draco is not included in their study. Marcolini et al (2006) presents the most sophisticated model, in that it includes a detailed study of the state of the ISM as a function of time within each of the *N* small volumes that together comprise the dSph galaxy. Star formation, SN explosions, etc are considered in a statistical manner within each volume. A dark matter halo is also included. Marcolini et al (2006) apply their model to predict [O/Fe] vs [Fe/H] for Draco, but do not consider any other elements. Our relationships for the other α -elements in Draco do not agree with their prediction for the behavior of [O/Fe].

As is the case for the Milky Way, conventional models similar to those reviewed by Matteucci (2008) can explain in general the abundance ratios seen in Draco. However, there are some problems when one looks in detail. For example, Lanfranchi, Matteucci & Cescutti (2008), who address the production of heavy elements beyond the Fe peak in dSph galaxies, overpredict by a factor of more than 10 the ratio Ba/Eu in the most metal-poor Draco stars. The cause of the (small) difference in behavior of [Mg and Si/Fe] vs [Ca, and Ti/Fe] at the lowest metallicities in Draco is not clear, particularly since Si is an explosive α -element while Mg is a hydrostatic one. How this behavior relates to the mass distribution of the SNII progenitors, given that one also needs to reproduce the odd-even effect at [Sc/Fe], is not obvious. Qualitatively similar differences in the behavior of the α -elements vs [Fe/H] are also seen in the Galactic bulge (Fulbright, McWilliam & Rich 2007), but again there are differences in detail as the separation between hydrostatic and explosive α -elements is cleaner there, i.e. [Si/Fe] behaves like [Ca/Fe] and [Ti/Fe] in the Galactic bulge.

Tsujimoto (2006) suggested that the low α -element signature in the dSph galaxies is a reflection of the contribution of massive stars with smaller rotation compared to solar neighborhood stars, instead of the conventional interpretation that this is a consequence of a low star formation rate. Current data are significantly better than what was available to him in 2006. They show that the values of [α /Fe] within the lowest Fe-metallicity Draco giants approach and often reach those of Galactic stars, providing additional support for the conventional interpretation that this results from a low star formation rate.

8. dSph Galaxies and the Formation of the Galactic Halo

Whether the Galactic halo could have been formed by accretion of satellite dwarf galaxies has become a question of great current interest; see e.g. Tolstoy et al (2003), Shetrone, Côté & Sargent (2001), among others. The cold dark matter cosmological model leads to hierarchical galaxy formation in which massive galaxies should be surrounded by numerous lower mass satellite halos; the stellar component of the Galactic halo presumably resulted at least in part from the dissolution of some of these satellites. But the small number of satellite galaxies known around our Galaxy was in conflict with this prediction, a situation often called the “missing satellites problem” (Klypin et al 1999). Recently, however, a substantial number of new satellite galaxies of the Milky Way have been discovered through searching the SDSS (see, e.g. Belokurov et al 2006). If one multiplies the new discoveries by the fraction of the sky not surveyed by the SDSS, taking into account the detection efficiency for finding a low luminosity satellite in the SDSS data as a function of distance and total luminosity of the satellite quantified by Koposov et al (2008), the “missing satellites” problem is well on the way to solution.

From the point of view of the chemical inventory of the Galactic halo versus that of the dSph satellites of the Galaxy, the initial answer to the question posed above given by Tolstoy et al (2003) was negative. Shetrone et al (2003) and his earlier work demonstrated that dSph galaxies clearly have a chemical inventory which reveals signatures of a lower star formation rate and these low

luminosity satellites appear to have a smaller fractional contribution of SNII in the total chemical inventory than in the Galactic halo itself. But since our work in Draco and that published for the Carina and for the Sgr dSph galaxies show that abundance ratios among stars in dSph galaxies tend to overlap those of Galactic halo giants at the lowest Fe-metallicities probed, it is possible that the satellites were accreted early in their development. Their properties as we observe them today would then not be relevant to this issue. Helmi et al (2006) claim, however, that early accretion is still ruled out because of the metallicity distribution function (MDF) they deduce for four dSph galaxies. Given the metallicity distribution function (MDF) they use for the Galactic halo, they claim that dSph galaxies would be expected to contain at least a few stars with $[\text{Fe}/\text{H}] < -3.0$ dex, while they have not to date detected any such stars in the four dSph galaxies in which they have extensive samples from the DART project.

However, we have contributed to refuting this argument by finding a giant in our Draco sample with $[\text{Fe}/\text{H}]$ from a high dispersion spectrum below -3 dex, the first such discovered. Kirby et al (2008) have found a few more such stars in the still lower luminosity satellite galaxies using moderate resolution spectra, as have (after this paper was submitted) Frebel *et al.* (2009)⁴. Furthermore, as is discussed in the appendix, the calibration adopted by the DART project to convert measurements of the strength of the Ca infrared triplet into Fe-metallicities is quite different at very low metallicities from that we use here, and with their adopted calibration, it is quite unlikely that they would have found any stars with $[\text{Fe}/\text{H}] < -3$ dex in their dSph samples, even if they did exist, an issue also discussed by Kirby et al (2008). In this context, it is interesting to note that the star in Sextans recently found to have $[\text{Fe}/\text{H}] -3.2$ dex by Aoki *et al.* (2009) has $[\text{Fe}/\text{H}](\text{CaT})$ from the DART team of -2.5 dex assigned in Helmi et al (2006), later revised to -2.7 dex by Battaglia *et al.* (2008) (see Fig. 6 of Aoki *et al.* 2009). In addition Schörck et al (2009) recently completed a determination of the halo MDF based based on the Hamburg/ESO Survey which shows that completeness corrections are important in the MDF derived from the HES.

Collectively this very recent work serves to help reestablish the scenario for the formation of the Galactic halo via accretion of satellite galaxies as viable. The material now in the inner halo of the Galaxy had to have been accreted early in the star formation history of the dSph galaxies, giving time for orbital mixing to eliminate traces of discrete stellar streams, while satellite galaxies accreted somewhat later could contribute to populating the outer halo, which shares many of the abundance anomalies of the dSph galaxies. Dissolved globular clusters had to disperse fairly quickly before the light element correlations among Na, Mg and Al developed, as these are not seen among halo field stars.

Finally we comment on the possible presence of a significant intermediate age population in the Draco dSph galaxy. Aaronson (1983) found several carbon stars in this dwarf galaxy.

⁴We suspect that the stars with $[\text{Fe}/\text{H}] < -3$ dex in the Bootes I dSph galaxy found by Norris et al (2008) may not actually be so Fe-poor, as their Fe-metallicities are from Ca lines assuming $[\text{Ca}/\text{Fe}] = +0.3$ dex, which is probably too large for stars in a dSph galaxy, so they require further verification.

Shetrone, Côté & Stetson (2001), in an effort to determine the highest metallicity reached in Draco, probed stars redward of the RGB, but found that they were either non-members or carbon stars, to establish an upper bound for this dSph of $[\text{Fe}/\text{H}] \sim -1.45$ dex (The highest metallicity star in our Draco sample has $[\text{Fe}/\text{H}]$ very close to this value.) Cioni & Habing (2005) recently surveyed Draco in the near-IR and found a few more carbon star candidates. The presence of these C stars has been used to argue for an intermediate age population in Draco, and for a difference between the stellar population of Draco vs that of the Galactic globular cluster system, where such C-rich stars are very rare.

Shetrone, Côté & Stetson (2001) point out that the carbon star specific frequency in Draco is 25 – 100 times higher than that of the Galactic globular clusters. However, study of the halo stellar population found in the Hamburg/ESO Survey by the OZ Project (Cohen *et al.* 2005) reveals the presence of numerous very carbon-rich stars at $[\text{Fe}/\text{H}] < -2.5$ dex. While the exact frequency of such stars is uncertain (see the discussion in Cohen *et al.* 2005), it is somewhere between 14 and 25%. This is a metallicity dependent phenomenon, with carbon rich stars becoming more frequent as $[\text{Fe}/\text{H}]$ decreases and the amount of C which must be dredged up to get to a situation where $\epsilon(\text{C}) > \epsilon(\text{O})$ consequently drops. It is for this reason that such C-stars are rare in the Galactic globular clusters, most of which have $[\text{Fe}/\text{H}]$ substantially larger than that of the mean of the Draco stellar population. In addition, the IR photometry of Cioni & Habing (2005) demonstrates that Draco’s C-stars are at luminosities near or well below the RGB tip; they are not the very luminous intermediate age C-stars seen in the LMC. We suggest instead that these are these just ordinary low metallicity C-stars similar to those in the Galactic halo, and in themselves do not imply the presence of an intermediate age population.

9. Summary

We present an abundance analysis based on high resolution spectra obtained with HIRES on the Keck I Telescope of 8 stars in the Draco dwarf spheroidal galaxy. The sample was selected to span the full range in metallicity inferred from Winnick (2003), who used moderate resolution spectroscopy for radial velocity members of this dSph galaxy found by earlier surveys, e.g. Armandroff, Olszewski & Pryor (1995) and others. Her CaT indices of the strength of the near-infrared Ca triplet correlate well with $[\text{Ca}/\text{H}]$ we derive from our detailed abundance analyses with differences from a linear fit of only $\sigma = 0.17$ dex; σ increases to 0.28 dex for linear fit of differences when considering how well the CaT indices predict $[\text{Fe}/\text{H}]$ as determined from our HIRES spectra. Winnick’s calibration differs significantly at low metallicities from that adopted by the DART project, an important issue in the search for extremely metal-poor stars in dSph galaxies discussed in the appendix.

We use classical plane-parallel (1D) LTE models from the Kurucz grid (Kurucz 1993) with a recent version of the stellar abundance code MOOG (Snedden 1973). $[\text{Fe}/\text{H}]$ for our sample stars ranges from -1.5 to -3.0 dex. Combining our sample with previously published work of

Shetrone, Bolte & Stetson (1998) and Shetrone, Côté & Sargent (2001) for 6 Draco giants, and using the analysis of better spectra for one of these 6 stars by Fulbright, Rich & Castro (2004), gives a total of 14 luminous Draco giants with detailed abundance analyses. We find that the abundance ratios $[\text{Na}/\text{Fe}]$, $[\text{Mg}/\text{Fe}]$, $[\text{Si}/\text{Fe}]$, $[\text{Cr}/\text{Fe}]$, $[\text{Ni}/\text{Fe}]$, $[\text{Zn}/\text{Fe}]$, and perhaps $[\text{Co}/\text{Fe}]$ for the Draco giants overlap those of Galactic halo giants at the lowest $[\text{Fe}/\text{H}]$ probed, but for the higher Fe-metallicity Draco stars are significantly lower than those of Milky Way halo giants. For the explosive α -elements Ca and Ti, the abundance ratios are low over the full metallicity range of the Draco dSph stars compared to Galactic halo giants, being closer, but still slightly low, at the lowest Fe-metallicities, traits shared by outer Galactic halo field stars. Nucleosynthetic yields sensitive to the neutron excess, hence to the initial metallicity of the SN progenitor (Timmes, Woosley & Weaver 1995), may be important in explaining the origin of differences between Draco giants and Galactic field stars for several of the abundance ratios studied here.

The heavy neutron capture elements Sr and Ba have abundance ratios with respect to Fe comparable to or lower than those of the lowest halo giants selected from much more extensive surveys. The *s*-process contribution to the production of heavy elements inferred from the ratio of Ba to Eu begins at significantly lower Fe-metallicity than in the Galactic halo.

The dominant uncertainty in these results is the possibility of differential non-LTE or 3D effects between the very cool luminous giants in our sample from the Draco dSph and the comparison halo field and globular cluster stars, which are somewhat hotter. With a 30-m telescope it will be possible to reach lower luminosity and somewhat hotter Draco giants where these issues will be less important.

We develop a toy model which we use to illuminate these trends, and to compare them with those of Galactic globular clusters and of giants from the Carina and Sgr dSph galaxies. The model has consists of a plateau in $[\text{X}/\text{Fe}]$ at low and at high $[\text{Fe}/\text{H}]$ connected by a straight line. There are four parameters determined directly from the data defining the plateau characteristics and two additional fit parameters which indicate the knee values. Since there is such good agreement in almost all cases for the abundance ratios at the lowest metallicity within a given sample and also the highest metallicities sampled, the fundamental contributors to their chemical inventory (SNII at the lowest metallicity and SNIa plus other sources at the highest $[\text{Fe}/\text{H}]$) behave in very similar ways in all these environments. We thus infer that the IMF for massive stars must be similar as well.

The key differences lie in the $[\text{Fe}/\text{H}]$ corresponding to the knee values, i.e. in the timescale at which the overall metallicity of the system increases. The Draco system has the slowest evolution of metallicity in its stars of the three, as well as the lowest mean $[\text{Fe}/\text{H}]$ for its giants, Sgr is intermediate, and the Carina dSph is closest to the Milky Way halo and the thick disk. This timescale is conventionally interpreted as a measure of the star formation efficiency combined with the rates of accretion of pristine materials and of gas lost via galactic winds. Our new data will enable much more sophisticated modelling of the chemical evolution of Draco with more detail than

our simple toy model can provide.

We note the presence of a Draco giant with $[\text{Fe}/\text{H}] < -3.0$ dex in our sample. This combined with other recent evidence for a small number of extremely low metallicity stars in other dSph galaxies reaffirms that the inner Galactic halo could have largely been formed by early accretion and dissolution of Galactic satellite galaxies and by globular clusters which dissolved prior to the imprinting of an AGB signature, while the outer halo could have formed largely from those dSph galaxies accreted later.

Shetrone, Côté & Sargent (2001) point out that the fraction of Carbon stars in Draco is 25 – 100 times higher than that of the Galactic globular clusters, and this has been viewed as an indication of the presence of an intermediate age stellar population. However, the 0Z Project (Cohen *et al.* 2005) has established that the frequency of carbon rich stars among very metal-poor Galactic halo field stars is surprisingly high. We thus suggest that the presence of carbon stars in the Draco dSph galaxy should not be regarded as a sign of an intermediate age stellar population there; this is instead a signpost of the low mean Fe-metallicity of the stellar component of this dSph galaxy.

The age–metallicity relationship established by combining photometry, spectroscopic metallicities, and isochrones suggests a fairly extended period of star formation in Draco with a duration of ~ 5 Gyr beginning about 10 Gyr ago over which the mean Fe-metallicity increased by a factor of ~ 5 . However, the uncertainty in the age of any individual star is high, there may be large systematic errors, and the apparently youngest stars could actually be older AGB stars.

The entire Keck/HIRES and LRIS user communities owes a huge debt to Jerry Nelson, Gerry Smith, Steve Vogt, and many other people who have worked to make the Keck Telescope and HIRES a reality and to operate and maintain the Keck Observatory. We are grateful to the W. M. Keck Foundation for the vision to fund the construction of the W. M. Keck Observatory. The authors wish to extend special thanks to those of Hawaiian ancestry on whose sacred mountain we are privileged to be guests. Without their generous hospitality, none of the observations presented herein would have been possible.

The authors are grateful to NSF grant AST-0507219 for partial support. This publication makes use of data from the Two Micron All-Sky Survey, which is a joint project of the University of Massachusetts and the Infrared Processing and Analysis Center, funded by the National Aeronautics and Space Administration and the National Science Foundation.

10. Appendix: The Validity of CaT and Stromgren Photometry for Draco

We have relied on the rough abundances determined from the infrared Ca triplet by Winnick (2003) to select our sample of stars in the Draco dSph galaxy. Here we examine the reliability of

her metallicities, relevant both for the present case and as an object lesson for the analysis of such data in other nearby galaxies. We only discuss calibration issues here; we assume that the actual measurements of the Ca triplet are correct, an issue which is complicated by how the wings of these strong lines are handled.

Winnick calibrates her results with observations of stars from Galactic globular clusters assuming $[\text{Ca}/\text{Fe}]$ is the same in Draco as it is in Galactic globular clusters. It should be noted that the corresponding relationship between $[\text{Fe}/\text{H}]$ and W' , the weighted sum of the equivalent widths of the three lines of the Ca triplet, corrected to the level of the horizontal branch, with the same assumption regarding $[\text{Ca}/\text{Fe}]$, adopted by the DART group (equations 7 and 13 of Battaglia *et al.* 2008) gives $[\text{Fe}/\text{H}]$ 0.44 dex higher than that of Winnick (2003) for $W' = 0$.

Fig. 22 shows a comparison for $[\text{Ca}/\text{H}]$ and for $[\text{Fe}/\text{H}]$ for the 8 stars in our sample in Draco with the values derived by Winnick (2003) from her infrared Ca triplet survey. For the entire metallicity range probed in Draco $[\text{Ca}/\text{Fe}]$ is essentially Solar, while in globular clusters it is $\sim +0.3$ dex. So we would expect Winnick's $[\text{Fe}/\text{H}]$ values to be low by this amount compared to our HIRES results, as is indeed seen in this figure. It is not clear why her $[\text{Ca}/\text{H}]$ values are somewhat higher than the HIRES results, but her calibration for that only includes one globular cluster below $[\text{Fe}/\text{H}] = -1.4$ dex, i.e. over the entire metallicity range of interest here.

Using our sample of 8 Draco luminous giants with HIRES detailed abundance analyses, we find a linear fit

$$[\text{Ca}/\text{H}] = -2.84(\pm 0.12) + 0.434(\pm 0.08) W'(Ca)$$

where $W'(Ca)$ is Winnick's measured line strength for the infrared Ca triplet, with a dispersion about the fit of 0.17 dex. This is in agreement to within the uncertainties with the relation given by Winnick. A linear fit for $[\text{Fe}/\text{H}]$ gives

$$[\text{Fe}/\text{H}] = -2.77(\pm 0.13) + 0.421(\pm 0.08) W'(Ca).$$

The constant here is 0.33 dex larger than that of Winnick, not surprising given that her relation is calibrated to globular clusters, which have $[\text{Ca}/\text{Fe}]$ typically $\sim +0.3$ dex. The dispersion about the linear fit, 0.28 dex, is somewhat larger than for $[\text{Ca}/\text{H}]$, again not surprising, since we are using a measurement of a Ca feature to determine a Fe abundance.

Four of the stars in our sample are included in the recent catalog of Draco members with metallicities derived from Stromgren photometry by Faria *et al.* (2007). The two most metal-poor of these (Draco 3157 and Draco 19219) have $[\text{Fe}/\text{H}](\text{Stromgren})$ 0.5 and 1.0 dex higher respectively than found from our detailed abundance analysis, presumably due to the low sensitivity of photometry at very low metallicity. The two higher metallicity stars in common show somewhat better agreement.

REFERENCES

- Aaronson, M., 1983, ApJ, 266, L11
- Adelman-McCarthy, J. K. et al, 2007, ApJS, 172, 634
- Andievsky, S. M., Spite, M., Korotin, S. A., Spite, F., Bonifacio, P., Cayrel, R., Hill, V. & Fracois, P., 2007 A&A, 464, 1081
- Aoki, W. *et al.*, 2009, A&A, in press (Astro-ph/0904.4307)
- Armandroff, T. E., Olszewski, E. W. & Pryor, C., 1995, AJ, 110, 2131
- Arnett, D., 1971, ApJ, 166, 153
- Asplund, M., Grevesse, N., Sauval, A. J., Allende Prieto, C. & Kisselman, D., 2004, A&A, 417, 751
- Asplund, M. 2005, ARA&A, 43, 481
- Asplund, M., Grevesse, N., Sauval, A. J., Allende Prieto, C. & Blomme, R., 2005, A&A, 431, 693
- Baade, W. & Swope, H., 1961, AJ, 66, 300
- Battagali, G., Irwin, M., Tolstoy, E., Hill, V., Helmi, A., Letarte, B. & Jablonka, P., 2008, MNRAS, 383, 183
- Belokurov, V. et al, 2006, ApJ, 654, 897
- Bonanos, A. Z., Stanke, K. Z., Szentgyorgyi, A. H., Sasselov, D. D. & Bakos, G. A., 2004, AJ, 127, 861
- Bonifacio, P. *et al.*, 2009, A&A, in press (Astro-ph/0903.4174)
- Busso, M., Gallino, R. & Wasserburg, G.J., 1999, ARA&A, 37, 239
- Carigi, L, Hernandez, X. & Gilmore, G., 2002, MNRAS, 334, 117
- Carigi, L. & Hernandez, X., 2008, MNRAS, in press
- Carpenter, J., 2001, AJ, 121, 2851
- Carollo, D. et al, 2007, Nature, 450, 1020
- Cayrel, R. et al, 2004, A&A, 416, 1117
- Cioni, M. R. L. & Habing, H., 2005, A&A, 442, 165
- Clayton, D., “Handbook of Isotopes in the Cosmos”, 2003, Cambridge U. Press
- Cohen, J. G., Christlieb, N., Beers, T. C., Gratton, R. G. & Carretta, E., 2002, AJ, 124, 470

- Cohen, J. G., Christlieb, N., McWilliam, A., Shectman, S., Thompson, I., Wasserburg, G. J., Ivans, I., Dehn, Karlsson, T. & Melendez, J., 2004, *ApJ*, 612, 1107
- Cohen, J. G. et al, 2005, *ApJ*, 633, L109
- Cohen, J. G. *et al.*, 2006, *AJ*, 132, 137
- Cohen, J. G., Christlieb, N., McWilliam, A., Shectman, S., Thompson, I., Melendez, J., Wisotzki, L. & Reimers, D., 2008, *ApJ*, 672, 320
- Cohen, J. G., Briley, M. M. & Stetson, P. B., 2005, *AJ*, 130, 1177
- Cohen, J. G. & Melendez, J., 2005, *AJ*, 129, 303
- Cohen et al 2007, *ApJ*, 659, L161
- Collet, R., Asplund, M. & Trampedach, R., 2007, *A&A*, 469, 687
- Cutri, R. M. *et al.*, 2003, “Explanatory Supplement to the 2MASS All-Sky Data Release, <http://www.ipac.caltech.edu/2mass/releases/allsky/doc/explsup.html>
- Dotter, A., Chaboyer, B., Jevremovic, D., Kotov, V., Baron, E. & Ferguson, J. W., 2008, *ApJS*, in press
- Faria, D., Feltzing, S., Lundstrom, I., Gilmore, G., Wahlgren, G. M., Ardeberg, A. & Linde, P., , 2007, *A&A*, 465,357
- Francois, P. et al, 2007, *A&A*, 476, 935
- Frebel, A., Simon, J. D., Geha, M. & Willman, B., 2009, *ApJ*, submitted (Astro-ph/0902.2395)
- Fuhrmann, K. Axer, M. & Gehren, T., 1995, *A&A*, 301, 492
- Fulbright, J. P., 2000, *AJ*, 120, 1841
- Fulbright, J., Rich, R. M. & Castro, S., 2004, *ApJ*, 612, 447
- Fulbright, J. P., McWilliam, A. & Rich, R. M., 2007, *ApJ*, 661, 1152
- Geisler, D., Smith, V V., Wallerstein, G., Gonzalez, G. & Charbonnel, C., 2005, *AJ*, 129, 1482
- Geisler, D., Wallerstein, G., Smith, V. V. & Casetti-Dinescu, D. I., 2008, *PASP*, 119, 859
- Gratton, R., Sneden, C. & Carretta, E., 2004, *ARA&A*, 42, 385
- Greggio, L., Renzini, A. & Daddi, E., 2008, *MNRAS*, 388, 829
- Grevesse, N. & Sauval, A. J., 1998, *Space Science Reviews*, 85, 161
- Grillmair, C. J. et al, 1998, *AJ*, 115, 144

- Helmi, A. et al, 2006, ApJ, 651, L121
- Hernandez,X., Gilmore, G. & Valls-Gabaud, D., 2000, MNRAS, 317, 831
- Houdashelt, M. L., Bell, R. A. & Sweigart, A. V., 2000, AJ, 119, 1448
- Huber, K. P. & Herzberg, G., 1979, *Constants of Diatomic Molecules*, (New York, Van Nostrand)
- Iwamoto, K., Brachwitz, F., Nomoto, K., Kishimoto, N., Umeda, H., Hix, W. R. & Thieleman, F. K., 1999, ApJS, 125, 439
- Johnson J. 2002, ApJS, 139, 219
- Kirby, E. N., Simon, J. D., Geha, M., Guhathakurta, P. & Frebel, A., 2008, ApJ, 685, L43
- Klypin, A., Kravtsov, A. V., Valenzuela, O. & Prada, F., 1999, ApJ, 522, 82
- Kobayashi, C., Umeda, H., Nomoto, K., Tominaga, N. & Ohkubo, T., 2003, ApJ, 653, 1145
- Koch, A., Grebel, E. K., Gilmore, G. F., Wyse, R. F. G., Kleyana, J. T., Harbeck, D. R., Wilkinson, M. I. & Evans, N. W., AJ, 135, 1580
- Koch, A., McWilliam, A., Grebel, E. K., Zucker, D. B. & Belokurov, V., 2008, ApJ, in press
- Koposov, S. et al, 2008, ApJ, 686, 279
- Kurucz, R. L., 1993, ATLAS9 Stellar Atmosphere Programs and 2 km/s Grid, (Kurucz CD-ROM No. 13)
- Lanfranchi, G. A. & Matteucci, F., 2004, MNRAS, 351, 1338
- Lanfranchi, G. A., Matteucci, F. & Cescutti, G., 2008, A&A, 481, 635
- Layden, A. C. & Sarajedini, A., 2000, AJ, 119, 1760
- Lehnert, M. D., Bell, R. A., Hesser, J. E. & Oke, J. B., 1992, ApJ, 395, 466
- Limongi, M. & Chieffi, A., 2003, ApJ, 592, 404
- Marcolini, A., D’Ercole, A., Brighenti, F. & Recchi, S., 2006, MNRAS, 371, 643
- Marin-Franch, A. et al 2009, ApJ, 694, 1498
- Martin, C. L., Kobulnicky, H. A. & Heckman, T. M., 2002, ApJ, 574, 663
- Mashonkina, L. & Gehren, T., 2001, A&A, 376, 232
- Mashonkina, L., Gehren, T., Travaglio, C. & Borkova, T., 2003, A&A, 397, 275

- Matteucci, F., 2008, in “Chemical Evolution of the Milky Way and Its Satellites”, in Saas-Fe Advance Course, “The Origin of the Galaxy and the Local Group”, ed. E. Grebel & B. Moore
- McWilliam, A., Preston, G. W., Sneden, C. & Shectman, S., 1995, *AJ*, 109, 2736
- McWilliam, A. & Smecker-Hane, T. A., 2005, in “Cosmic Abundances as Records of Stellar Evolution and Nucleosynthesis”, ed. F.N.Bash & T.G.Barnes
- Melendez, J., Shchukina, N. G., Vasiljeva, I. E. & Ramirez, I., 2006, *ApJ*, 641, 1082
- Mishenina, T. V., Kovtyukh, V. V., Soubiran, C., Travaglio, C. & Busso, M., 2002, *A&A*, 396, 189
- Monaco, L. et al, 2005, *A&A*, 441, 141
- Munoz, R. R. et al, 2005, *ApJ*, 631, L137
- Nissen, P. E. & Schuster, W. J., 1997, *A&A*, 326, 751
- Nissen, P. E. et al 2000, *A&A*, 353, 722
- Nissen, P. E., Primas, F., Asplund, M. & Lambert, D. L., 2002, *A&A*, 390, 325
- Nissen, P. E., Ackerman, C., Asplund, M., Fabian, D., Kerber, F., Kaufl, H. U. & Pettini, M., 2008, *A&A*, 649, 319
- Norris, J. E., Gilmore G., Wyse, R. F. G., Wilkinson, M. I., Belokurov, V., Wyn Evans, N. & Zucker, D. B., 2008, *ApJ*, 689, L113
- Ohkubo, T., Umeda, H., Nomoto, K. & Yoshida, T., 2006, *AIPC*, 847, 458
- Orban, C., Gnedin, O. Y., Weisz, D. R., Skillman, E. D., Dolphin, A. E. & Holtzman, J. A., 2008, *AJ*, 686, 1030
- Piatek, S., Pryor, C., Armandroff, T. E. & Olszewski, E. W., 2001, *AJ*, 121, 841
- Prantzos, N., 2008, in “Stellar Nucleosynthesis: 50 Years After B2FH”, 2008, ed. C. Charbonnel & J. P. Zahn, EAS Publications Series
- Prochaska, J. X., Naumov, S. O., Carney, B. W., McWilliam, A. & Wolfe, A. M., 2000, *AJ*, 120, 2513
- Qian, Y. Z. & Wasserburg, G J., 2003. *ApJ*, 588, 1099
- Qian, Y. Z. & Wasserburg, G J., 2007, *Physics Reports, Review Section of Physics Letters*, 442, 237
- Qian, Y. Z. & Wasserburg, G J., 2008, *ApJ*, 687, 272
- Ramirez, I., Allende Prieto, C. & Lambert, D. L., 2007, *A&A*, 465, 271

- Reddy, B. E., Tomkin, J., Lambert, D. L., & Allende Prieto, C., 2003, MNRAS, 340, 304
- Reddy, B. E., Lambert, D. L. & Allende Prieto, C., 2006, MNRAS, 367, 1329
- Roederer, I. U., 2008, AJ, 137, 272
- Sbordone, L., Bonifacio, P., Marconi, G., Buonanno, R. & Zaggia, S., 2005, A&A, 437, 905
- Sbordone, L., Bonifacio, P., Buonanno, R., Marconi, G., Monaco, L. & Zaggia, S., 2007, A&A, 465, 815
- Schlegel, D., Finkbeiner, D. P. & Davis, M., 1998, ApJ, 500, 525
- Schörck, T. et al, 2009, A&A, submitted (Astro-ph/0809.1172)
- Schuler, S. C., Hatzes, A. P., King, J. R., Kurster, M. & The, L.-S., 2005, ApJ, 636, 432
- Segall, M., Ibata, R. A., Irwin, M. J., Martin, M. F. & Chapman, S., 2007, MNRAS, 375, 831
- Shetrone, M. D., Bolte, M. & Stetson, P. B., 1998, AJ, 115, 1888
- Shetrone, M. D., Côté, P. & Sargent, W. L. W., 2001, ApJ, 548, 592
- Shetrone, M. D., Côté, P. & Stetson, P. B., 2001, PASP, 113, 1122
- Shetrone, M. D. et al, 2003, AJ, 125, 684
- Shetrone, M. D., Siegel, M H., Cook, D. O. & Bosler, T., 2009, AJ, in press
- Short, C. I. & Hauschildt, P. H., 2006, ApJ, 641, 494
- Shortridge K. 1993, in *Astronomical Data Analysis Software and Systems II*, A.S.P. Conf. Ser., Vol 52, eds. R.J. Hannisch, R.J.V. Brissenden, & J. Barnes, 219
- Siegel, M. H. et al, 2007, ApJ, 667, L57
- Simmerer, J., Sneden, C., Cowan, J. J., Collier, J., Woolf, V. M. & Lawler, J. E., 2004, ApJ, 617, 1091
- Skrutskie, M. F., Schneider, S.E., Stiening, R., Strom, S.E., Weinberg, M.D., Beichman, C., Chester, T. *et al.*, 1997, in *The Impact of Large Scale Near-IR Sky Surveys*, ed. F.Garzon *et al.* (Dordrecht: Kluwer), p. 187
- Smith, G. & Raggett, D. St. J., 1981, J.Phys.B, 14, 4015
- Smith, J. A. *et al.*, 2002, AJ, 123, 2121
- Sneden, C., 1973, Ph.D. thesis, Univ. of Texas
- Spite, M. et al, 2005, A&A, 430, 655

- Stephens, A., 1999, *AJ*, 117, 1771
- Takeda, Y., Zhao, G., Chen, Y. Q., Qui, H. M. & Takada-Hidei, M., 2002, *PASJ*, 54, 275
- Takeda, Zhao, Takeda-Hidai et al 2003, *Chinese Jrl Astron & Astrophys*, 3, 316
- Timmes, F. X., Woosley, S. E. & Weaver, T. A., 1995, *ApJS*, 98, 617
- Tinsley, B. M., 1973, *ApJ*, 186, 35
- Tolstoy, E. et al, 2003, *AJ*, 125, 707
- Travaglio, C., Gallino, R., Arnone, E., Cowan, J., Jordan, F. & Sneden, C., 2004, *ApJ*, 601, 864
- Tsujimoto, T., 2006, *A&A*, 447, 81
- Vogt, S. E. *et al.* 1994, *SPIE*, 2198, 362
- Wallace, L., Hinkle, K. & Livingston, W. C., 1998, “An Atlas of the Spectrum of the Solar Photosphere from 13,500 to 28,000 cm^{-1} ”, N.S.O. Technical Report 98-001, ftp:
nsokp.nso.edu/pub/atlas/visatl.
- Walker, M. G., Mateo, M., Olszewski, E. W., Gnedin, O. Y., Wang, W., Sen, B. & Woodroffe, M., 2007., *ApJ*, 667, L53
- Winnick, R. A., 2003, PhD thesis, Yale University, “Metallicity Distributions in the Draco, Ursa Minor and Sculptor Dwarf Spheroidal Galaxies”
- Woosley, S. E. & Weaver, T. A., 1995, *ApJ*, 101, 181
- Yi, S., Demarque, P., Kim, Y.-C. , Lee, Y.-W., Ree, C. Lejeune, Th. & Barnes, S., 2001, *ApJS*, 136, 417
- Yong, D., Lambert, D. L., Allende Prieto, C. & Paulson, D. B., 2003, *ApJ*. 500. 1357
- York, D. G., Adelman, J., Anderson Jr., J. E. *et al.*, 2000, *AJ*, 120, 1579
- Young, L. M., 1999, *AJ*, 117, 1758
- Zinn, R. J., 1988, *ApJ*, 225, 790

Table 1. The Sample of Stars in the Draco dSph

| ID ^a | Coords. ^a (J2000) | | | V (mag, from SDSS) | I (mag, from SDSS) | Date Obs. | Exp. Time (sec) |
|-----------------|---------------------------------|--------------|--|-----------------------|-----------------------|----------------------|--------------------|
| 361 | 17 20 34.19 | +57 53 32.14 | | 17.53 | 16.15 | 09/2006 | 7200 |
| 3053 | 17 19 35.46 | +57 58 46.78 | | 17.48 | 16.09 | 09/2006 | 7200 |
| 3150 | 17 19 36.37 | +57 51 25.1 | | 17.38 | 15.98 | 06/2005 | 7200 |
| 3157 | 17 19 41.85 | +57 52 19.47 | | 16.91 | 15.56 | 09/2006 ^b | 7200 |
| 19219 | 17 21 43.69 | +57 57 12.49 | | 17.32 | 16.01 | 09/2006 | 7200 |
| 19629 | 17 21 58.23 | +57 56 04.31 | | 17.33 | 15.97 | 09/2006 | 7200 |
| 21456 | 17 18 10.43 | +57 52 09.2 | | 17.08 | 15.63 | 06/2005 | 7200 |
| XI-2 | 17 19 17.53 | +58 01 07.1 | | 16.96 | 15.38 | 06/2005 | 7200 |

^aThe star names and coordinates are from Winnick (2003). Many of the names were originally assigned by Baade & Swope (1961).

^bThe 2 hour exposure from 06/2005 is not as good and was not used.

Table 2. Stellar Parameters for the Draco Giants

| ID | T_{eff} (K) (phot) | $\log(g)$ (dex) (phot) | T_{eff} (K) (spec) | $\log(g)$ (dex) (spec) | v_t (km s ⁻¹) | v_r (km s ⁻¹) |
|-------|--------------------------------|---------------------------|--------------------------------|---------------------------|--------------------------------|--------------------------------|
| 361 | 4375 | 0.75 | 4420 | 0.75 | 2.0 | -288.4 |
| 3053 | 4394 | 1.0 | 4350 | 1.0 | 2.1 | -279.2 |
| 3150 | 4430 | 0.6 | 4380 | 0.6 | 2.3 | -279.8 |
| 3157 | 4490 | 0.7 | 4510 | 0.7 | 2.4 | -295.7 |
| 19219 | 4490 | 0.75 | 4500 | 0.75 | 2.9 | -295.7 |
| 19629 | 4445 | 0.8 | 4460 | 0.8 | 2.9 | -303.2 |
| 21456 | 4263 | 0.7 | 4430 | 0.7 | 2.3 | -305.6 |
| XI-2 | 4184 | 0.5 | 4350 | 0.6 | 2.4 | -316.0 |

Table 3. Equivalent Widths for Eight Stars in the Draco dSph

| λ Å | Ion | χ (eV) | $\log(gf)$ (dex) | 361 (mÅ) | 3053 (mÅ) | 3150 (mÅ) | 3157 (mÅ) | 19219 (mÅ) | 19629 (mÅ) | 21456 (mÅ) | XI–2 (mÅ) |
|----------------|-------|----------------|---------------------|-------------|--------------|--------------|--------------|---------------|---------------|---------------|------------------|
| 6300.30 | [O I] | 0.00 | −9.780 | 17.5 | 36.0 | ... | 10.5 | ... | ... | 14.7 | 9.0 ^a |
| 6363.78 | [O I] | 0.02 | −10.300 | 11.0 | 14.0 | ... | ... | ... | ... | ... | ... |
| 5682.63 | Na I | 2.10 | −0.700 | ... | 12.8 | ... | 10.0 | ... | ... | ... | ... |
| 5688.19 | Na I | 2.10 | −0.420 | 25.4 | 21.3 | ... | 10.0 | ... | ... | ... | ... |
| 5889.95 | Na I | 0.00 | 0.110 | 299.6 | 262.7 | 257.1 | 220.6 | 173.3 | 207.4 | 217.4 | 212.8 |
| 5895.92 | Na I | 0.00 | −0.190 | 277.5 | 225.3 | 235.7 | 197.4 | 135.6 | 174.5 | ... | ... |
| 4703.00 | Mg I | 4.34 | −0.670 | 111.6 | 110.5 | 108.1 | 64.3 | 42.3 | 50.7 | 90.5 | 89.0 |
| 5172.70 | Mg I | 2.71 | −0.380 | 353.6 | 326.6 | 294.5 | 234.6 | 192.7 | 222.4 | 246.9 | 243.0 |
| 5183.62 | Mg I | 2.72 | −0.160 | 429.9 | 380.3 | 384.4 | 263.6 | 214.9 | 243.2 | 285.4 | 278.9 |
| 5528.40 | Mg I | 4.34 | −0.480 | 151.4 | 149.5 | 123.1 | 82.1 | 62.1 | 82.8 | 93.8 | 83.3 |
| 5711.09 | Mg I | 4.34 | −1.670 | 64.9 | 46.7 | 52.8 | ... | ... | 14.4 | ... | 14.5 |
| 3961.52 | Al I | 0.00 | −0.340 | ... | ... | ... | 130.0 | ... | ... | ... | ... |
| 4102.94 | Si I | 1.91 | −3.140 | 106.0 | 110.0 | ... | 90.0 | 65.9 | 101.1 | ... | ... |
| 5948.54 | Si I | 5.08 | −1.230 | ... | 29.5 | 19.6 | ... | ... | ... | 19.8 | ... |
| 7405.77 | Si I | 5.61 | −0.820 | 26.8 | 21.6 | 21.3 | 7.2 | ... | ... | ... | ... |
| 7415.95 | Si I | 5.61 | −0.730 | 21.8 | 21.8 | 14.3 | ... | ... | ... | ... | ... |
| 7423.50 | Si I | 5.62 | −0.580 | 33.2 | 28.7 | 25.9 | 11.9 | ... | ... | ... | 11.7 |
| 7698.97 | K I | 0.00 | −0.168 | ... | 132.3 | ... | 52.2 | 44.8 | 55.1 | 92.5 | ... |
| 4226.74 | Ca I | 0.00 | 0.240 | ... | ... | ... | ... | 172.3 | ... | ... | ... |
| 4318.66 | Ca I | 1.90 | −0.210 | 122.5 | ... | ... | ... | ... | ... | ... | ... |
| 4425.44 | Ca I | 1.88 | −0.360 | 103.5 | ... | 95.8 | 62.7 | ... | 59.2 | ... | ... |
| 4435.69 | Ca I | 1.89 | −0.520 | ... | ... | ... | 76.2 | ... | 42.6 | ... | ... |
| 4454.79 | Ca I | 1.90 | 0.260 | ... | ... | ... | 99.6 | 55.9 | 92.9 | ... | ... |
| 4578.56 | Ca I | 2.52 | −0.558 | ... | 38.3 | ... | ... | ... | ... | ... | ... |
| 5512.99 | Ca I | 2.93 | −0.300 | 37.3 | 36.7 | 33.9 | ... | ... | ... | ... | ... |
| 5581.96 | Ca I | 2.52 | −0.710 | 78.3 | 50.3 | 42.6 | 23.2 | ... | ... | 22.2 | 37.5 |
| 5588.75 | Ca I | 2.52 | 0.210 | 115.3 | 106.4 | 105.3 | 64.3 | 27.7 | 59.2 | 61.7 | 85.2 |
| 5590.11 | Ca I | 2.52 | −0.710 | 62.8 | 53.1 | 45.2 | 21.1 | ... | ... | 18.2 | 30.6 |
| 5594.46 | Ca I | 2.52 | −0.050 | 94.7 | ... | 88.8 | 48.3 | ... | 43.1 | ... | ... |
| 5601.28 | Ca I | 2.52 | −0.690 | 74.8 | 63.6 | 52.0 | 20.4 | ... | 19.2 | 26.3 | 41.5 |
| 5857.45 | Ca I | 2.93 | 0.230 | 91.6 | 77.9 | 84.3 | 40.0 | ... | 25.4 | 32.5 | 46.4 |
| 6161.30 | Ca I | 2.52 | −1.030 | 34.8 | 27.7 | 31.1 | ... | ... | ... | ... | ... |
| 6162.17 | Ca I | 1.90 | −0.090 | ... | 162.7 | 154.1 | 109.8 | 52.5 | 103.8 | 117.5 | 134.1 |
| 6166.44 | Ca I | 2.52 | −0.900 | 42.4 | 35.9 | 24.1 | ... | ... | ... | ... | 13.2 |
| 6169.04 | Ca I | 2.52 | −0.540 | 63.1 | 55.4 | 42.4 | 19.5 | ... | 11.4 | ... | 20.5 |
| 6169.56 | Ca I | 2.52 | −0.270 | 85.5 | 74.3 | 62.8 | 31.0 | ... | 16.8 | 27.6 | 35.0 |
| 6471.66 | Ca I | 2.52 | −0.590 | 66.2 | 60.1 | 52.4 | 17.0 | ... | 14.7 | 24.0 | 23.1 |
| 6493.78 | Ca I | 2.52 | 0.140 | 109.3 | 97.4 | 93.4 | 49.7 | 18.0 | 38.9 | 55.5 | 72.4 |
| 6499.65 | Ca I | 2.54 | −0.590 | 62.5 | 58.9 | 40.8 | 24.7 | ... | ... | ... | 32.3 |
| 6717.68 | Ca I | 2.71 | −0.610 | 72.2 | 70.8 | 45.2 | 22.1 | ... | ... | 21.3 | 35.8 |
| 7148.15 | Ca I | 2.71 | 0.218 | 124.3 | 110.9 | 103.2 | 62.9 | 19.7 | 51.5 | 56.0 | 78.1 |
| 4246.82 | Sc II | 0.32 | 0.242 | ... | ... | ... | 166.0 | 127.3 | 150.5 | ... | ... |
| 4670.41 | Sc II | 1.36 | −0.580 | 102.4 | 70.0 | ... | 55.3 | 28.9 | 32.6 | 64.3 | 61.2 |
| 5526.79 | Sc II | 1.77 | 0.130 | 94.3 | 80.0 | 93.2 | 56.5 | 40.3 | 52.2 | 81.3 | 55.9 |
| 5657.90 | Sc II | 1.51 | −0.500 | 91.1 | 80.5 | 92.2 | 48.0 | 19.9 | 39.4 | 62.0 | 42.2 |

Table 3—Continued

| λ Å | Ion | χ (eV) | $\log(gf)$ (dex) | 361 (mÅ) | 3053 (mÅ) | 3150 (mÅ) | 3157 (mÅ) | 19219 (mÅ) | 19629 (mÅ) | 21456 (mÅ) | XI–2 (mÅ) |
|----------------|-------|----------------|---------------------|-------------|--------------|--------------|--------------|---------------|---------------|---------------|--------------|
| 5667.15 | Sc II | 1.50 | –1.240 | 35.5 | 33.1 | 33.3 | 20.5 | ... | ... | ... | 12.2 |
| 5669.04 | Sc II | 1.50 | –1.120 | 54.2 | 46.4 | 57.7 | 17.8 | ... | ... | 35.4 | ... |
| 5684.20 | Sc II | 1.51 | –1.080 | 42.6 | 49.0 | 38.9 | 31.5 | ... | 16.2 | 26.5 | 31.2 |
| 6245.64 | Sc II | 1.51 | –1.130 | 56.1 | 50.8 | 62.0 | 20.5 | ... | ... | ... | 21.9 |
| 6604.60 | Sc II | 1.36 | –1.480 | 45.2 | 38.7 | 39.3 | 12.2 | ... | ... | 17.6 | 18.9 |
| 4512.74 | Ti I | 0.84 | –0.480 | 70.8 | 79.8 | 56.0 | 21.6 | ... | ... | ... | 46.1 |
| 4518.03 | Ti I | 0.83 | –0.230 | ... | 85.3 | 77.8 | 34.2 | ... | 25.5 | ... | ... |
| 4533.25 | Ti I | 0.85 | 0.480 | 121.5 | 134.2 | 128.9 | 76.3 | 35.3 | 58.3 | ... | 94.2 |
| 4534.78 | Ti I | 0.84 | 0.280 | 126.4 | 101.9 | 108.9 | 60.5 | ... | 57.0 | ... | 80.3 |
| 4548.77 | Ti I | 0.83 | –0.350 | 86.4 | 84.0 | 77.6 | 37.6 | ... | ... | ... | 55.0 |
| 4555.49 | Ti I | 0.85 | –0.490 | 97.4 | 78.9 | ... | 32.2 | ... | ... | ... | 34.2 |
| 4681.92 | Ti I | 0.05 | –1.070 | 127.0 | 126.2 | 95.5 | 60.6 | ... | 41.6 | 69.4 | 101.2 |
| 4981.74 | Ti I | 0.85 | 0.500 | 132.2 | 128.1 | 132.4 | 95.2 | 38.7 | 78.3 | 92.2 | 126.1 |
| 4999.51 | Ti I | 0.83 | 0.250 | 140.8 | 126.9 | 135.6 | 68.8 | 38.2 | 55.1 | 89.0 | 106.1 |
| 5022.87 | Ti I | 0.83 | –0.430 | 103.8 | 87.0 | 72.9 | 38.2 | ... | 22.7 | 41.4 | 53.5 |
| 5039.96 | Ti I | 0.02 | –1.130 | 120.7 | 112.4 | 109.5 | 61.7 | 14.2 | 35.0 | 81.9 | 98.2 |
| 5173.75 | Ti I | 0.00 | –1.120 | 137.5 | 129.3 | 112.7 | 66.4 | 18.4 | 57.4 | 100.5 | 106.1 |
| 5210.39 | Ti I | 0.05 | –0.880 | 137.2 | 131.0 | 127.7 | 74.1 | 28.1 | 55.4 | 93.5 | 121.9 |
| 5426.26 | Ti I | 0.02 | –3.010 | 15.1 | ... | ... | ... | ... | ... | ... | ... |
| 5490.15 | Ti I | 1.46 | –0.933 | 28.6 | 17.5 | ... | ... | ... | ... | ... | ... |
| 5644.14 | Ti I | 2.27 | 0.050 | ... | 15.0 | ... | ... | ... | ... | ... | ... |
| 5866.45 | Ti I | 1.07 | –0.840 | 61.0 | 52.7 | 56.9 | ... | ... | ... | ... | 29.0 |
| 5922.11 | Ti I | 1.05 | –1.470 | 25.4 | 27.1 | 18.4 | ... | ... | ... | ... | ... |
| 5941.75 | Ti I | 1.05 | –1.520 | 20.3 | 19.1 | 13.6 | ... | ... | ... | ... | ... |
| 5953.16 | Ti I | 1.89 | –0.329 | 26.9 | ... | 11.4 | ... | ... | ... | ... | ... |
| 5965.83 | Ti I | 1.88 | –0.409 | 25.5 | 18.1 | ... | ... | ... | ... | ... | ... |
| 6126.22 | Ti I | 1.07 | –1.420 | 30.9 | 18.6 | ... | ... | ... | ... | ... | ... |
| 6258.10 | Ti I | 1.44 | –0.355 | 54.2 | 41.5 | 37.1 | ... | ... | ... | 14.5 | 14.6 |
| 6258.71 | Ti I | 1.46 | –0.240 | 68.6 | 61.2 | 42.4 | ... | ... | ... | 14.7 | 19.8 |
| 6261.10 | Ti I | 1.43 | –0.479 | 48.2 | 47.2 | 43.7 | ... | ... | ... | 12.3 | 21.4 |
| 6743.12 | Ti I | 0.90 | –1.630 | 32.1 | 20.2 | 16.5 | ... | ... | ... | ... | ... |
| 7344.69 | Ti I | 1.46 | –0.992 | 22.7 | 14.6 | ... | ... | ... | ... | ... | ... |
| 4300.05 | Ti II | 1.18 | –0.490 | ... | ... | ... | ... | ... | 139.3 | ... | ... |
| 4395.03 | Ti II | 1.08 | –0.510 | ... | ... | ... | ... | 123.8 | 151.2 | ... | ... |
| 4399.77 | Ti II | 1.24 | –1.290 | 147.2 | ... | 124.9 | ... | 86.2 | 101.7 | 113.5 | 118.3 |
| 4417.72 | Ti II | 1.16 | –1.160 | 153.0 | ... | 140.7 | 129.3 | 81.7 | 106.6 | 123.0 | 139.9 |
| 4443.81 | Ti II | 1.08 | –0.700 | ... | ... | ... | 159.9 | 116.7 | 129.1 | ... | 164.4 |
| 4468.51 | Ti II | 1.13 | –0.600 | ... | ... | ... | 164.9 | 127.7 | 122.4 | ... | 173.0 |
| 4501.28 | Ti II | 1.12 | –0.760 | ... | 166.5 | 160.0 | 154.0 | 110.9 | 147.6 | ... | 172.6 |
| 4533.97 | Ti II | 1.24 | –0.640 | ... | ... | ... | ... | 123.0 | 147.5 | 143.6 | ... |
| 4563.77 | Ti II | 1.22 | –0.820 | 160.8 | 151.1 | 153.4 | 140.3 | 102.1 | 118.6 | 139.2 | 150.7 |
| 4571.98 | Ti II | 1.57 | –0.340 | ... | ... | 157.1 | 159.2 | 99.3 | 135.9 | ... | ... |
| 4583.41 | Ti II | 1.16 | –2.870 | ... | 69.0 | ... | 43.4 | ... | ... | ... | 42.8 |
| 4589.95 | Ti II | 1.24 | –1.650 | 123.4 | 130.2 | 103.8 | 106.2 | 53.8 | 87.1 | 101.7 | 120.8 |
| 4657.20 | Ti II | 1.24 | –2.320 | ... | 78.0 | 63.1 | 76.0 | ... | 25.8 | 60.8 | ... |

Table 3—Continued

| λ Å | Ion | χ (eV) | $\log(gf)$ (dex) | 361 (mÅ) | 3053 (mÅ) | 3150 (mÅ) | 3157 (mÅ) | 19219 (mÅ) | 19629 (mÅ) | 21456 (mÅ) | XI–2 (mÅ) |
|----------------|-------|----------------|---------------------|-------------|--------------|--------------|--------------|---------------|---------------|---------------|--------------|
| 4708.67 | Ti II | 1.24 | –2.370 | ... | ... | 75.1 | 63.7 | 19.9 | 35.9 | 49.4 | ... |
| 4762.78 | Ti II | 1.08 | –2.710 | ... | ... | ... | 45.3 | ... | 30.9 | ... | 57.3 |
| 4798.54 | Ti II | 1.08 | –2.670 | ... | ... | ... | 68.9 | ... | 51.4 | ... | 82.6 |
| 4865.62 | Ti II | 1.12 | –2.810 | 76.6 | 55.5 | 68.9 | 47.3 | 16.7 | 30.3 | 41.3 | 56.9 |
| 4911.20 | Ti II | 3.12 | –0.340 | 53.2 | ... | 39.0 | 20.4 | ... | ... | ... | ... |
| 5185.91 | Ti II | 1.89 | –1.460 | 86.5 | 89.0 | 82.4 | 63.9 | 21.4 | 43.9 | 56.2 | 72.5 |
| 5670.85 | V I | 1.08 | –0.425 | 32.0 | ... | ... | ... | ... | ... | ... | ... |
| 5703.57 | V I | 1.05 | –0.212 | 22.3 | ... | ... | ... | ... | ... | ... | ... |
| 6090.22 | V I | 1.08 | –0.062 | 35.7 | 25.9 | 30.1 | ... | ... | ... | ... | ... |
| 6199.20 | V I | 0.29 | –1.280 | ... | 19.9 | ... | ... | ... | ... | ... | ... |
| 6243.10 | V I | 0.30 | –0.978 | 42.8 | 29.1 | 29.0 | ... | ... | ... | ... | ... |
| 6251.82 | V I | 0.29 | –1.340 | 24.9 | ... | ... | ... | ... | ... | ... | ... |
| 4254.33 | Cr I | 0.00 | –0.110 | ... | ... | ... | ... | 113.1 | 128.2 | ... | ... |
| 4274.79 | Cr I | 0.00 | –0.230 | ... | ... | ... | ... | ... | 143.2 | ... | ... |
| 4545.96 | Cr I | 0.94 | –1.380 | ... | 89.5 | 83.1 | 43.9 | ... | ... | ... | 59.7 |
| 4600.76 | Cr I | 1.00 | –1.280 | ... | 85.0 | 64.1 | 50.2 | ... | ... | 43.8 | 67.7 |
| 4613.37 | Cr I | 0.96 | –1.670 | ... | ... | ... | 35.6 | ... | ... | ... | ... |
| 4616.13 | Cr I | 0.98 | –1.210 | 110.4 | 102.9 | 82.5 | 45.8 | ... | 30.7 | 50.5 | 62.2 |
| 4626.18 | Cr I | 0.97 | –1.340 | 117.6 | 83.6 | 78.3 | 45.2 | ... | 20.0 | ... | 59.5 |
| 4652.17 | Cr I | 1.00 | –1.030 | 111.9 | 109.3 | 96.2 | 47.2 | ... | 34.5 | 62.5 | 81.4 |
| 5206.04 | Cr I | 0.94 | 0.030 | ... | ... | ... | 132.5 | 81.6 | 111.9 | 144.2 | 163.6 |
| 5298.28 | Cr I | 0.98 | –1.170 | ... | ... | 99.9 | ... | ... | ... | 68.9 | 93.2 |
| 5409.80 | Cr I | 1.03 | –0.710 | 174.9 | 140.2 | 144.2 | 85.4 | 31.8 | 61.9 | 88.2 | 128.5 |
| 5783.89 | Cr I | 3.32 | –0.295 | 20.2 | ... | ... | ... | ... | ... | ... | ... |
| 4030.75 | Mn I | 0.00 | –0.470 | ... | ... | ... | ... | 137.0 | 193.6 | ... | ... |
| 4033.06 | Mn I | 0.00 | –0.620 | ... | ... | ... | ... | 126.2 | 204.7 | ... | ... |
| 4451.59 | Mn I | 2.89 | 0.280 | 86.2 | ... | ... | ... | ... | ... | ... | ... |
| 4709.69 | Mn I | 2.89 | –0.339 | ... | ... | 25.5 | ... | ... | ... | ... | ... |
| 4754.04 | Mn I | 2.28 | –0.090 | 97.6 | 94.1 | 77.1 | 40.3 | ... | 24.0 | 39.4 | 73.5 |
| 4783.42 | Mn I | 2.30 | 0.042 | 131.3 | 114.2 | 100.0 | 35.6 | ... | 31.0 | 39.1 | 66.8 |
| 4823.51 | Mn I | 2.32 | 0.140 | 132.6 | 106.1 | 110.0 | 40.2 | ... | 36.6 | 51.6 | 72.7 |
| 5394.69 | Mn I | 0.00 | –3.503 | ... | ... | 73.1 | ... | ... | ... | ... | 66.7 |
| 6021.80 | Mn I | 3.08 | 0.034 | 54.9 | 33.2 | 35.6 | ... | ... | ... | ... | 26.3 |
| 4202.04 | Fe I | 1.49 | –0.710 | ... | ... | ... | ... | 139.6 | 161.4 | ... | ... |
| 4222.22 | Fe I | 2.45 | –0.970 | ... | ... | ... | 89.8 | ... | 86.3 | ... | ... |
| 4233.61 | Fe I | 2.48 | –0.600 | ... | ... | ... | 108.6 | 77.6 | 116.1 | ... | ... |
| 4250.13 | Fe I | 2.47 | –0.404 | ... | ... | ... | 123.6 | ... | 105.0 | ... | ... |
| 4250.80 | Fe I | 1.56 | –0.720 | ... | ... | ... | 174.0 | 140.0 | ... | ... | ... |
| 4260.49 | Fe I | 2.40 | 0.140 | ... | ... | ... | 156.6 | 127.1 | 140.0 | ... | ... |
| 4271.16 | Fe I | 2.45 | –0.350 | ... | ... | ... | 136.7 | ... | 120.5 | ... | ... |
| 4282.41 | Fe I | 2.18 | –0.780 | ... | ... | ... | 123.3 | 78.3 | 107.8 | ... | ... |
| 4325.77 | Fe I | 1.61 | 0.010 | ... | ... | ... | ... | 197.8 | ... | ... | ... |
| 4337.05 | Fe I | 1.56 | –1.690 | ... | ... | 169.8 | 117.0 | ... | 112.3 | ... | ... |
| 4375.94 | Fe I | 0.00 | –3.030 | ... | ... | ... | ... | 109.4 | 163.4 | ... | ... |
| 4404.76 | Fe I | 1.56 | –0.140 | ... | ... | ... | ... | 170.7 | ... | ... | ... |

Table 3—Continued

| λ Å | Ion | χ (eV) | $\log(gf)$ (dex) | 361 (mÅ) | 3053 (mÅ) | 3150 (mÅ) | 3157 (mÅ) | 19219 (mÅ) | 19629 (mÅ) | 21456 (mÅ) | XI–2 (mÅ) |
|----------------|------|----------------|---------------------|-------------|--------------|--------------|--------------|---------------|---------------|---------------|--------------|
| 4415.13 | Fe I | 1.61 | –0.610 | ... | ... | ... | ... | 149.0 | 172.3 | ... | ... |
| 4430.62 | Fe I | 2.22 | –1.660 | 138.7 | ... | 110.1 | 85.7 | 49.3 | 67.6 | 81.3 | ... |
| 4442.35 | Fe I | 2.20 | –1.250 | ... | ... | 138.1 | 108.8 | 84.7 | 99.4 | 119.9 | ... |
| 4447.73 | Fe I | 2.22 | –1.340 | ... | ... | 121.6 | 96.8 | 76.6 | 100.8 | 102.8 | 155.5 |
| 4459.14 | Fe I | 2.18 | –1.280 | 154.5 | ... | ... | ... | 85.3 | 112.6 | 130.5 | ... |
| 4461.66 | Fe I | 0.09 | –3.210 | ... | ... | ... | 163.2 | 149.1 | 159.7 | ... | ... |
| 4489.75 | Fe I | 0.12 | –3.970 | ... | ... | 157.5 | 130.7 | 92.6 | 130.3 | ... | 173.4 |
| 4494.57 | Fe I | 2.20 | –1.140 | ... | ... | 145.2 | 132.5 | 71.1 | 105.8 | 126.2 | ... |
| 4531.16 | Fe I | 1.49 | –2.150 | ... | 167.9 | ... | 120.3 | 85.6 | 104.1 | 146.4 | ... |
| 4592.66 | Fe I | 1.56 | –2.450 | ... | ... | 134.5 | ... | 56.6 | 89.3 | ... | ... |
| 4602.95 | Fe I | 1.49 | –2.220 | 167.0 | 156.6 | 155.3 | 115.8 | 89.6 | ... | 128.5 | 151.5 |
| 4625.05 | Fe I | 3.24 | –1.348 | 94.3 | 93.2 | ... | 24.7 | ... | 20.9 | ... | 69.8 |
| 4788.77 | Fe I | 3.24 | –1.806 | 66.6 | ... | 48.6 | ... | ... | ... | ... | 41.9 |
| 4871.33 | Fe I | 2.86 | –0.360 | 158.2 | 159.9 | 138.1 | 101.4 | 69.5 | 93.2 | 124.9 | 146.5 |
| 4872.14 | Fe I | 2.88 | –0.570 | 166.6 | 152.2 | 156.2 | 85.9 | 46.3 | 83.8 | 93.4 | 151.5 |
| 4891.50 | Fe I | 2.85 | –0.110 | ... | 166.9 | 154.8 | 119.5 | 87.9 | 110.0 | 134.4 | 159.7 |
| 4919.00 | Fe I | 2.86 | –0.340 | 168.9 | 156.6 | 155.4 | 108.7 | 91.3 | 100.7 | 119.3 | 154.3 |
| 4920.51 | Fe I | 2.83 | 0.150 | ... | ... | ... | 132.0 | 97.0 | 142.9 | ... | ... |
| 4957.61 | Fe I | 2.81 | 0.230 | ... | ... | ... | 144.2 | 107.3 | 144.9 | ... | ... |
| 5083.34 | Fe I | 0.96 | –2.960 | ... | ... | 148.6 | 121.3 | 94.2 | 118.7 | 149.6 | 166.3 |
| 5166.28 | Fe I | 0.00 | –4.200 | ... | ... | ... | 147.4 | 107.1 | 129.6 | 156.4 | ... |
| 5171.61 | Fe I | 1.48 | –1.790 | ... | ... | 172.3 | 145.1 | 120.4 | 138.8 | 157.2 | ... |
| 5192.35 | Fe I | 3.00 | –0.420 | 149.6 | 152.5 | 145.2 | 90.0 | 54.2 | 89.9 | 108.7 | 138.2 |
| 5194.95 | Fe I | 1.56 | –2.090 | ... | 160.6 | 162.1 | 116.5 | 88.4 | 119.7 | 135.4 | 170.7 |
| 5198.72 | Fe I | 2.22 | –2.140 | 122.8 | 123.8 | 106.7 | 58.5 | 36.4 | 64.0 | 85.7 | 112.8 |
| 5216.28 | Fe I | 1.61 | –2.150 | 166.4 | 157.0 | 146.7 | 115.0 | 85.7 | 113.0 | 140.7 | 152.7 |
| 5217.40 | Fe I | 3.21 | –1.070 | 103.1 | 88.3 | 78.6 | 39.6 | ... | 42.3 | 50.7 | 91.9 |
| 5227.19 | Fe I | 1.56 | –1.350 | ... | ... | ... | 166.9 | 129.7 | 167.3 | ... | ... |
| 5232.95 | Fe I | 2.94 | –0.100 | ... | 161.6 | 154.3 | 117.9 | 82.7 | 106.6 | 126.1 | 165.1 |
| 5393.18 | Fe I | 3.24 | –0.720 | 125.9 | 118.7 | 114.7 | 62.7 | 28.8 | 54.6 | 83.0 | 113.0 |
| 5405.79 | Fe I | 0.99 | –1.840 | ... | ... | ... | ... | 160.3 | ... | ... | ... |
| 5409.14 | Fe I | 4.37 | –1.200 | 30.9 | ... | ... | ... | ... | ... | ... | ... |
| 5410.92 | Fe I | 4.47 | 0.400 | 93.4 | 74.2 | 82.8 | 35.3 | ... | 29.5 | 47.6 | 73.4 |
| 5415.21 | Fe I | 4.39 | 0.640 | 110.4 | 108.5 | 102.8 | 48.8 | 23.5 | 48.5 | 54.2 | 97.2 |
| 5424.08 | Fe I | 4.32 | 0.510 | 128.4 | 112.1 | 105.8 | 62.5 | 32.9 | 51.9 | 78.8 | 91.2 |
| 5434.53 | Fe I | 1.01 | –2.130 | ... | ... | ... | 173.5 | 139.9 | 174.2 | ... | ... |
| 5445.05 | Fe I | 4.39 | –0.030 | 86.9 | 78.8 | 70.4 | 31.5 | ... | ... | 44.2 | 64.7 |
| 5466.39 | Fe I | 4.37 | –0.620 | 47.7 | 51.0 | 44.0 | ... | ... | ... | 11.4 | 21.4 |
| 5473.90 | Fe I | 4.15 | –0.690 | 50.9 | 41.5 | 26.1 | ... | ... | ... | ... | 29.9 |
| 5487.14 | Fe I | 4.41 | –1.430 | ... | 12.2 | ... | ... | ... | ... | ... | ... |
| 5487.77 | Fe I | 4.14 | –0.620 | 59.5 | 44.8 | 37.6 | ... | ... | ... | ... | 32.6 |
| 5497.52 | Fe I | 1.01 | –2.830 | ... | ... | ... | 143.9 | 99.1 | 128.1 | 164.3 | ... |
| 5501.46 | Fe I | 0.96 | –3.050 | ... | ... | ... | 138.1 | 95.8 | 131.7 | 164.0 | ... |
| 5506.79 | Fe I | 0.99 | –2.790 | ... | ... | ... | 143.0 | 109.4 | 136.2 | ... | ... |
| 5522.45 | Fe I | 4.21 | –1.450 | 21.1 | ... | ... | ... | ... | ... | ... | 15.7 |

Table 3—Continued

| λ Å | Ion | χ (eV) | $\log(gf)$ (dex) | 361 (mÅ) | 3053 (mÅ) | 3150 (mÅ) | 3157 (mÅ) | 19219 (mÅ) | 19629 (mÅ) | 21456 (mÅ) | XI–2 (mÅ) |
|----------------|------|----------------|---------------------|-------------|--------------|--------------|--------------|---------------|---------------|---------------|--------------|
| 5525.55 | Fe I | 4.23 | −1.080 | 27.9 | 23.2 | 15.2 | ... | ... | ... | ... | ... |
| 5554.88 | Fe I | 4.55 | −0.350 | 54.1 | 33.5 | 24.0 | ... | ... | ... | ... | 29.6 |
| 5560.21 | Fe I | 4.43 | −1.100 | 24.7 | ... | ... | ... | ... | ... | ... | ... |
| 5567.39 | Fe I | 2.61 | −2.670 | 71.7 | 64.2 | 48.3 | ... | ... | ... | 19.6 | 54.6 |
| 5569.62 | Fe I | 3.42 | −0.486 | 127.2 | 120.8 | 111.2 | 59.0 | 28.0 | 49.9 | 75.2 | 112.9 |
| 5572.84 | Fe I | 3.40 | −0.275 | 146.7 | 134.5 | 137.4 | 76.7 | 45.4 | 67.8 | 88.4 | 126.6 |
| 5576.09 | Fe I | 3.43 | −0.920 | 121.4 | 96.3 | 90.8 | 38.4 | ... | 34.0 | 49.5 | 88.9 |
| 5586.76 | Fe I | 3.37 | −0.140 | 158.2 | 142.5 | 132.9 | 81.4 | 51.0 | 78.5 | 94.3 | 142.7 |
| 5618.63 | Fe I | 4.21 | −1.630 | 20.6 | ... | ... | ... | ... | ... | ... | ... |
| 5624.04 | Fe I | 4.39 | −1.220 | 23.6 | ... | ... | ... | ... | ... | ... | ... |
| 5624.54 | Fe I | 3.42 | −0.755 | 129.5 | 109.5 | 103.5 | 46.6 | ... | 45.2 | 66.9 | 92.5 |
| 5641.44 | Fe I | 4.26 | −1.080 | 35.4 | 24.4 | 15.3 | ... | ... | ... | ... | ... |
| 5662.52 | Fe I | 4.18 | −0.570 | 71.3 | 56.4 | 50.8 | ... | ... | ... | ... | 36.1 |
| 5667.52 | Fe I | 4.48 | −1.500 | 21.3 | ... | ... | ... | ... | ... | ... | ... |
| 5679.02 | Fe I | 4.65 | −0.820 | 26.5 | ... | ... | ... | ... | ... | ... | ... |
| 5701.54 | Fe I | 2.56 | −2.140 | 120.1 | 82.6 | 87.6 | 39.4 | ... | 49.0 | 52.3 | 80.7 |
| 5705.98 | Fe I | 4.61 | −0.490 | 47.2 | 36.6 | ... | ... | ... | ... | ... | 21.0 |
| 5731.76 | Fe I | 4.26 | −1.200 | 29.0 | 28.1 | 21.1 | ... | ... | ... | ... | ... |
| 5752.04 | Fe I | 4.55 | −0.940 | 17.8 | ... | ... | ... | ... | ... | ... | ... |
| 5753.12 | Fe I | 4.26 | −0.690 | 53.6 | 49.9 | 34.8 | ... | ... | ... | ... | 27.0 |
| 5762.99 | Fe I | 4.21 | −0.410 | 77.1 | 65.3 | 53.5 | 15.7 | ... | 18.2 | 21.5 | 43.1 |
| 5775.06 | Fe I | 4.22 | −1.300 | 33.3 | 29.0 | ... | ... | ... | ... | ... | ... |
| 5778.46 | Fe I | 2.59 | −3.430 | 31.5 | ... | ... | ... | ... | ... | ... | ... |
| 5806.72 | Fe I | 4.61 | −0.950 | ... | 12.3 | ... | ... | ... | ... | ... | ... |
| 5859.60 | Fe I | 4.55 | −0.550 | 47.5 | 27.2 | 22.7 | ... | ... | ... | ... | ... |
| 5862.35 | Fe I | 4.55 | −0.330 | 54.0 | 37.1 | 27.4 | ... | ... | ... | 21.9 | 28.0 |
| 5883.81 | Fe I | 3.96 | −1.260 | 38.0 | 43.2 | ... | ... | ... | ... | ... | 15.9 |
| 5930.17 | Fe I | 4.65 | −0.140 | ... | 49.9 | ... | ... | ... | ... | ... | 28.1 |
| 5934.65 | Fe I | 3.93 | −1.070 | 60.9 | 46.3 | 44.6 | ... | ... | ... | 9.9 | 42.9 |
| 5952.72 | Fe I | 3.98 | −1.340 | 51.1 | 21.6 | 22.7 | ... | ... | ... | ... | 13.9 |
| 5956.69 | Fe I | 0.86 | −4.500 | 117.6 | 99.6 | 92.0 | 32.9 | ... | 38.3 | 49.9 | 100.2 |
| 5976.79 | Fe I | 3.94 | −1.330 | 58.1 | 34.9 | 23.5 | ... | ... | ... | ... | 29.5 |
| 5983.69 | Fe I | 4.55 | −0.660 | 42.8 | ... | 24.8 | ... | ... | ... | ... | ... |
| 5984.83 | Fe I | 4.73 | −0.260 | 45.7 | 35.6 | 34.2 | ... | ... | ... | ... | 23.0 |
| 6024.05 | Fe I | 4.55 | 0.030 | 79.3 | 65.9 | 50.8 | ... | ... | 14.8 | 31.4 | 55.6 |
| 6027.05 | Fe I | 4.07 | −1.090 | 49.7 | ... | 36.0 | ... | ... | ... | ... | 29.6 |
| 6055.99 | Fe I | 4.73 | −0.370 | 31.0 | 30.3 | 13.8 | ... | ... | ... | ... | 14.1 |
| 6065.48 | Fe I | 2.61 | −1.410 | 145.0 | 128.7 | 135.8 | 74.5 | 36.3 | 65.7 | 90.2 | 138.5 |
| 6078.50 | Fe I | 4.79 | −0.330 | 30.2 | 22.9 | ... | ... | ... | ... | ... | 16.0 |
| 6079.00 | Fe I | 4.65 | −1.020 | 18.1 | ... | ... | ... | ... | ... | ... | ... |
| 6089.57 | Fe I | 5.02 | −0.900 | 21.9 | ... | ... | ... | ... | ... | ... | ... |
| 6136.62 | Fe I | 2.45 | −1.410 | 165.4 | 148.2 | 148.3 | 99.9 | 55.0 | 89.2 | 122.3 | 158.5 |
| 6136.99 | Fe I | 2.20 | −2.930 | 103.3 | 84.6 | 76.2 | 22.8 | ... | ... | ... | ... |
| 6137.69 | Fe I | 2.59 | −1.350 | 163.9 | 147.0 | 139.7 | 89.2 | 48.6 | 85.9 | 117.3 | 135.1 |
| 6151.62 | Fe I | 2.18 | −3.370 | 72.4 | 61.5 | 53.2 | 12.9 | ... | ... | 23.5 | 56.5 |

Table 3—Continued

| λ Å | Ion | χ (eV) | $\log(gf)$ (dex) | 361 (mÅ) | 3053 (mÅ) | 3150 (mÅ) | 3157 (mÅ) | 19219 (mÅ) | 19629 (mÅ) | 21456 (mÅ) | XI–2 (mÅ) |
|----------------|------|----------------|---------------------|-------------|--------------|--------------|--------------|---------------|---------------|---------------|--------------|
| 6157.73 | Fe I | 4.07 | –1.160 | 50.6 | 36.0 | 32.2 | ... | ... | ... | ... | 18.9 |
| 6165.36 | Fe I | 4.14 | –1.470 | 32.8 | ... | ... | ... | ... | ... | ... | ... |
| 6173.34 | Fe I | 2.22 | –2.880 | 93.8 | 88.4 | 70.8 | 27.0 | ... | 23.3 | 41.4 | 72.1 |
| 6180.20 | Fe I | 2.73 | –2.650 | 65.9 | 58.5 | 46.2 | ... | ... | ... | 21.5 | 42.3 |
| 6187.99 | Fe I | 3.94 | –1.620 | 29.2 | ... | 14.1 | ... | ... | ... | ... | ... |
| 6191.56 | Fe I | 2.43 | –1.420 | 170.2 | 163.5 | 146.4 | 99.9 | 46.9 | 93.5 | 119.0 | 149.5 |
| 6200.31 | Fe I | 2.61 | –2.370 | 94.3 | 86.6 | 76.2 | 22.7 | ... | ... | 45.6 | 75.1 |
| 6240.65 | Fe I | 2.22 | –3.170 | 80.8 | 56.4 | 52.7 | ... | ... | ... | ... | 48.1 |
| 6246.32 | Fe I | 3.60 | –0.880 | 119.6 | 110.8 | 79.8 | 49.8 | ... | 48.5 | 41.1 | 96.6 |
| 6252.55 | Fe I | 2.40 | –1.770 | 155.5 | 147.4 | 131.3 | 88.3 | 45.4 | 80.2 | 110.5 | 138.6 |
| 6254.26 | Fe I | 2.28 | –2.430 | 130.1 | 112.8 | 105.8 | 47.8 | 16.4 | 44.8 | 64.7 | 102.2 |
| 6265.13 | Fe I | 2.18 | –2.540 | 126.8 | 114.3 | 99.5 | 51.5 | 17.3 | 48.8 | 69.0 | 115.4 |
| 6271.28 | Fe I | 3.33 | –2.700 | 14.8 | 10.1 | ... | ... | ... | ... | ... | ... |
| 6290.97 | Fe I | 4.73 | –0.730 | 24.3 | 20.3 | ... | ... | ... | ... | ... | ... |
| 6297.79 | Fe I | 2.22 | –2.640 | 112.3 | 110.2 | 91.8 | 33.4 | ... | 26.6 | 48.2 | 94.5 |
| 6301.51 | Fe I | 3.65 | –0.718 | 106.1 | 93.4 | 84.9 | ... | ... | 44.8 | 57.1 | 89.8 |
| 6302.50 | Fe I | 3.69 | –1.110 | 70.4 | 54.2 | 45.8 | ... | ... | ... | 35.5 | 72.2 |
| 6311.50 | Fe I | 2.83 | –3.140 | ... | 34.2 | ... | ... | ... | ... | ... | 17.6 |
| 6315.31 | Fe I | 4.14 | –1.230 | 39.4 | ... | ... | ... | ... | ... | ... | ... |
| 6355.03 | Fe I | 2.84 | –2.290 | 87.2 | 76.9 | 54.3 | 20.6 | ... | ... | ... | 47.1 |
| 6380.75 | Fe I | 4.19 | –1.380 | 31.8 | 20.1 | 14.9 | ... | ... | ... | ... | ... |
| 6392.54 | Fe I | 2.28 | –3.990 | 26.9 | 13.8 | ... | ... | ... | ... | ... | ... |
| 6393.60 | Fe I | 2.43 | –1.580 | 161.4 | 145.3 | 134.4 | 91.2 | 55.5 | 87.4 | 119.9 | 143.6 |
| 6408.03 | Fe I | 3.69 | –1.020 | 87.5 | 75.5 | 61.8 | 23.8 | ... | 14.7 | 29.0 | 48.0 |
| 6411.65 | Fe I | 3.65 | –0.720 | 116.7 | 102.2 | 102.0 | 41.4 | 14.8 | 31.1 | 63.7 | 92.1 |
| 6421.35 | Fe I | 2.28 | –2.010 | ... | ... | 135.4 | ... | ... | ... | ... | 143.6 |
| 6469.21 | Fe I | 4.83 | –0.730 | 24.0 | 28.5 | ... | ... | ... | ... | ... | 9.5 |
| 6475.63 | Fe I | 2.56 | –2.940 | 85.0 | 62.8 | 37.7 | 13.7 | ... | ... | ... | 57.2 |
| 6481.87 | Fe I | 2.28 | –3.010 | 111.0 | 95.6 | 68.0 | ... | ... | ... | 36.7 | 71.9 |
| 6494.98 | Fe I | 2.40 | –1.240 | ... | 170.3 | 168.6 | 118.1 | 75.0 | 111.6 | 138.8 | 172.2 |
| 6498.94 | Fe I | 0.96 | –4.690 | 123.5 | 101.0 | 92.7 | 29.4 | ... | ... | 43.1 | 87.2 |
| 6546.24 | Fe I | 2.76 | –1.540 | ... | ... | 111.2 | ... | ... | ... | 88.1 | 120.5 |
| 6581.21 | Fe I | 1.48 | –4.680 | 66.9 | 37.5 | 27.0 | ... | ... | ... | ... | 33.6 |
| 6592.91 | Fe I | 2.73 | –1.470 | 146.1 | 133.1 | 119.3 | 75.1 | 36.6 | 74.2 | 85.2 | 121.0 |
| 6593.87 | Fe I | 2.43 | –2.370 | 118.7 | 107.8 | 92.9 | 39.7 | ... | 35.3 | 62.0 | 93.8 |
| 6597.56 | Fe I | 4.79 | –0.970 | 14.6 | ... | ... | ... | ... | ... | ... | ... |
| 6608.02 | Fe I | 2.28 | –3.930 | 26.7 | ... | ... | ... | ... | ... | ... | 14.2 |
| 6609.11 | Fe I | 2.56 | –2.660 | 90.0 | 77.8 | 61.7 | 18.5 | ... | ... | 29.3 | 55.3 |
| 6625.02 | Fe I | 1.01 | –5.370 | 47.1 | 38.2 | 34.3 | ... | ... | ... | ... | 38.7 |
| 6633.75 | Fe I | 4.79 | –0.800 | 30.0 | 14.6 | ... | ... | ... | ... | ... | ... |
| 6648.12 | Fe I | 1.01 | –5.920 | ... | 16.0 | ... | ... | ... | ... | ... | ... |
| 6703.57 | Fe I | 2.76 | –3.060 | 37.4 | 34.8 | 28.4 | ... | ... | ... | ... | 17.1 |
| 6726.67 | Fe I | 4.61 | –1.070 | 16.7 | ... | ... | ... | ... | ... | ... | ... |
| 6739.52 | Fe I | 1.56 | –4.790 | 32.1 | 24.9 | 14.8 | ... | ... | ... | ... | 12.6 |
| 6750.15 | Fe I | 2.42 | –2.580 | 109.8 | 93.4 | 81.8 | 26.9 | ... | 31.6 | 39.2 | 87.5 |

Table 3—Continued

| λ Å | Ion | χ (eV) | $\log(gf)$ (dex) | 361 (mÅ) | 3053 (mÅ) | 3150 (mÅ) | 3157 (mÅ) | 19219 (mÅ) | 19629 (mÅ) | 21456 (mÅ) | XI–2 (mÅ) |
|----------------|-------|----------------|---------------------|-------------|--------------|--------------|--------------|---------------|---------------|---------------|--------------|
| 6786.86 | Fe I | 4.19 | −1.970 | 16.9 | ... | ... | ... | ... | ... | ... | ... |
| 6839.83 | Fe I | 2.56 | −3.350 | 41.1 | 32.1 | 20.5 | ... | ... | ... | ... | 14.4 |
| 6843.65 | Fe I | 4.55 | −0.830 | 28.2 | 22.5 | 20.3 | ... | ... | ... | ... | ... |
| 6855.18 | Fe I | 4.56 | −0.740 | 35.1 | 31.4 | 16.2 | ... | ... | ... | ... | 18.8 |
| 6858.15 | Fe I | 4.61 | −0.930 | 19.0 | ... | ... | ... | ... | ... | ... | ... |
| 6861.95 | Fe I | 2.42 | −3.850 | 20.5 | 14.9 | ... | ... | ... | ... | ... | 9.6 |
| 6978.85 | Fe I | 2.48 | −2.450 | 106.9 | 96.5 | 81.8 | 28.7 | ... | 30.5 | ... | ... |
| 6988.52 | Fe I | 2.40 | −3.560 | 49.4 | 35.2 | 17.4 | ... | ... | ... | 10.0 | 33.2 |
| 6999.88 | Fe I | 4.10 | −1.460 | ... | ... | 16.4 | ... | ... | ... | ... | 18.0 |
| 7022.95 | Fe I | 4.19 | −1.150 | ... | 57.9 | 38.1 | ... | ... | ... | ... | 16.3 |
| 7038.22 | Fe I | 4.22 | −1.200 | 41.2 | 24.4 | ... | ... | ... | ... | ... | ... |
| 7112.17 | Fe I | 2.99 | −3.000 | 32.2 | ... | 13.1 | ... | ... | ... | ... | 17.6 |
| 7130.92 | Fe I | 4.22 | −0.750 | 64.4 | 45.2 | 34.3 | ... | ... | ... | 14.3 | 38.7 |
| 7132.98 | Fe I | 4.07 | −1.630 | ... | 13.9 | ... | ... | ... | ... | ... | ... |
| 7151.47 | Fe I | 2.48 | −3.660 | 27.3 | 22.5 | 11.6 | ... | ... | ... | ... | 18.5 |
| 7179.99 | Fe I | 1.48 | −4.750 | ... | ... | 28.9 | ... | ... | ... | ... | ... |
| 7181.20 | Fe I | 4.22 | −1.250 | ... | 21.0 | ... | ... | ... | ... | ... | ... |
| 7189.15 | Fe I | 3.07 | −2.220 | 30.5 | ... | ... | ... | ... | ... | ... | ... |
| 7288.74 | Fe I | 4.22 | −1.280 | 49.4 | ... | ... | ... | ... | ... | ... | ... |
| 7401.69 | Fe I | 4.19 | −1.350 | 17.4 | ... | ... | ... | ... | ... | ... | ... |
| 7411.16 | Fe I | 4.28 | −0.280 | 80.7 | 58.8 | 51.5 | 17.8 | ... | ... | 24.0 | 48.3 |
| 7418.67 | Fe I | 4.14 | −1.380 | 17.7 | ... | 10.6 | ... | ... | ... | ... | ... |
| 7440.92 | Fe I | 4.91 | −0.720 | 25.5 | ... | ... | ... | ... | ... | ... | ... |
| 7445.75 | Fe I | 4.26 | 0.030 | 93.9 | 83.3 | ... | 25.8 | ... | 16.0 | ... | 67.7 |
| 7461.52 | Fe I | 2.56 | −3.530 | 31.1 | 27.2 | ... | ... | ... | ... | ... | 9.6 |
| 7491.65 | Fe I | 4.30 | −1.070 | 42.9 | 29.9 | ... | ... | ... | ... | ... | 34.4 |
| 7495.06 | Fe I | 4.22 | 0.230 | 109.4 | 100.3 | 84.1 | ... | ... | ... | 53.0 | 86.2 |
| 7568.91 | Fe I | 4.28 | −0.940 | 53.4 | 43.7 | 24.3 | ... | ... | ... | ... | 28.5 |
| 7583.79 | Fe I | 3.02 | −1.890 | 96.8 | 89.1 | 66.4 | 23.6 | ... | 23.1 | 37.4 | 74.8 |
| 7586.04 | Fe I | 4.31 | −0.130 | 86.7 | 73.0 | 69.1 | ... | ... | 20.2 | 41.0 | 56.5 |
| 7748.27 | Fe I | 2.95 | −1.750 | 115.4 | 103.9 | 90.6 | 34.0 | ... | 33.1 | 60.0 | 87.2 |
| 7780.57 | Fe I | 4.47 | −0.040 | 80.2 | ... | 55.7 | ... | ... | 13.0 | ... | 58.7 |
| 4178.86 | Fe II | 2.57 | −2.530 | ... | ... | ... | 64.4 | ... | 65.9 | ... | ... |
| 4233.17 | Fe II | 2.57 | −2.000 | ... | ... | ... | ... | 80.4 | ... | ... | ... |
| 4416.82 | Fe II | 2.77 | −2.430 | 104.1 | ... | 89.4 | 69.8 | 41.4 | 50.1 | 73.2 | 64.8 |
| 4491.40 | Fe II | 2.84 | −2.600 | 80.4 | ... | 84.7 | 44.9 | ... | 48.6 | ... | 73.8 |
| 4508.30 | Fe II | 2.84 | −2.280 | 112.0 | 88.5 | 76.6 | 77.1 | 54.8 | 68.8 | ... | 85.7 |
| 4555.89 | Fe II | 2.82 | −2.170 | ... | ... | ... | 76.2 | 44.7 | 64.5 | ... | ... |
| 4576.34 | Fe II | 2.83 | −2.900 | 71.0 | 60.7 | 63.1 | 38.6 | ... | 28.3 | 56.2 | 53.8 |
| 4583.84 | Fe II | 2.81 | −2.020 | ... | ... | 124.0 | ... | 73.8 | ... | 97.9 | ... |
| 4923.93 | Fe II | 2.88 | −1.320 | 162.5 | 145.6 | 145.5 | 135.2 | 94.8 | 132.3 | 133.5 | 144.8 |
| 5018.45 | Fe II | 2.89 | −1.220 | ... | ... | 164.7 | 149.7 | 107.8 | 133.2 | 151.7 | 157.9 |
| 5197.58 | Fe II | 3.23 | −2.230 | 98.2 | 82.6 | 90.0 | 52.5 | 33.2 | 46.4 | 69.7 | 81.7 |
| 5234.63 | Fe II | 3.22 | −2.220 | 91.6 | 82.6 | 82.2 | 67.6 | 35.3 | 52.0 | 63.5 | 83.6 |
| 5414.08 | Fe II | 3.22 | −3.620 | ... | ... | ... | ... | ... | 6.4 | ... | ... |

Table 3—Continued

| λ Å | Ion | χ (eV) | $\log(gf)$ (dex) | 361 (mÅ) | 3053 (mÅ) | 3150 (mÅ) | 3157 (mÅ) | 19219 (mÅ) | 19629 (mÅ) | 21456 (mÅ) | XI–2 (mÅ) |
|----------------|-------|----------------|---------------------|-------------|--------------|--------------|--------------|---------------|---------------|---------------|--------------|
| 5425.26 | Fe II | 3.00 | –3.240 | 33.6 | 38.5 | 31.0 | 16.6 | ... | ... | ... | 29.2 |
| 5534.85 | Fe II | 3.25 | –2.640 | 75.6 | 56.5 | 47.3 | ... | ... | 20.0 | ... | 59.5 |
| 5991.38 | Fe II | 3.15 | –3.570 | 25.2 | ... | ... | ... | ... | ... | ... | 15.5 |
| 6149.26 | Fe II | 3.89 | –2.690 | 27.9 | 22.4 | ... | ... | ... | ... | ... | 14.8 |
| 6247.56 | Fe II | 3.89 | –2.360 | 53.9 | 41.7 | 35.6 | ... | ... | 17.5 | ... | 35.0 |
| 6369.46 | Fe II | 2.89 | –4.200 | 18.2 | ... | ... | ... | ... | ... | ... | 9.9 |
| 6416.92 | Fe II | 3.89 | –2.690 | 31.5 | 25.4 | 32.6 | ... | ... | ... | ... | 15.0 |
| 6516.08 | Fe II | 2.89 | –3.450 | 55.2 | 53.4 | 37.4 | 32.1 | ... | ... | 27.0 | 44.9 |
| 4121.31 | Co I | 0.92 | –0.315 | ... | ... | ... | 130.7 | 93.0 | 123.3 | ... | ... |
| 5483.34 | Co I | 1.71 | –1.490 | 66.9 | 57.9 | 61.4 | 13.7 | ≤15.0 | 15.2 | 43.0 | 29.8 |
| 4401.55 | Ni I | 3.19 | 0.084 | ... | ... | ... | ... | ... | 54.6 | ... | ... |
| 5578.72 | Ni I | 1.68 | –2.640 | 68.4 | 61.9 | 52.8 | ... | ... | 10.9 | 39.9 | 35.1 |
| 5587.86 | Ni I | 1.93 | –2.140 | 62.2 | 61.5 | 64.3 | 13.2 | ... | ... | 31.0 | 33.3 |
| 5592.26 | Ni I | 1.95 | –2.590 | 60.1 | 58.7 | 53.8 | ... | ... | 15.7 | 25.4 | 26.9 |
| 5593.74 | Ni I | 3.90 | –0.840 | 13.7 | ... | ... | ... | ... | ... | ... | ... |
| 5748.35 | Ni I | 1.68 | –3.260 | 33.2 | 22.8 | ... | ... | ... | ... | ... | 9.6 |
| 5846.99 | Ni I | 1.68 | –3.210 | 21.7 | 19.6 | ... | ... | ... | ... | ... | 18.4 |
| 5892.87 | Ni I | 1.99 | –2.340 | 84.7 | 65.7 | 63.7 | 25.0 | ... | ... | ... | 38.8 |
| 6128.97 | Ni I | 1.68 | –3.330 | ... | ... | 19.3 | ... | ... | ... | ... | ... |
| 6176.81 | Ni I | 4.09 | –0.529 | 12.0 | ... | ... | ... | ... | ... | ... | ... |
| 6482.80 | Ni I | 1.93 | –2.630 | 42.3 | 37.6 | 19.6 | ... | ... | ... | 17.5 | ... |
| 6586.31 | Ni I | 1.95 | –2.810 | 34.9 | 29.2 | 19.7 | ... | ... | ... | 16.8 | 15.7 |
| 6643.63 | Ni I | 1.68 | –2.300 | 114.2 | 102.6 | 95.6 | 40.4 | 18.9 | 33.3 | 82.4 | 88.2 |
| 6767.77 | Ni I | 1.83 | –2.170 | 100.1 | 84.5 | 82.6 | 34.8 | 11.0 | 25.4 | 73.1 | 73.8 |
| 7110.88 | Ni I | 1.93 | –2.970 | 28.1 | 27.9 | 17.4 | ... | ... | ... | ... | 16.7 |
| 7122.20 | Ni I | 3.54 | 0.048 | 76.0 | 63.5 | 63.6 | 27.3 | ... | 16.4 | 54.7 | 38.8 |
| 7197.01 | Ni I | 1.93 | –2.680 | 56.7 | 56.8 | 37.0 | ... | ... | ... | 25.6 | 32.6 |
| 7261.92 | Ni I | 1.95 | –2.700 | 52.1 | 53.0 | 41.9 | 11.4 | ... | ... | 27.2 | 23.2 |
| 7409.35 | Ni I | 3.80 | –0.100 | 50.9 | 39.6 | ... | ... | ... | ... | ... | ... |
| 7414.50 | Ni I | 1.99 | –2.570 | 66.3 | 63.0 | 50.5 | ... | ... | ... | 36.9 | 44.9 |
| 7422.27 | Ni I | 3.63 | –0.129 | 65.4 | 57.8 | 59.5 | 17.6 | ... | 17.8 | 34.7 | 31.4 |
| 7574.05 | Ni I | 3.83 | –0.580 | 31.8 | 18.1 | 23.2 | ... | ... | ... | ... | ... |
| 7727.62 | Ni I | 3.68 | –0.162 | 58.7 | 57.6 | 47.5 | ... | ... | ... | 32.3 | 25.6 |
| 7748.89 | Ni I | 3.70 | –0.130 | 54.1 | 42.1 | 44.2 | ... | ... | ... | ... | 24.0 |
| 7788.93 | Ni I | 1.95 | –2.420 | 104.2 | 92.5 | 86.0 | 30.8 | ... | 19.7 | 66.8 | 67.0 |
| 7797.59 | Ni I | 3.90 | –0.180 | 39.4 | 35.0 | 23.6 | ... | ... | ... | 16.2 | ... |
| 5105.54 | Cu I | 1.39 | –1.505 | 70.1 | 55.8 | 44.4 | ... | ... | ... | ... | 16.0 |
| 5782.12 | Cu I | 1.64 | –1.780 | 31.2 | 19.2 | ... | ... | ... | ... | ... | ... |
| 4722.16 | Zn I | 4.03 | –0.390 | 37.0 | 32.8 | ... | 27.6 | ... | ... | ... | ... |
| 4810.54 | Zn I | 4.08 | –0.170 | 39.7 | 37.7 | 54.9 | 38.1 | ... | ... | ... | 47.1 |
| 4607.33 | Sr I | 0.00 | 0.280 | 33.0 | ... | ... | ... | ... | ... | ... | ... |
| 4077.71 | Sr II | 0.00 | 0.170 | ... | ... | ... | 157.9 | 109.1 | 140.8 | ... | ... |
| 4215.52 | Sr II | 0.00 | –0.140 | 242.1 | 232.2 | 279.0 | 168.9 | 102.2 | 123.4 | ... | 165.0 |
| 4554.04 | Ba II | 0.00 | 0.170 | 241.3 | 239.8 | 254.9 | 177.4 | 125.4 | 143.2 | 219.9 | 156.6 |
| 4934.16 | Ba II | 0.00 | –0.150 | ... | ... | ... | 163.0 | ... | 144.3 | ... | ... |

Table 3—Continued

| λ Å | Ion | χ (eV) | $\log(gf)$ (dex) | 361 (mÅ) | 3053 (mÅ) | 3150 (mÅ) | 3157 (mÅ) | 19219 (mÅ) | 19629 (mÅ) | 21456 (mÅ) | XI–2 (mÅ) |
|----------------|-------|----------------|---------------------|-------------|--------------|--------------|--------------|---------------|---------------|---------------|--------------|
| 5853.70 | Ba II | 0.60 | –1.010 | 121.4 | 108.1 | 122.4 | 45.5 | 18.5 | 42.5 | 102.7 | 42.5 |
| 6141.70 | Ba II | 0.70 | –0.070 | 183.2 | 175.8 | 191.6 | 102.9 | 69.7 | 83.4 | 169.2 | 97.0 |
| 6496.90 | Ba II | 0.60 | –0.380 | 187.3 | 169.2 | 186.6 | 118.9 | 74.3 | 84.8 | 164.4 | 87.2 |
| 4398.01 | Y II | 0.13 | –1.000 | 85.2 | 73.8 | 86.4 | ... | ... | ... | ... | ... |
| 4883.69 | Y II | 1.08 | 0.070 | 85.6 | 68.4 | 94.6 | ... | ... | ... | 59.4 | ... |
| 5087.43 | Y II | 1.08 | –0.170 | 59.0 | 51.3 | 60.6 | ... | ... | ... | 40.4 | ... |
| 5200.42 | Y II | 0.99 | –0.570 | 46.2 | 42.7 | 67.9 | ... | ... | ... | 42.0 | ... |
| 4208.99 | Zr II | 0.71 | –0.460 | ... | ... | 72.8 | 27.4 | ... | ... | ... | ... |
| 4486.91 | Ce II | 0.30 | –0.360 | ... | 32.6 | ... | ... | ... | ... | ... | ... |
| 4562.37 | Ce II | 0.48 | 0.330 | 50.6 | 37.4 | 64.8 | ... | ... | ... | ... | ... |
| 4628.16 | Ce II | 0.52 | 0.260 | 45.3 | 45.4 | 52.3 | ... | ... | ... | 41.2 | ... |
| 4061.09 | Nd II | 0.47 | 0.550 | 77.6 | 66.6 | ... | ... | ... | ... | ... | ... |
| 4446.39 | Nd II | 0.20 | –0.350 | ... | ... | 65.9 | ... | ... | ... | 56.5 | ... |
| 4462.99 | Nd II | 0.56 | 0.040 | ... | ... | ... | ... | ... | ... | 53.2 | ... |
| 4959.12 | Nd II | 0.06 | –0.800 | 46.2 | 49.6 | 63.6 | ... | ... | ... | 64.6 | ... |
| 5092.79 | Nd II | 0.38 | –0.610 | 32.4 | 34.8 | 54.8 | ... | ... | ... | 47.0 | ... |
| 5130.59 | Nd II | 1.30 | 0.450 | ... | 19.2 | 37.9 | ... | ... | ... | ... | ... |
| 5212.35 | Nd II | 0.20 | –0.960 | 20.8 | 35.3 | 41.5 | ... | ... | ... | 38.8 | ... |
| 5249.58 | Nd II | 0.98 | 0.200 | 36.7 | 37.7 | 56.9 | ... | ... | ... | 35.0 | ... |
| 6645.11 | Eu II | 1.38 | 0.120 | 19.0 | 22.1 | 43.2 | ≤10.0 | ... | ≤13.0 | 26.0 | ≤10.0 |
| 4103.31 | Dy II | 0.10 | –0.370 | 46.0 | ... | ... | ... | ... | ... | ... | ... |
| 5169.69 | Dy II | 0.10 | –1.660 | ... | ... | 21.0 | ... | ... | ... | ... | ... |

^aVery uncertain. Could be an upper limit.

Table 4. Fit Fe I Slopes With EP, Equivalent Width, and Wavelength

| Star ID | $\Delta[X/Fe]/\Delta(\text{EP})^a$ (dex/eV) | $\Delta[X/Fe]/\Delta[W_\lambda/\lambda]$ (dex) | $\Delta[X/Fe]/\Delta\lambda$ ($10^{-4}\text{dex}/\text{\AA}$) |
|---------|--|---|--|
| 361 | -0.05 | +0.02 | -0.31 |
| 3053 | -0.04 | -0.07 | +0.05 |
| 3150 | -0.03 | -0.01 | -0.18 |
| 3157 | -0.10 | 0.00 | -0.09 |
| 19219 | -0.08 | 0.00 | +0.18 |
| 19629 | -0.05 | -0.07 | +0.26 |
| 21456 | -0.08 | -0.01 | +0.08 |
| XI-2 | -0.07 | -0.03 | +0.06 |

^aTypical range of EP is 4 eV. This slope decreases by ~ 0.2 dex/eV for an increase in T_{eff} of 250 K.

Table 5. Sensitivity of Absolute Abundances

| Species | $\Delta \log(\epsilon)$ ($\Delta T_{\text{eff}} - 250 \text{ K}$) (dex) | $\Delta \log(\epsilon)$ ($\Delta \log(g)$ -0.5 dex) (dex) | $\Delta \log(\epsilon)$ ($\Delta Z(\text{model})$ -0.5 dex) (dex) | $\Delta \log(\epsilon)$ (Δv_t $+0.3 \text{ km s}^{-1}$) (dex) |
|---------|---|---|---|---|
| C(CH) | -0.15 | 0.21 | 0.10 | 0.02 |
| O I | -0.05 | -0.18 | 0.06 | 0.00 |
| Na I | -0.66 | 0.17 | -0.19 | 0.15 |
| Mg I | -0.32 | 0.19 | -0.10 | 0.10 |
| Al I | -0.69 | 0.28 | -0.34 | 0.15 |
| Si I | -0.11 | 0.03 | -0.03 | 0.01 |
| K I | -0.39 | 0.06 | -0.07 | 0.06 |
| Ca I | -0.27 | 0.07 | -0.05 | 0.03 |
| Sc II | 0.01 | -0.14 | 0.03 | 0.03 |
| Ti I | -0.63 | 0.11 | -0.13 | 0.06 |
| Ti II | 0.03 | -0.07 | -0.01 | 0.12 |
| V I | -0.55 | 0.08 | -0.07 | 0.01 |
| Cr I | -0.53 | 0.13 | -0.13 | 0.07 |
| Mn I | -0.37 | 0.11 | -0.08 | 0.03 |
| Fe I | -0.41 | 0.09 | -0.11 | 0.08 |
| Fe II | 0.17 | -0.09 | 0.00 | 0.12 |
| Co I | -0.44 | 0.06 | 0.01 | 0.07 |
| Ni I | -0.38 | 0.05 | -0.06 | 0.02 |
| Cu I | -0.44 | 0.08 | -0.07 | 0.02 |
| Zn I | 0.05 | -0.03 | -0.02 | 0.02 |
| Sr II | -0.10 | 0.00 | -0.03 | 0.24 |
| Y II | -0.02 | -0.13 | 0.03 | 0.03 |
| Zr II | 0.04 | -0.02 | -0.02 | 0.11 |
| Ba II | -0.14 | -0.11 | 0.01 | 0.19 |
| Ce II | -0.07 | -0.11 | 0.02 | 0.03 |
| Nd II | -0.09 | -0.12 | 0.02 | 0.04 |
| Eu II | -0.03 | -0.17 | 0.05 | 0.01 |
| Dy II | -0.07 | -0.11 | 0.01 | 0.02 |

Table 6. Sensitivity of Relative Abundances

| Species | $\Delta[X/Fe]$ (ΔT_{eff} –150 K) (dex) | $\Delta[X/Fe]$ ($\Delta \log(g)$ –0.4 dex) (dex) | $\Delta[X/Fe]$ ($\Delta Z(\text{model})$ –0.5 dex) (dex) | $\Delta[X/Fe]$ (Δv_t +0.3 km s ^{–1}) (dex) | $\Delta[X/Fe]$ ΔW_λ^a (dex) | Ion. Code ^b (dex) | Total Unc. ^c (dex) |
|--------------------|--|--|--|--|---|------------------------------------|----------------------------------|
| C(CH) | 0.16 | 0.10 | 0.21 | –0.06 | 0.10 | 1 | 0.30 |
| O I | –0.13 | –0.07 | 0.02 | 0.00 | 0.08 | 2 | 0.17 |
| Na I | –0.15 | 0.06 | –0.03 | 0.15 | 0.08 | 1 | 0.24 |
| Mg I | 0.05 | 0.08 | 0.00 | 0.10 | 0.04 | 1 | 0.14 |
| Al I | –0.17 | 0.15 | –0.23 | 0.07 | 0.08 | 1 | 0.34 |
| Si I | 0.18 | –0.05 | 0.03 | 0.01 | 0.08 | 1 ^d | 0.21 |
| K I | 0.01 | –0.02 | 0.02 | 0.06 | 0.08 | 1 | 0.10 |
| Ca I | 0.08 | –0.02 | 0.02 | 0.03 | 0.02 | 1 | 0.10 |
| Sc II | –0.10 | –0.04 | 0.01 | 0.03 | 0.03 | 2 | 0.11 |
| Ti I | –0.13 | 0.02 | –0.01 | 0.06 | 0.03 | 1 | 0.15 |
| Ti II | –0.08 | 0.02 | 0.00 | 0.12 | 0.03 | 2 | 0.15 |
| Ti12 ^e | –0.04 | 0.02 | –0.02 | –0.01 | 0.02 | ... | 0.05 |
| V I | –0.08 | –0.01 | 0.04 | –0.07 | 0.05 | 1 | 0.13 |
| Cr I | –0.07 | 0.03 | –0.01 | 0.07 | 0.03 | 1 | 0.11 |
| Mn I | 0.02 | 0.02 | 0.01 | 0.03 | 0.05 | 1 | 0.06 |
| Fe I ^f | –0.35 | 0.14 | –0.04 | 0.08 | 0.01 | 2 | 0.39 ^f |
| Fe II ^f | 0.35 | –0.14 | 0.04 | 0.12 | 0.03 | 1 | 0.40 ^f |
| Co I | –0.02 | –0.02 | 0.12 | –0.01 | 0.08 | 1 | 0.15 |
| Ni I | 0.02 | –0.03 | 0.02 | 0.02 | 0.02 | 1 | 0.05 |
| Cu I | –0.02 | –0.01 | 0.04 | –0.06 | 0.06 | 1 | 0.10 |
| Zn I | –0.07 | –0.05 | –0.02 | –0.10 | 0.08 | 2 | 0.13 |
| Sr II | –0.16 | 0.07 | –0.03 | 0.12 | 0.06 | 2 | 0.19 |
| Y II | –0.11 | –0.03 | 0.01 | 0.03 | 0.05 | 2 | 0.13 |
| Zr II | –0.08 | 0.06 | –0.02 | –0.01 | 0.06 | 2 | 0.11 |
| Ba II | –0.19 | –0.02 | 0.00 | 0.19 | 0.04 | 2 | 0.27 |
| Ce II | –0.14 | –0.02 | 0.01 | 0.03 | 0.08 | 2 | 0.17 |
| Nd II | –0.16 | –0.02 | 0.01 | 0.04 | 0.03 | 2 | 0.17 |
| Eu II | –0.12 | –0.06 | 0.02 | 0.01 | 0.08 | 2 | 0.16 |
| Dy II | –0.14 | –0.02 | 0.01 | –0.10 | 0.08 | 2 | 0.17 |

^aUncertainty from errors in W_λ taken as 20% (0.08 dex)/ \sqrt{Nlines} .

^bIon. code is 1 if with respect to Fe I, 2 if with respect to Fe II.

^cThe rms sum of the 5 contributing terms.

^dThe total uncertainty for [Si/Fe] is the same using either Fe I or Fe II, although the values of the individual terms contributing are different.

^eAverage of [Ti/Fe](Ti I,Fe I) and [Ti/Fe](Ti II,Fe II).

^fThis is [Fe/H](Fe I) – [Fe/H](Fe II) and vice versa, given for illustrative purposes only.

Table 7a. Abundances for the First Four Draco Stars

| Species | Draco 361 [Fe/H] -1.49 | | | | Draco 3053 [Fe/H] -1.73 | | | | Draco 3150 [Fe/H] -1.89 | | | | Draco 3157 [Fe/H] -2.45 | | | |
|--------------------|------------------------|----------------------------|--------------|---------------------|-------------------------|----------------------------|--------------|---------------------|-------------------------|----------------------------|--------------|---------------------|-------------------------|----------------------------|--------------|---------------------|
| | [X/Fe] (dex) | log $\epsilon(X)$ (dex) | No. Lines | σ^a (dex) | [X/Fe] (dex) | log $\epsilon(X)$ (dex) | No. Lines | σ^a (dex) | [X/Fe] (dex) | log $\epsilon(X)$ (dex) | No. Lines | σ^a (dex) | [X/Fe] (dex) | log $\epsilon(X)$ (dex) | No. Lines | σ^a (dex) |
| C(CH) ^b | -0.54 | 6.56 | 1 | ... | -0.80 | 6.06 | 1 | ... | -0.64 | 6.06 | 1 | ... | -0.29 | 5.85 | 1 | ... |
| O I | 0.00 | 7.34 | 2 | 0.04 | 0.32 | 7.42 | 2 | 0.04 | ... | ... | ... | ... | 0.40 | 6.78 | 1 | ... |
| Na I | -0.48 | 4.35 | 3 | 0.25 | -0.62 | 3.96 | 4 | 0.28 | -0.47 | 3.96 | 2 | 0.08 | 0.01 | 3.88 | 4 | 0.20 |
| Mg I | -0.01 | 6.05 | 5 | 0.14 | 0.00 | 5.81 | 5 | 0.32 | 0.18 | 5.83 | 5 | 0.22 | 0.19 | 5.28 | 4 | 0.06 |
| Al I | ... | ... | ... | ... | ... | ... | ... | ... | ... | ... | ... | ... | -0.62 | 3.40 | 1 | ... |
| Si I | -0.23 | 5.83 | 4 | 0.23 | -0.01 | 5.81 | 5 | 0.13 | 0.08 | 5.74 | 4 | 0.13 | 0.26 | 5.36 | 3 | 0.12 |
| K I | ... | ... | ... | ... | 0.25 | 3.64 | 1 | ... | ... | ... | ... | ... | 0.10 | 2.77 | 1 | ... |
| Ca I | -0.16 | 4.71 | 18 | 0.15 | -0.08 | 4.55 | 17 | 0.18 | 0.00 | 4.47 | 18 | 0.14 | 0.15 | 4.06 | 17 | 0.17 |
| Sc II | -0.20 | 1.41 | 8 | 0.20 | -0.25 | 1.11 | 8 | 0.14 | -0.04 | 1.17 | 7 | 0.16 | 0.04 | 0.69 | 9 | 0.16 |
| Ti I | -0.17 | 3.33 | 25 | 0.16 | -0.08 | 3.18 | 25 | 0.16 | -0.05 | 3.05 | 20 | 0.16 | 0.07 | 2.61 | 13 | 0.13 |
| Ti II | 0.00 | 3.50 | 7 | 0.26 | 0.03 | 3.29 | 7 | 0.20 | -0.03 | 3.07 | 11 | 0.14 | 0.31 | 2.85 | 15 | 0.18 |
| V I | -0.28 | 2.23 | 5 | 0.20 | -0.31 | 1.96 | 3 | 0.09 | -0.08 | 2.03 | 2 | 0.18 | ... | ... | ... | ... |
| Cr I | -0.11 | 4.07 | 5 | 0.26 | -0.28 | 3.66 | 6 | 0.12 | -0.30 | 3.48 | 7 | 0.16 | -0.11 | 3.11 | 8 | 0.18 |
| Mn I | -0.37 | 3.53 | 5 | 0.27 | -0.43 | 3.23 | 4 | 0.22 | -0.33 | 3.17 | 6 | 0.15 | -0.41 | 2.53 | 3 | 0.10 |
| Fe I | -1.49 ^c | 5.96 | 132 | 0.18 | -1.73 ^c | 5.72 | 114 | 0.19 | -1.89 ^c | 5.56 | 111 | 0.16 | -2.45 ^c | 5.00 | 79 | 0.18 |
| Fe II | -0.11 | 5.85 | 15 | 0.19 | -0.11 | 5.60 | 11 | 0.11 | -0.04 | 5.52 | 14 | 0.22 | -0.02 | 4.98 | 12 | 0.16 |
| Co I | -0.15 | 3.28 | 1 | ... | -0.07 | 3.12 | 1 | ... | 0.20 | 3.23 | 1 | ... | 0.14 | 2.61 | 2 | 0.10 |
| Ni I | -0.35 | 4.41 | 24 | 0.20 | -0.28 | 4.24 | 22 | 0.22 | -0.18 | 4.18 | 20 | 0.20 | -0.07 | 3.73 | 8 | 0.21 |
| Cu I | -0.85 | 1.87 | 2 | 0.04 | -1.09 | 1.39 | 2 | 0.13 | -0.77 | 1.54 | 1 | ... | ... | ... | ... | ... |
| Zn I | -0.56 | 2.55 | 2 | 0.08 | -0.41 | 2.46 | 2 | 0.06 | 0.01 | 2.72 | 1 | ... | 0.20 | 2.35 | 2 | 0.04 |
| Sr I | -0.67 | 0.74 | 1 | -15.00 | ... | ... | ... | ... | ... | ... | ... | ... | ... | ... | ... | ... |
| Sr II | -0.50 | 0.91 | 1 | -15.00 | -0.53 | 0.64 | 1 | ... | -0.07 | 0.94 | 1 | ... | -0.77 | -0.32 | 2 | 0.27 |
| Y II | -0.62 | 0.13 | 4 | 0.18 | -0.68 | -0.17 | 4 | 0.11 | -0.26 | 0.09 | 4 | 0.20 | ... | ... | ... | ... |
| Zr II | ... | ... | ... | ... | ... | ... | ... | ... | -0.07 | 0.63 | 1 | ... | -0.38 | -0.23 | 1 | ... |
| Ba II | 0.02 | 0.66 | 4 | 0.13 | -0.15 | 0.24 | 4 | 0.12 | 0.14 | 0.37 | 4 | 0.15 | -0.46 | -0.78 | 5 | 0.16 |
| Ce II | -0.38 | -0.32 | 2 | 0.00 | -0.29 | -0.47 | 3 | 0.20 | 0.04 | -0.30 | 2 | 0.09 | ... | ... | ... | ... |
| Nd II | -0.17 | -0.16 | 5 | 0.14 | -0.05 | -0.28 | 6 | 0.14 | 0.33 | -0.06 | 6 | 0.07 | ... | ... | ... | ... |
| Eu II | 0.19 | -0.79 | 1 | ... | 0.39 | -0.83 | 1 | ... | 0.84 | -0.54 | 1 | ... | ≤0.69 | ≤1.24 | 1 | ... |
| Dy II | -0.18 | -0.57 | 1 | ... | ... | ... | ... | ... | 0.61 | -0.18 | 1 | ... | ... | ... | ... | ... |

^a σ is the dispersion of the abundance ratio for each absorption line about the mean for the species.

^bThe 4320 Å region of the G band of CH was used.

^c[Fe/H](Fe I) is given instead of [X/Fe].

Table 7b. Abundances for the Last Four Draco Stars

| Species | Draco 19219 [Fe/H] –3.01 | | | | Draco 19629 [Fe/H] –2.65 | | | | Draco 21456 [Fe/H] –2.34 | | | | Draco XI-2 [Fe/H] –1.99 | | | |
|--------------------|--------------------------|----------------------------|--------------|---------------------|--------------------------|----------------------------|--------------|---------------------|--------------------------|----------------------------|--------------|---------------------|-------------------------|----------------------------|--------------|---------------------|
| | [X/Fe] (dex) | log $\epsilon(X)$ (dex) | No. Lines | σ^a (dex) | [X/Fe] (dex) | log $\epsilon(X)$ (dex) | No. Lines | σ^a (dex) | [X/Fe] (dex) | log $\epsilon(X)$ (dex) | No. Lines | σ^a (dex) | [X/Fe] (dex) | log $\epsilon(X)$ (dex) | No. Lines | σ^a (dex) |
| C(CH) ^b | 0.32 | 5.90 | 1 | ... | –0.44 | 5.50 | 1 | ... | –0.49 | 5.76 | 1 | ... | –0.84 | 5.76 | 1 | ... |
| O I | ... | ... | ... | ... | ... | ... | ... | ... | 0.38 | 6.87 | 1 | ... | –0.13 ^c | 6.71 ^c | 1 | ... |
| Na I | –0.30 | 3.02 | 2 | 0.15 | –0.29 | 3.38 | 2 | 0.10 | –0.46 | 3.52 | 1 | ... | –1.06 | 3.27 | 1 | ... |
| Mg I | 0.33 | 4.86 | 4 | 0.17 | 0.20 | 5.09 | 5 | 0.10 | 0.19 | 5.39 | 4 | 0.25 | –0.37 | 5.18 | 5 | 0.31 |
| Si I | 0.35 | 4.89 | 1 | ... | 0.51 | 5.41 | 1 | ... | 0.51 | 5.71 | 1 | ... | –0.21 | 5.34 | 1 | ... |
| K I | 0.56 | 2.67 | 1 | ... | 0.28 | 2.75 | 1 | ... | 0.36 | 3.13 | 1 | ... | ... | ... | ... | ... |
| Ca I | –0.09 | 3.26 | 6 | 0.18 | 0.09 | 3.81 | 13 | 0.16 | –0.06 | 3.95 | 11 | 0.16 | –0.29 | 4.07 | 14 | 0.17 |
| Sc II | –0.01 | 0.08 | 4 | 0.24 | –0.08 | 0.38 | 5 | 0.15 | 0.09 | 0.85 | 6 | 0.12 | –0.39 | 0.72 | 7 | 0.21 |
| Ti I | –0.05 | 1.93 | 6 | 0.12 | –0.04 | 2.31 | 10 | 0.11 | –0.05 | 2.60 | 10 | 0.15 | –0.40 | 2.60 | 16 | 0.19 |
| Ti II | –0.02 | 1.96 | 13 | 0.17 | 0.00 | 2.34 | 17 | 0.22 | 0.09 | 2.74 | 9 | 0.11 | 0.05 | 3.05 | 12 | 0.16 |
| Cr I | –0.54 | 2.12 | 3 | 0.37 | –0.50 | 2.52 | 7 | 0.20 | –0.36 | 2.97 | 6 | 0.08 | –0.58 | 3.10 | 8 | 0.11 |
| Mn I | –0.56 | 1.82 | 2 | 0.02 | –0.27 | 2.47 | 5 | 0.28 | –0.55 | 2.50 | 3 | 0.07 | –0.62 | 2.78 | 5 | 0.12 |
| Fe I | –3.01 ^d | 4.44 | 56 | 0.21 | –2.65 ^d | 4.80 | 77 | 0.19 | –2.34 ^d | 5.11 | 73 | 0.19 | –1.99 ^d | 5.46 | 106 | 0.20 |
| Fe II | –0.01 | 4.43 | 9 | 0.19 | 0.00 | 4.80 | 13 | 0.16 | 0.05 | 5.16 | 8 | 0.12 | –0.05 | 5.41 | 16 | 0.16 |
| Co I | 0.12 | 2.03 | 1 | ... | 0.09 | 2.37 | 1 | ... | 0.54 | 3.12 | 1 | ... | –0.15 | 2.78 | 1 | ... |
| Ni I | 0.05 | 3.29 | 2 | 0.15 | 0.00 | 3.60 | 8 | 0.26 | 0.10 | 4.01 | 15 | 0.19 | –0.37 | 3.89 | 18 | 0.24 |
| Cu I | ... | ... | ... | ... | ... | ... | ... | ... | ... | ... | ... | ... | –1.32 | 0.90 | 1 | ... |
| Zn I | ... | ... | ... | ... | ... | ... | ... | ... | ... | ... | ... | ... | –0.06 | 2.55 | 1 | ... |
| Sr II | –1.50 | –1.61 | 2 | 0.08 | –1.41 | –1.15 | 2 | 0.09 | ... | ... | ... | ... | –1.12 | –0.21 | 1 | ... |
| Y II | ... | ... | ... | ... | ... | ... | ... | ... | –0.24 | –0.34 | 3 | 0.15 | ... | ... | ... | ... |
| Ba II | –0.56 | –1.43 | 4 | 0.11 | –0.73 | –1.24 | 5 | 0.14 | 0.26 | 0.05 | 4 | 0.15 | –1.12 | –0.98 | 4 | 0.09 |
| Ce II | ... | ... | ... | ... | ... | ... | ... | ... | 0.27 | –0.53 | 1 | ... | ... | ... | ... | ... |
| Nd II | ... | ... | ... | ... | ... | ... | ... | ... | 0.67 | –0.17 | 6 | 0.13 | ... | ... | ... | ... |
| Eu II | ... | ... | ... | ... | ≤0.97 | ≤ –1.17 | 1 | ... | 1.05 | –0.78 | 1 | ... | ≤0.24 | ≤ –1.24 | 1 | ... |

^a σ is the dispersion of the abundance ratio for each absorption line about the mean for the species.

^bThe 4320 Å region of the G band of CH was used.

^cExtremely uncertain, could be upper limit.

^d[Fe/H](Fe I) is given instead of [X/Fe].

Table 8. Parameters for the Toy Model of Abundance Ratios^a Applied to the Draco Giants

| Species [X/Fe] | A(X) (dex) | B(X) (dex) | [Fe/H](A) (dex) | [Fe/H](B) (dex) | [Fe/H](low,X) (dex) | [Fe/H](high,X) (dex) |
|-------------------------|---------------|---------------|--------------------|--------------------|------------------------|-------------------------|
| [Na/Fe] | 0.07 | −0.34 | −2.96 | −1.53 | −2.86 | −2.29 |
| [Mg/Fe] | 0.47 | −0.03 | −2.96 | −1.53 | −2.86 | −2.10 |
| thick disk ^b | 0.35 | 0.00 | −1.00 | 0.00 | −0.53 | −0.07 |
| thin disk ^b | 0.11 | 0.02 | −0.70 | 0.05 | −0.50 | −0.10 |
| [Si/Fe] ^c | 0.28 | 0.01 | −2.96 | −1.53 | −2.31 | −2.02 |
| [Ca/Fe] | −0.05 | 0.00 | −2.96 | −1.53 | −1.72 | −1.72 |
| [Ti12/Fe] ^d | 0.13 | −0.04 | −2.96 | −1.53 | −2.39 | −2.39 |
| [Cr/Fe] | −0.45 | −0.07 | −2.96 | −1.53 | −1.82 | −1.63 |
| [Mn/Fe] | −0.59 | −0.39 | −2.96 | −1.53 | −2.86 | −2.67 |
| [Ni/Fe] | −0.01 | −0.13 | −2.96 | −1.53 | −2.29 | −2.01 |
| [Sr/Fe] ^{c,e} | −1.99 | 0.08 | −2.96 | −1.61 | −2.87 | −1.70 |
| [Ba/Fe] ^c | −1.54 | 0.04 | −2.96 | −1.53 | −2.86 | −2.29 |

^aThe model and its parameters are described in §6.

^bFits to the Milky Way thin and thick disk sample of Reddy et al (2003) and Reddy, Lambert & Allende Prieto (2006) for [Mg/Fe] vs [Fe/H].

^cThe upper limits for Draco 119 of Fulbright, Rich & Castro (2004) for [Si/Fe], [Sr/Fe] and for [Ba/Fe] are treated as detections.

^d[Ti12/Fe] = [Ti from TiI/Fe from FeI] + [Ti from TiII/Fe from FeII])/2.

^e[Sr/Fe] is only available for the 8 Draco giants whose analyses are presented here.

Table 9. Abundance Range for Eight Draco Giants

| Species [X/Fe] | Nu. stars (dex) | Mean [X/Fe] (dex) | σ (dex) | Min. (dex) | Max. (dex) |
|-------------------------|--------------------|----------------------|-------------------|---------------|---------------|
| [C(CH)/Fe] ^a | 8 | −0.46 | 0.37 | −0.84 | 0.32 |
| [O(6300)/Fe] | 5 | 0.20 | 0.24 | −0.13 | 0.40 |
| [Na/Fe] | 8 | −0.46 | 0.31 | −1.06 | 0.01 |
| [Mg/Fe] | 8 | 0.09 | 0.22 | −0.37 | 0.33 |
| [Al/Fe] ^b | 1 | −0.62 | ... | ... | ... |
| [Si/Fe] | 8 | 0.16 | 0.30 | −0.23 | 0.51 |
| [K/Fe] | 5 | 0.31 | 0.17 | 0.10 | 0.57 |
| [Ca/Fe] | 8 | −0.05 | 0.14 | −0.29 | 0.15 |
| [Sc/Fe] | 8 | −0.10 | 0.16 | −0.39 | 0.09 |
| [Ti/Fe] ^c | 8 | −0.10 | 0.14 | −0.40 | 0.07 |
| [Ti/Fe] ^d | 8 | 0.06 | 0.21 | −0.03 | 0.31 |
| [Ti12/Fe] ^e | 8 | 0.00 | 0.10 | −0.15 | 0.20 |
| [V/Fe] | 3 | −0.22 | 0.13 | −0.31 | −0.08 |
| [Cr/Fe] | 8 | −0.35 | 0.18 | −0.58 | −0.11 |
| [Mn/Fe] | 8 | −0.44 | 0.12 | −0.62 | −0.27 |
| [FeII/FeI] | 8 | −0.04 | 0.06 | −0.11 | 0.05 |
| [Co/Fe] | 8 | 0.11 | 0.23 | −0.15 | 0.54 |
| [Ni/Fe] | 8 | −0.14 | 0.18 | −0.37 | 0.10 |
| [Cu/Fe] | 4 | −1.01 | 0.25 | −1.32 | −0.77 |
| [Zn/Fe] | 5 | −0.16 | 0.31 | −0.56 | 0.20 |
| [Sr/Fe] | 7 | −0.84 | 0.52 | −1.50 | −0.07 |
| [Y/Fe] | 4 | −0.45 | 0.23 | −0.68 | −0.24 |
| [Zr/Fe] | 2 | −0.23 | 0.22 | −0.39 | −0.07 |
| [Ba/Fe] | 8 | −0.32 | 0.47 | −1.12 | 0.26 |
| [Ce/Fe] | 4 | −0.09 | 0.30 | −0.39 | 0.27 |
| [Nd/Fe] | 4 | 0.19 | 0.38 | −0.17 | 0.67 |
| [Eu/Fe] | 4 | 0.62 | 0.40 | 0.19 | 1.05 |
| [Dy/Fe] | 2 | 0.22 | 0.56 | −0.18 | 0.61 |

^aThe 4320 Å region of the G band of CH was used.

^bNon-LTE correction of +0.6 dex has been applied for [Al/Fe] from

the 3950 Å doublet.

^cFrom Ti I lines.

^dFrom Ti II lines

^e $[\text{Ti12/Fe}] = [\text{Ti from TiI/Fe from FeI}] + [\text{Ti from TiII/Fe from FeII}]/2.$

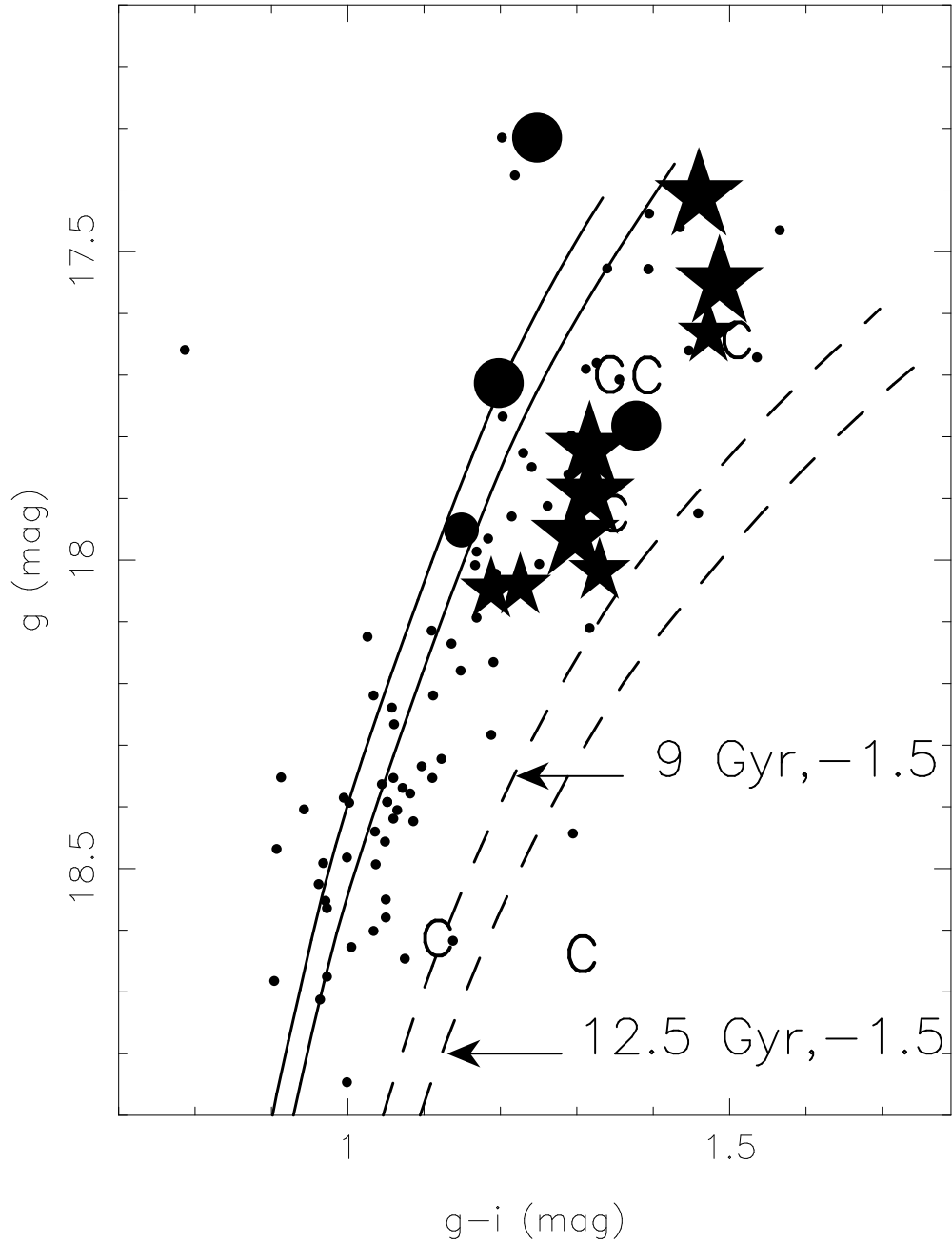


Fig. 1.— Our Draco HIRES sample is shown in a plot of $g' - i$ versus g' (large symbols), where filled circles indicate giants with $[\text{Fe}/\text{H}] < -2.5$ dex, and star symbols have higher metallicity. The sample of Draco stars studied by Shetrone, Bolte & Stetson (1998) and by Shetrone, Côté & Sargent (2001) are indicated by the smaller symbols. The dots indicate Draco members from Winnick (2003) with photometry from Segall *et al.* (2007) or, for the brightest stars, from the SDSS. Carbon stars that are confirmed members of Draco (see, e.g. Cioni & Habing 2005) are indicated by the letter C. All observational data are corrected for interstellar reddening. Isochrones from the Dartmouth Stellar Evolution Database (Dotter *et al.* 2008) for $[\text{Fe}/\text{H}] -2.5$ dex with $[\alpha/\text{Fe}] = +0.2$ dex (solid lines) and for $[\text{Fe}/\text{H}] -1.5$ dex with $[\alpha/\text{Fe}]$ Solar (dashed lines) for ages 9 and 12.5 Gyr are shown.

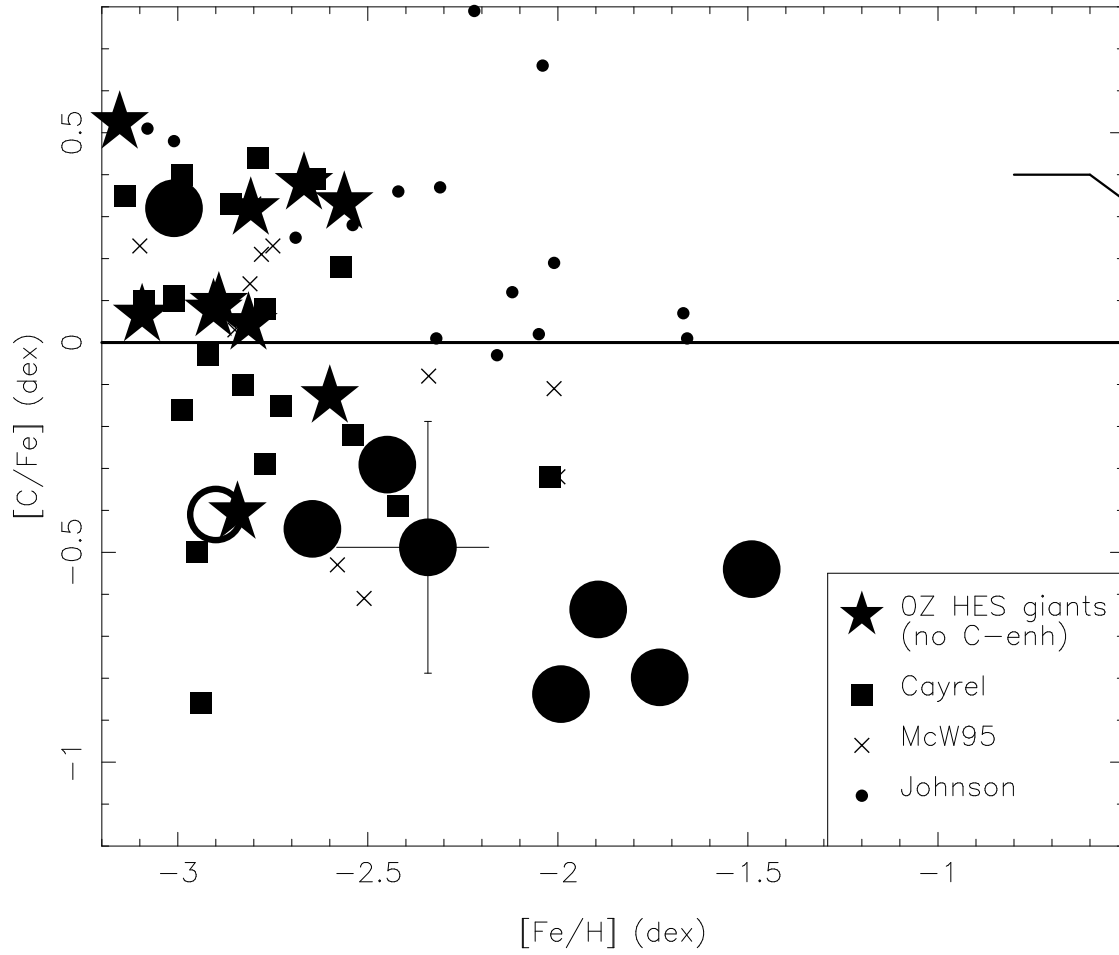


Fig. 2.— $[C/Fe]$ from the G band of CH vs $[Fe/H]$ for Draco stars from our sample (large filled circles) with that of Draco 119 from Fulbright, Rich & Castro (2004) (large open circle); these symbols are used for the remaining figures. The symbol key for the other sources is given on each figure. Typical uncertainties are shown for one star. The line represents the behavior of halo dwarfs from Reddy, Lambert & Allende Prieto (2006).

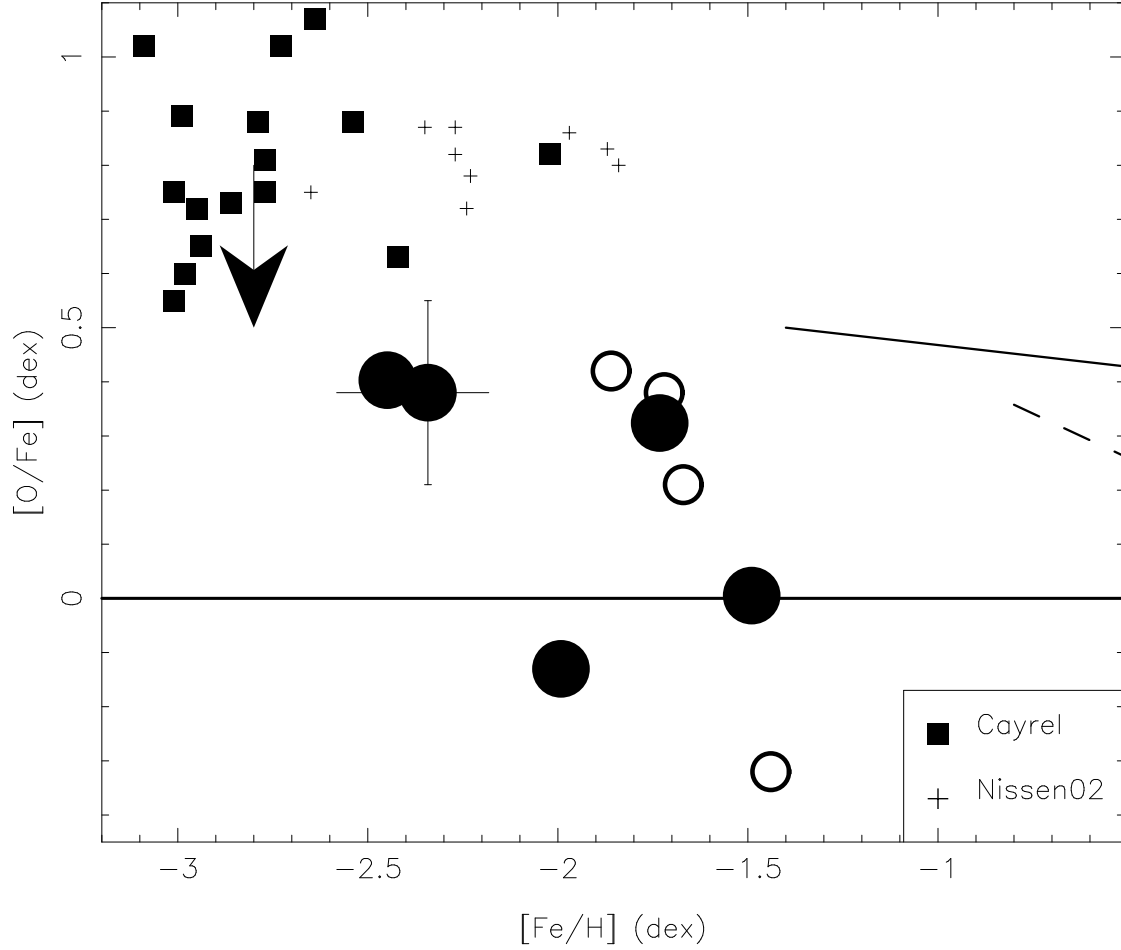


Fig. 3.— $[O/Fe]$ vs $[Fe/H]$. Draco stars from our sample (large filled circles) with those of Shetrone, Côté & Sargent (2001) indicated by the somewhat smaller open circles. Typical uncertainties are shown for one star. The small crosses are from Nissen et al (2002). Linear fits to the thick disk and halo stars (solid line) and thin disk (dashed line) relations of Ramirez, Allende Prieto & Lambert (2007) are shown. The arrow indicates the probable magnitude of 1D to 3D model corrections required for the Cayrel et al (2004) and the Draco $[O/Fe]$ values.

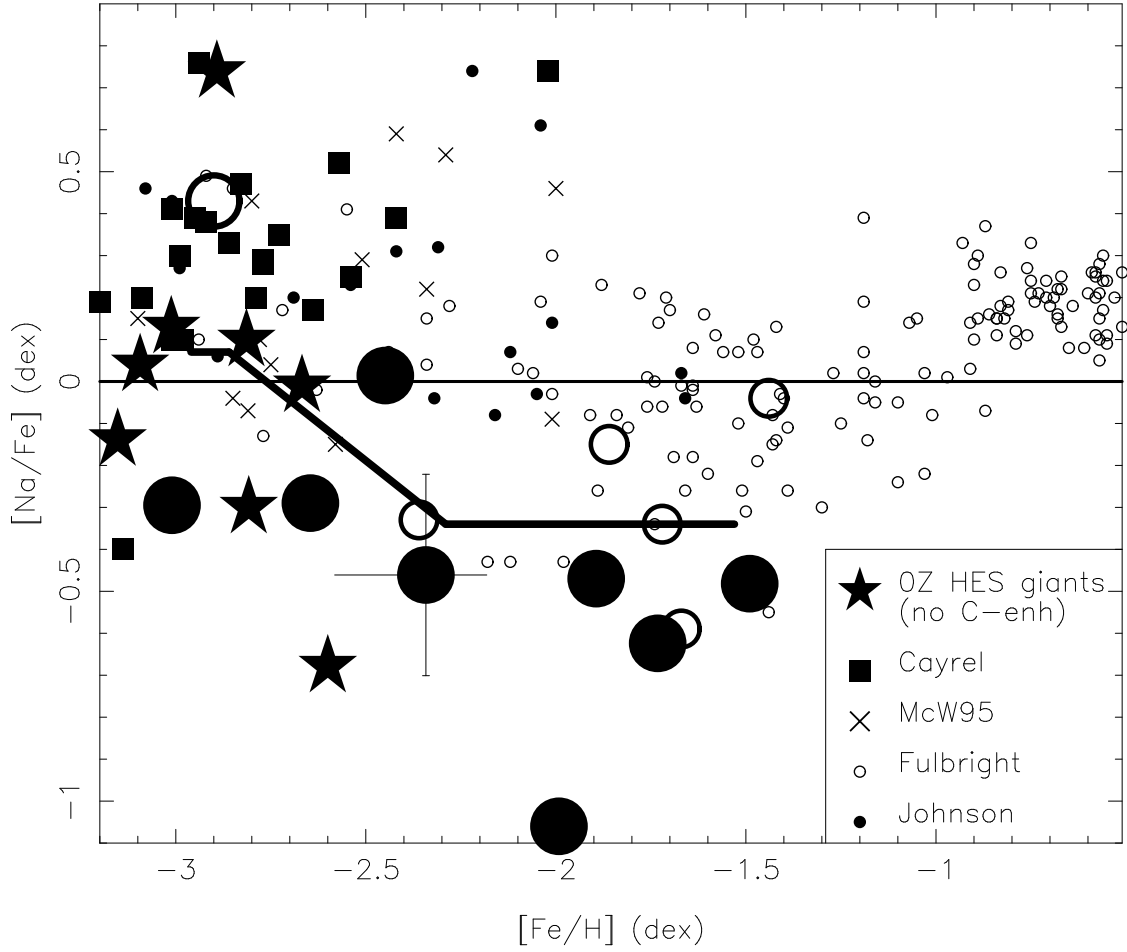


Fig. 4.— $[Na/Fe]$ vs $[Fe/H]$ for Draco stars. Draco stars from our sample (large filled circles) with those of Shetrone, Côté & Sargent (2001) indicated by the somewhat smaller open circles and the updated value for Draco 119 from Fulbright, Rich & Castro (2004) as the large open circle. Typical uncertainties are shown for one star. The symbol key for other sources is shown on the figure. The thick line indicates the fit of the toy model described in §6 (see also Table 8) to the Draco data.

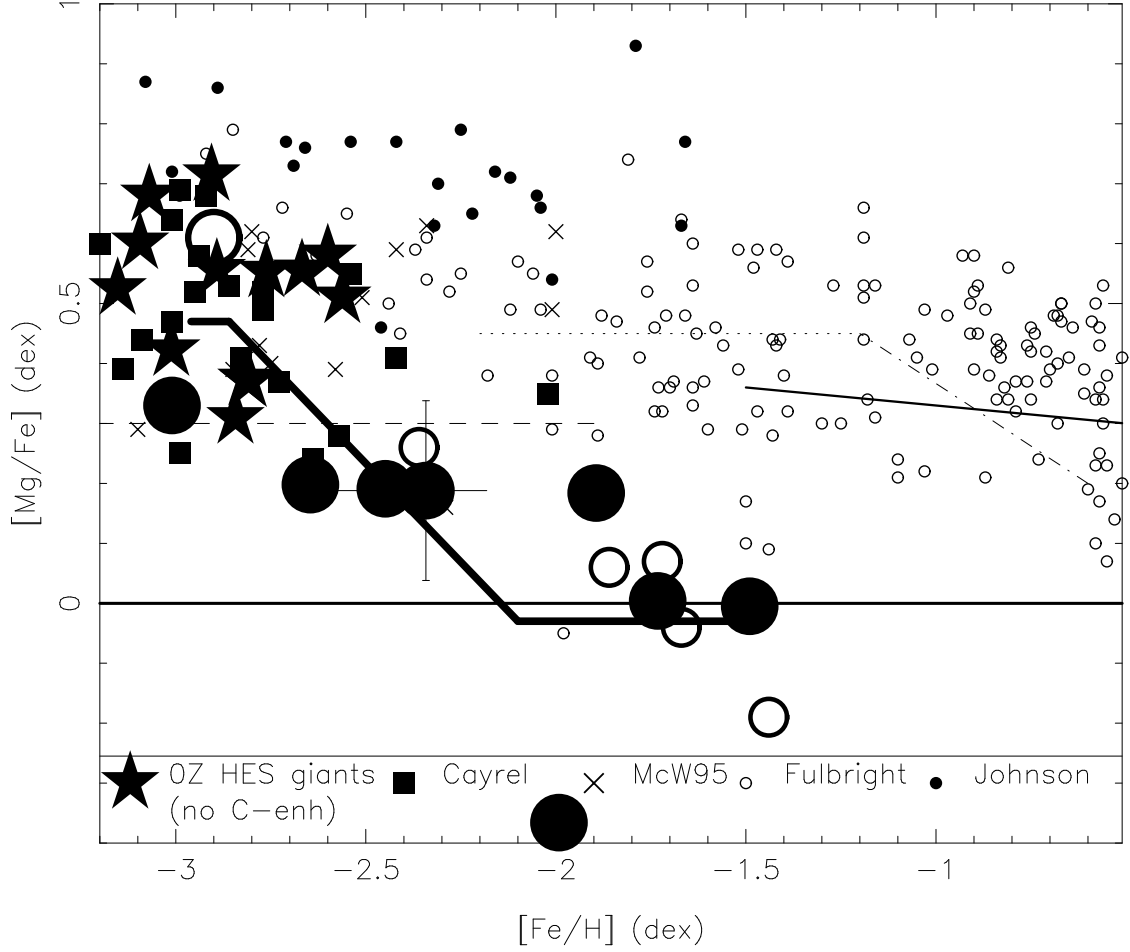


Fig. 5.— $[Mg/Fe]$ vs $[Fe/H]$ for Draco stars. See Fig. 4 for details regarding the symbols for the Draco stars and uncertainties. The symbol key for sources of data for Galactic halo field stars is shown on the figure. Note that 0.15 dex has been added to the $[Mg/Fe]$ values from Cayrel et al (2004); see the text for details. The thick line indicates the fit of the toy model described in §6 (see also Table 8) to the Draco data. The solid line is the mean relation for thick disk stars from Reddy, Lambert & Allende Prieto (2006). The dotted line is the mean relation for inner halo stars from Roederer (2008), while his outer halo mean is shown as the dashed line.

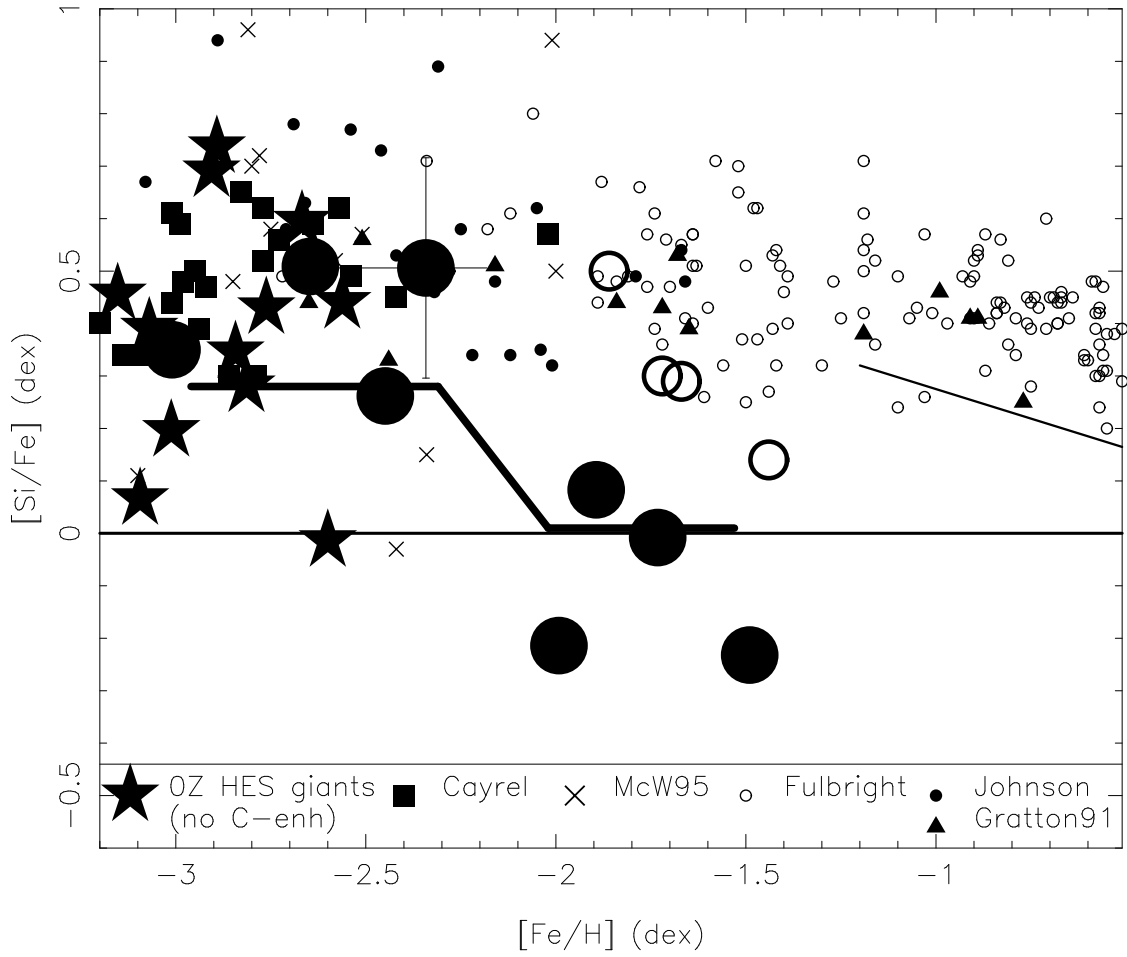


Fig. 6.— $[\text{Si}/\text{Fe}]$ vs $[\text{Fe}/\text{H}]$ for Draco stars. See Fig. 4 for details regarding the symbols for the Draco stars and uncertainties. The symbol key for sources of data for Galactic halo field stars is shown on the figure. The thick line indicates the fit of the toy model described in §6 (see also Table 8) to the Draco data. The solid line is the mean relation for thick disk stars from Reddy, Lambert & Allende Prieto (2006).

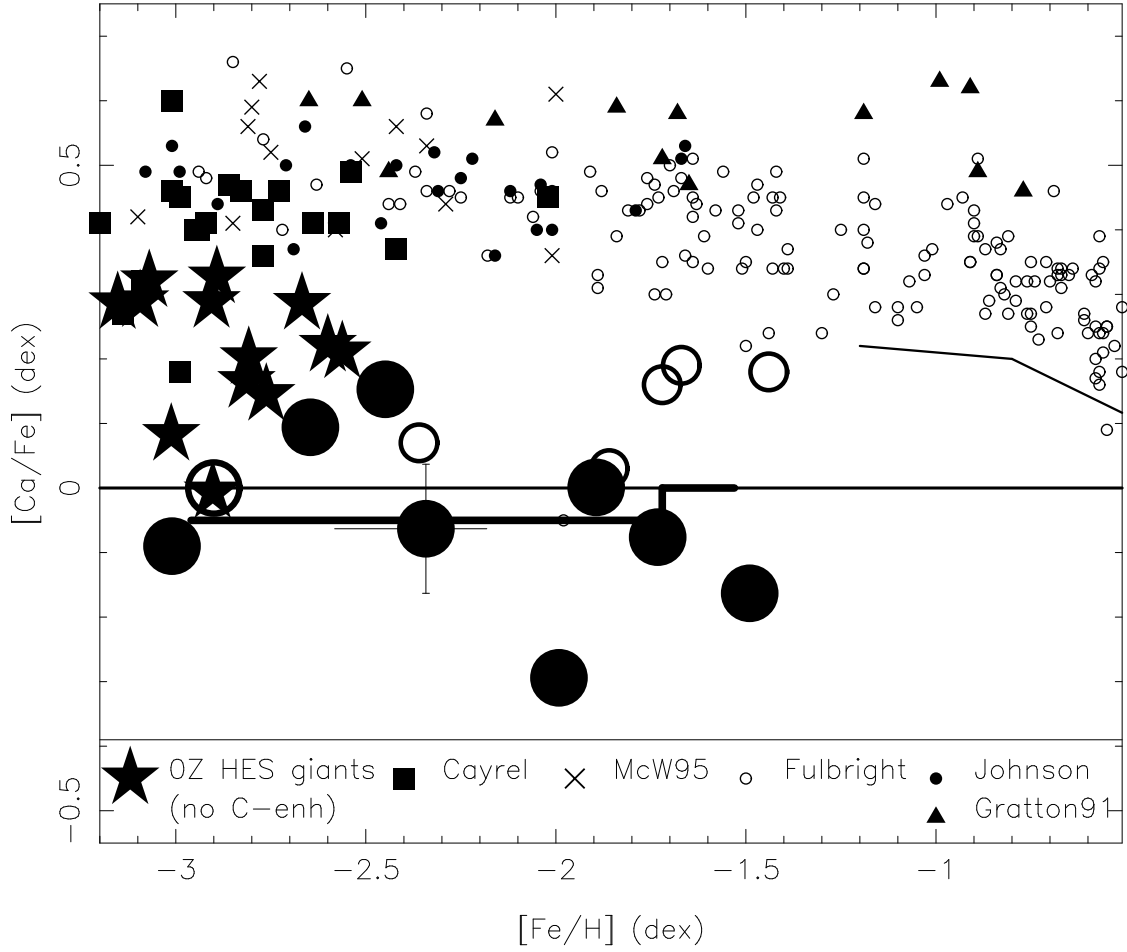


Fig. 7.— $[Ca/Fe]$ vs $[Fe/H]$ for Draco stars. See Fig. 4 for details regarding the symbols for the Draco stars and uncertainties. The symbol key for sources of data for Galactic halo field stars is shown on the figure. The thick line indicates the fit of the toy model described in §6 (see also Table 8) to the Draco data. The solid line is the mean relation for thick disk stars from Reddy, Lambert & Allende Prieto (2006).

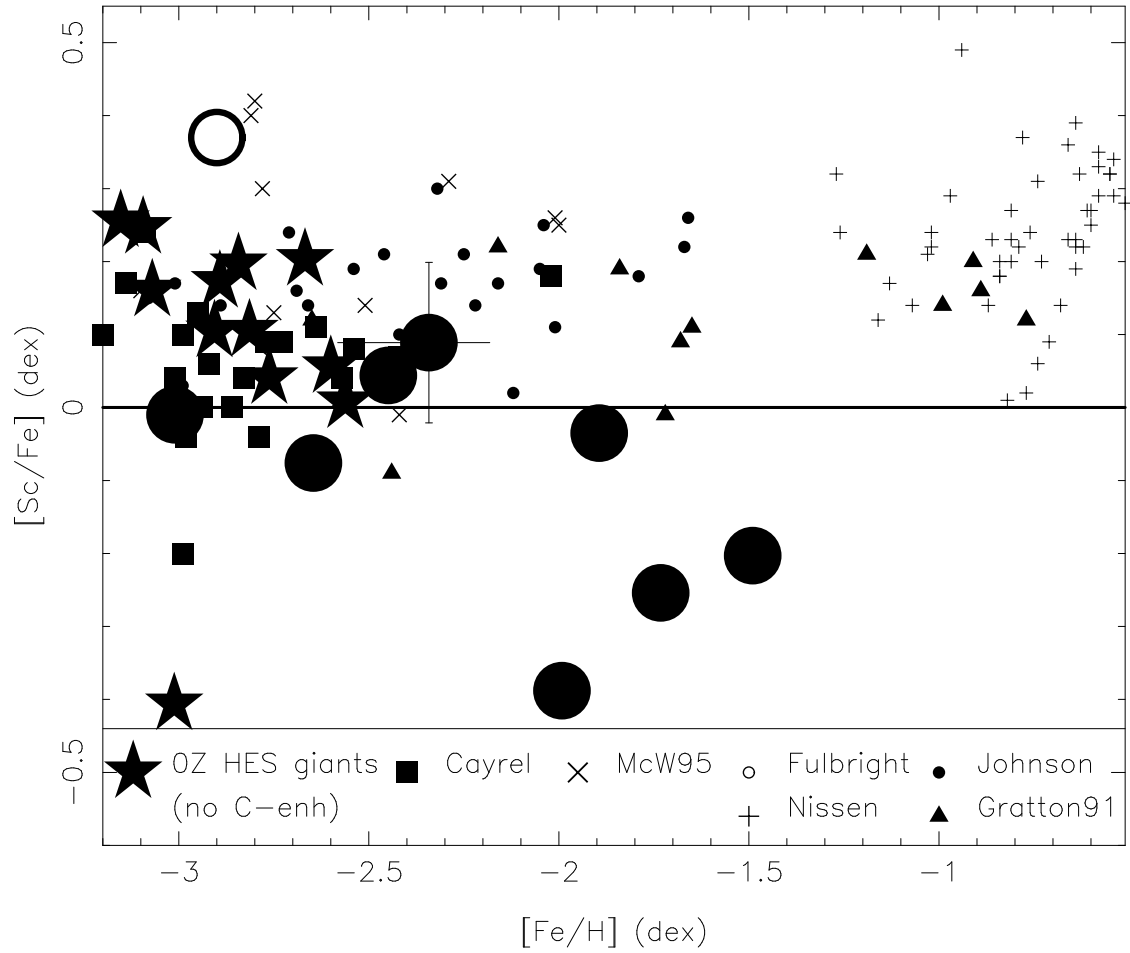


Fig. 8.— $[\text{Sc}/\text{Fe}]$ vs $[\text{Fe}/\text{H}]$ for Draco giants. See Fig. 4 for details regarding the symbols for the Draco stars and uncertainties. The symbol key for sources of data for Galactic halo field stars is shown on the figure.

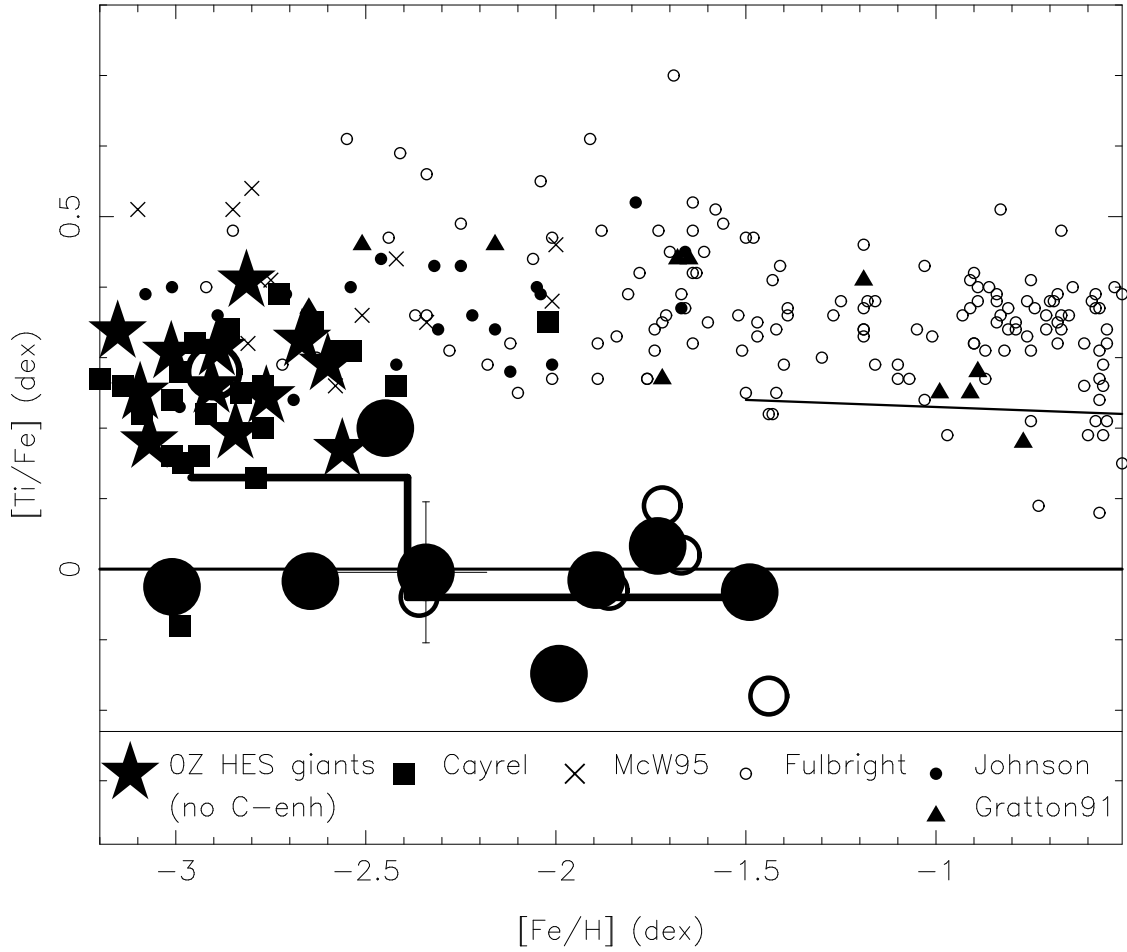


Fig. 9.— $[\text{Ti}/\text{Fe}]$ vs $[\text{Fe}/\text{H}]$ for Draco stars. $[\text{Ti}12/\text{Fe}12]$, which relates ionized Ti to ionized Fe, and neutral Ti to Fe I, is shown for our Draco stars. See Fig. 4 for details regarding the symbols for the Draco stars and uncertainties. The symbol key for sources of data for Galactic halo field stars is shown on the figure. The thick line indicates the fit of the toy model described in §6 (see also Table 8) to the Draco data. The solid line denotes the mean relation for the thick disk stars from Reddy, Lambert & Allende Prieto (2006).

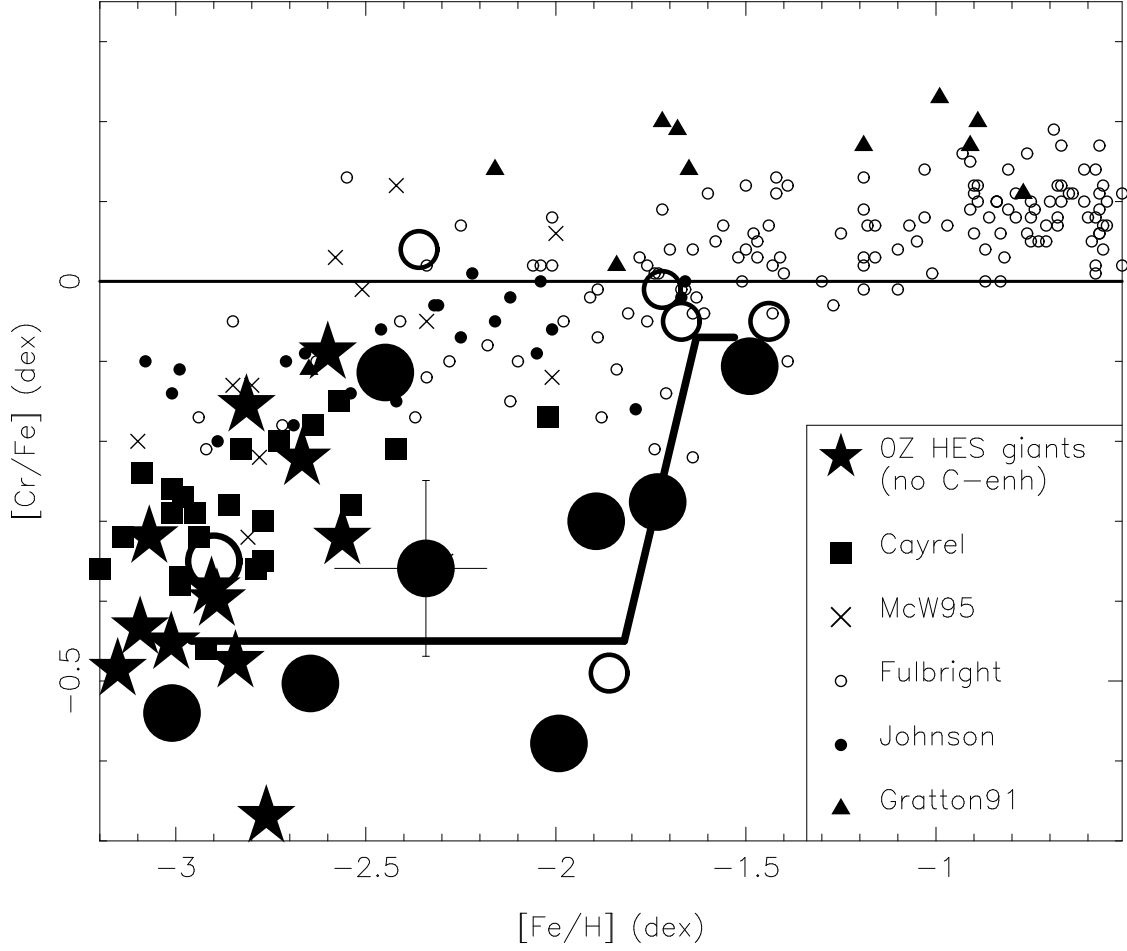


Fig. 10.— $[\text{Cr}/\text{Fe}]$ vs $[\text{Fe}/\text{H}]$ for Draco stars. See Fig. 4 for details regarding the symbols for the Draco stars and uncertainties. The symbol key for sources of data for Galactic halo field stars is shown on the figure. The thick line indicates the fit of the toy model described in §6 (see also Table 8) to the Draco data.

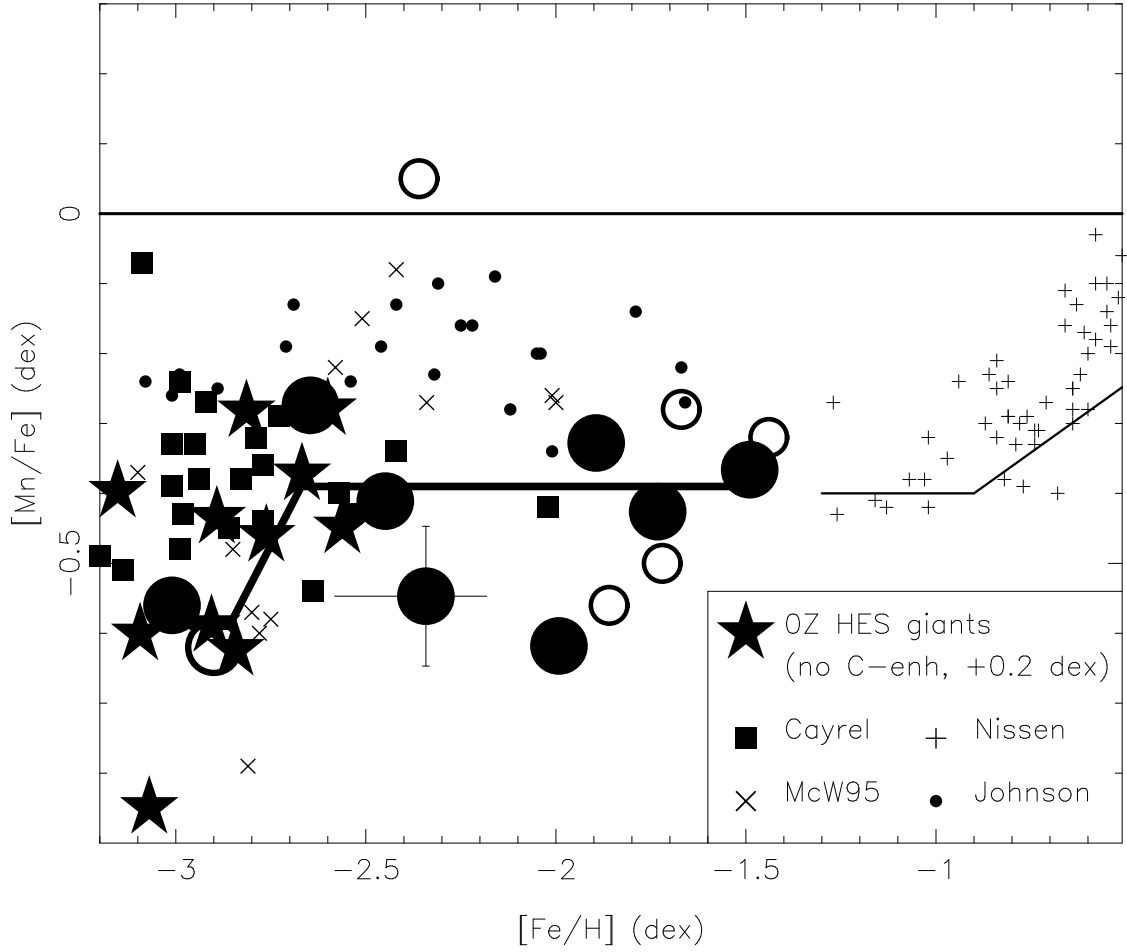


Fig. 11.— $[Mn/Fe]$ vs. $[Fe/H]$ for Draco giants. See Fig. 4 for details regarding the symbols for the Draco stars and uncertainties. The symbol key for sources of data for Galactic halo field stars is shown on the figure. The thick line indicates the fit of the toy model described in §6 (see also Table 8) to the Draco data. The solid line denotes the mean relation for the thick disk stars from Reddy, Lambert & Allende Prieto (2006).

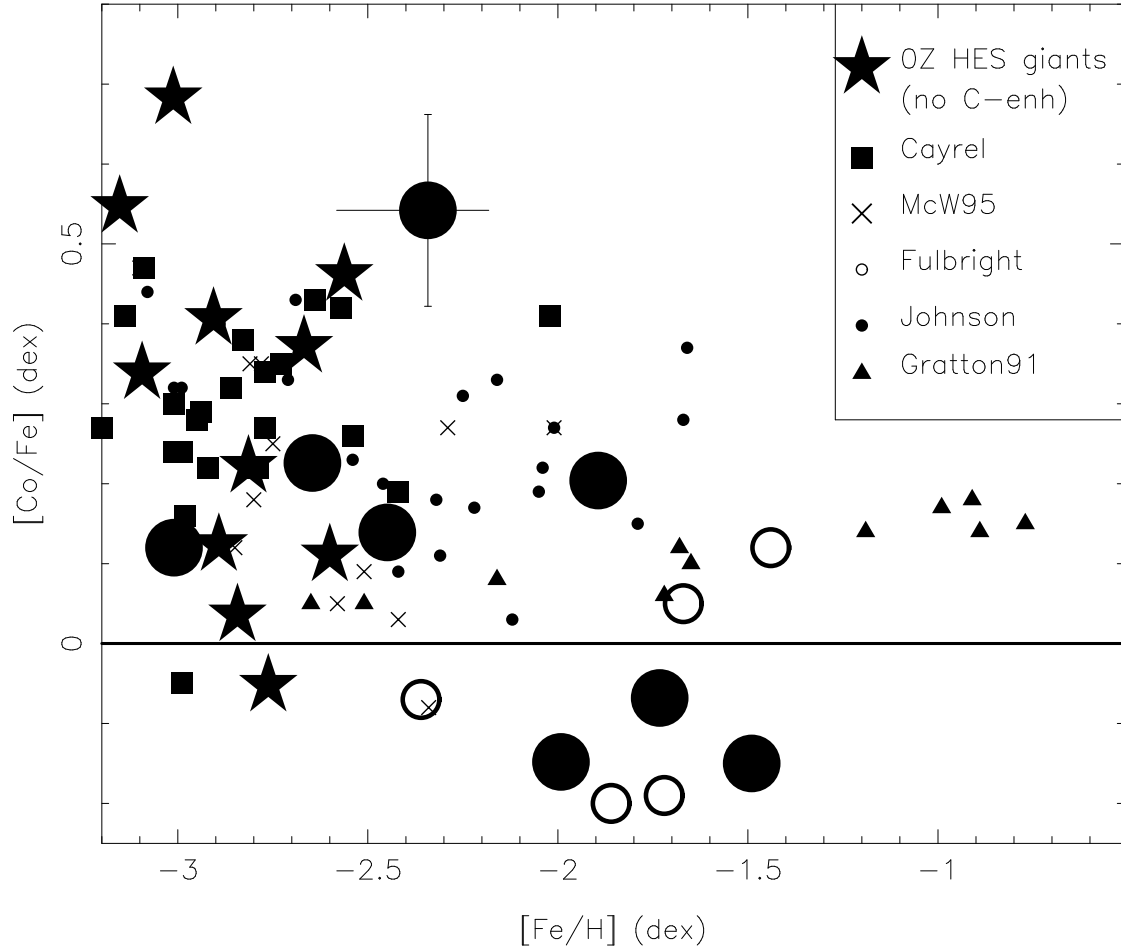


Fig. 12.— $[\text{Co}/\text{Fe}]$ vs $[\text{Fe}/\text{H}]$ for Draco stars. See Fig. 4 for details regarding the symbols for the Draco stars and uncertainties. The symbol key for sources of data for Galactic halo field stars is shown on the figure.

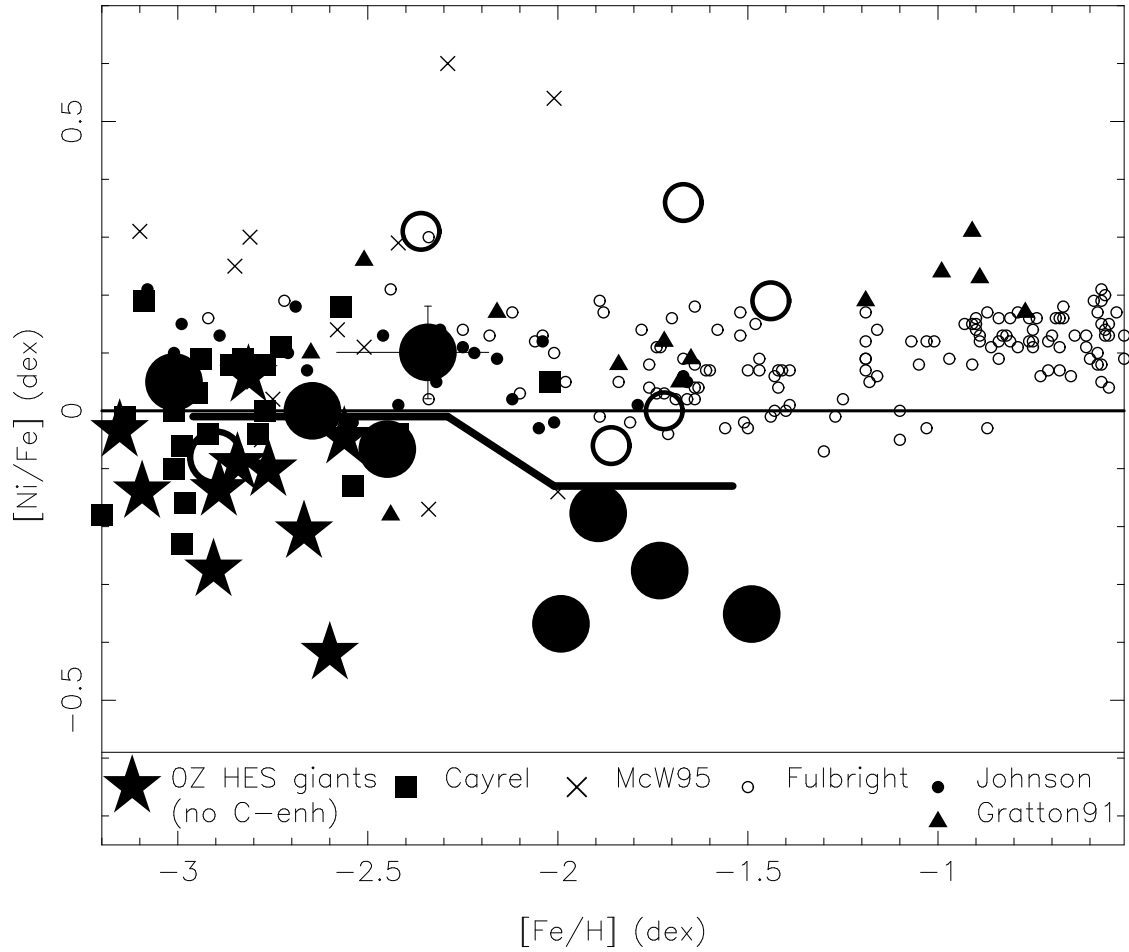


Fig. 13.— $[\text{Ni}/\text{Fe}]$ vs $[\text{Fe}/\text{H}]$ for Draco stars. See Fig. 4 for details regarding the symbols for the Draco stars and uncertainties. The symbol key for sources of data for Galactic halo field stars is shown on the figure. The thick line indicates the fit of the toy model described in §6 (see also Table 8) to the Draco data.

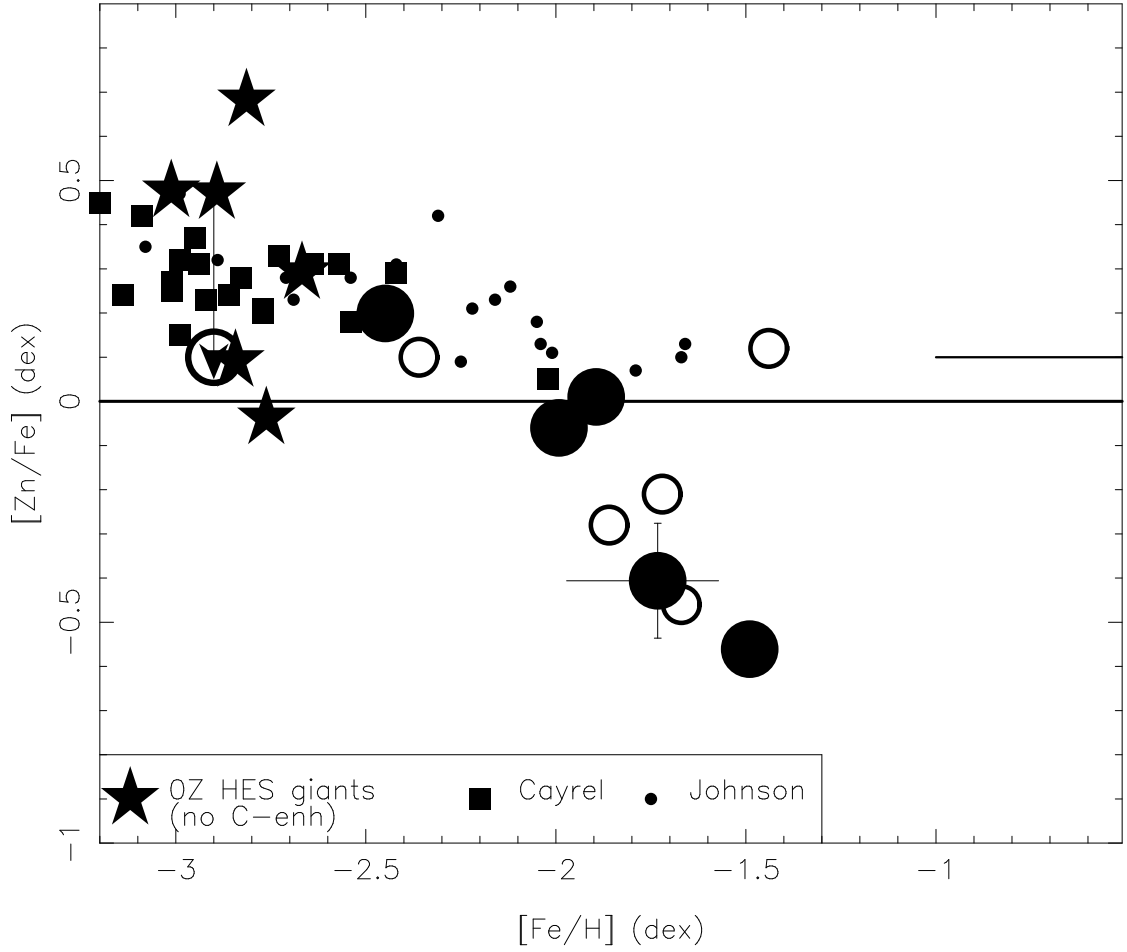


Fig. 14.— $[Zn/Fe]$ vs $[Fe/H]$ for Draco stars. See Fig. 4 for details regarding the symbols for the Draco stars and uncertainties. The upper limit for Draco 119 from Fulbright, Rich & Castro (2004) is indicated by an arrow. The symbol key for sources of data for Galactic halo field stars is shown on the figure. The behavior of this abundance ratio in thick disk dwarfs from Reddy, Lambert & Allende Prieto (2006) is indicated as a solid line.

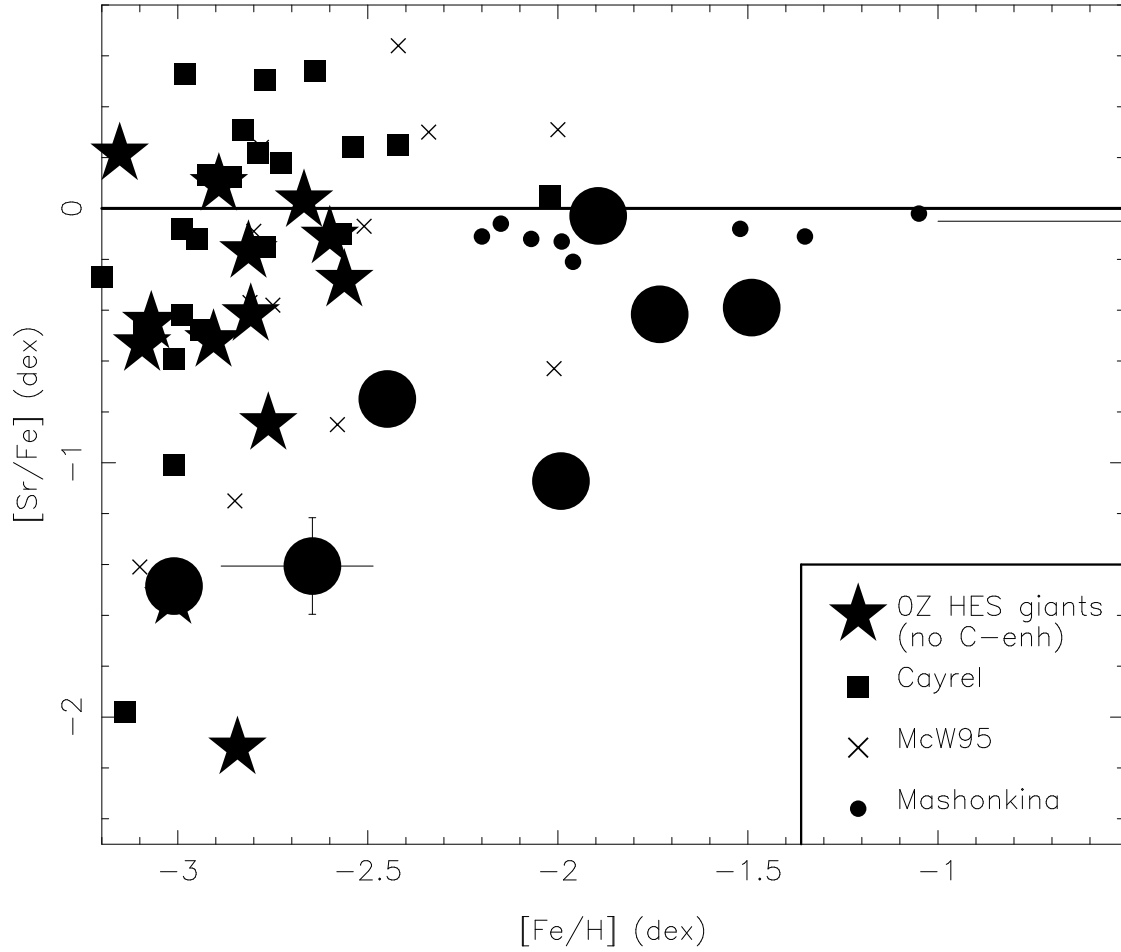


Fig. 15.— $[\text{Sr}/\text{Fe}]$ vs $[\text{Fe}/\text{H}]$ for Draco stars. See Fig. 4 for details regarding the symbols for the Draco stars and uncertainties. The upper limit for Draco 119 from Fulbright, Rich & Castro (2004) is indicated by an arrow. The First Stars data is from Francois et al (2007). The symbol key for sources of data for Galactic halo field stars is shown on the figure. The thick line indicates the fit of the toy model described in §6 (see also Table 8) to the Draco data. The behavior of this abundance ratio in thick disk dwarfs from Mashonkina & Gehren (2001) is shown as the solid line.

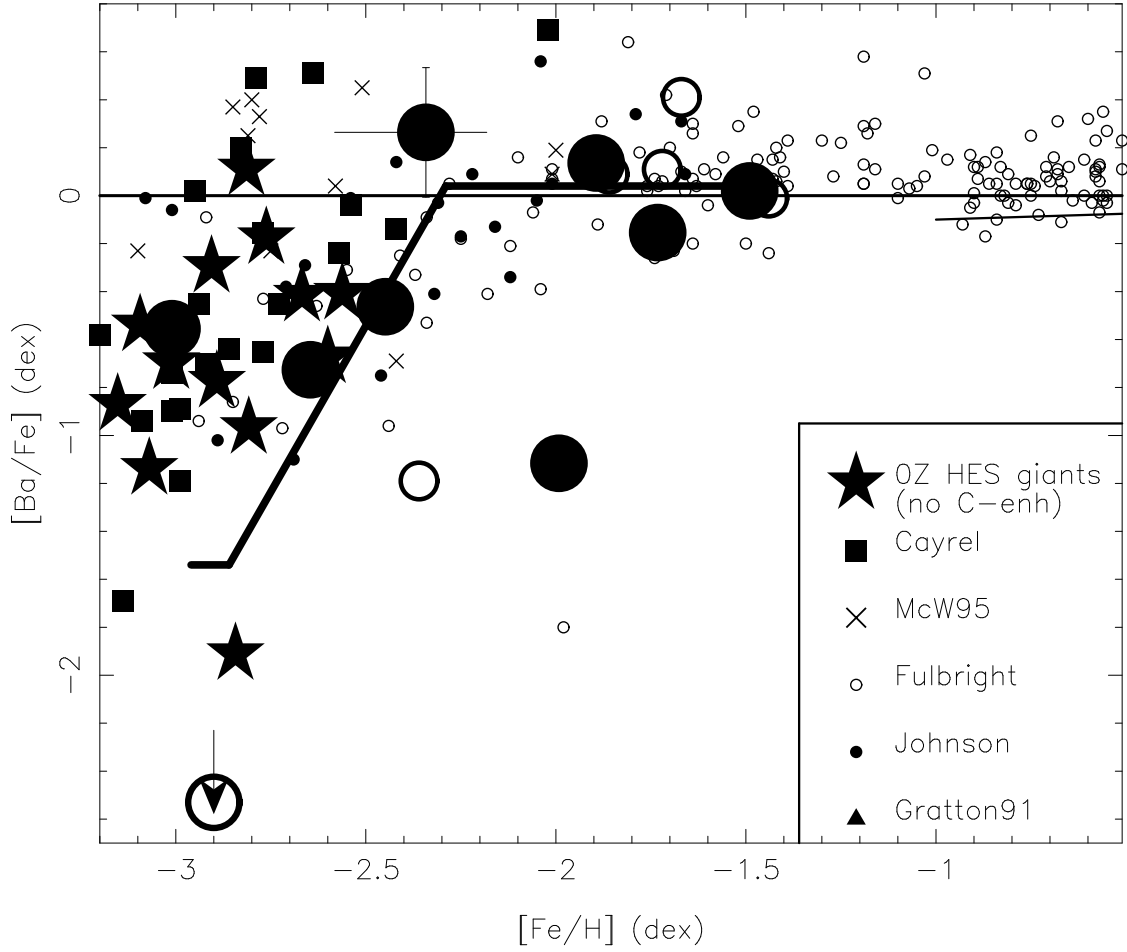


Fig. 16.— $[Ba/Fe]$ vs $[Fe/H]$ for Draco stars. See Fig. 4 for details regarding the symbols for the Draco stars and uncertainties. The upper limit for Draco 119 from Fulbright, Rich & Castro (2004) is indicated by an arrow. The First Stars data is from Francois et al (2007). The symbol key for sources of data for Galactic halo field stars is shown on the figure. The thick line indicates the fit of the toy model described in §6 (see also Table 8) to the Draco data.

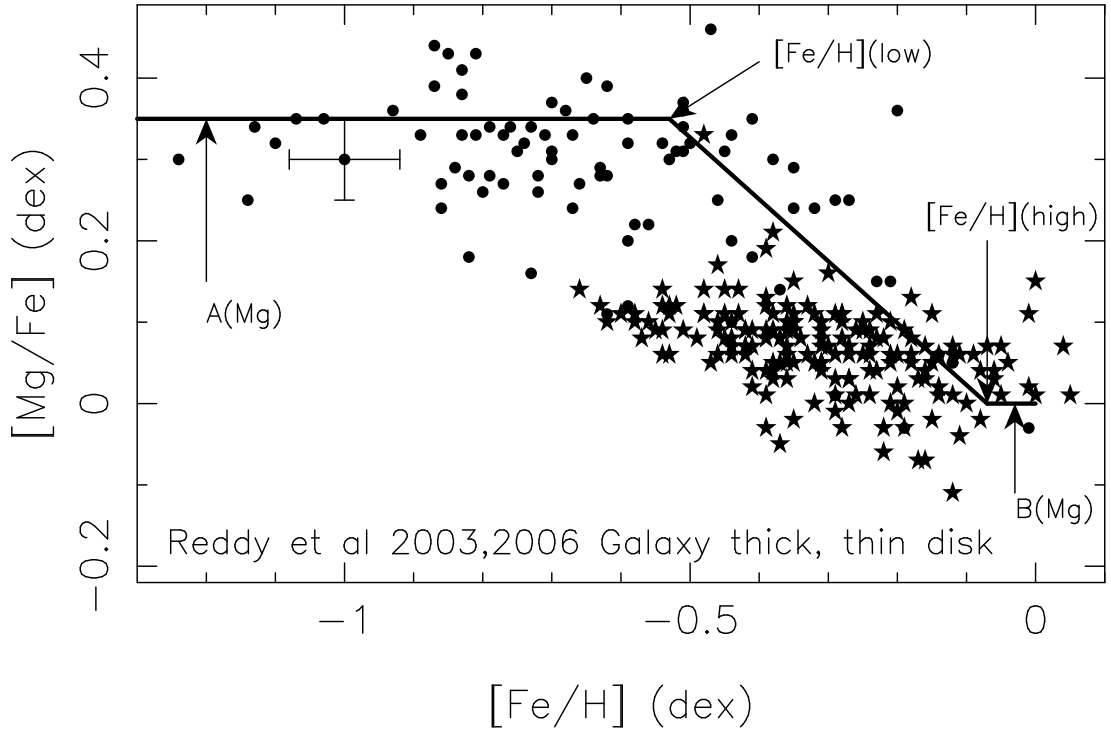


Fig. 17.— Abundance ratios $[\text{Mg}/\text{Fe}]$ are shown as a function of $[\text{Fe}/\text{H}]$ for a large sample of Galactic thick disk stars (filled circles) from Reddy, Lambert & Allende Prieto (2006) and thin disk stars (star symbols) from Reddy et al (2003). Typical errors are shown for a single star. The best fit using our toy model for the thick disk stars is indicated by the solid lines. The values of the key parameters are marked.

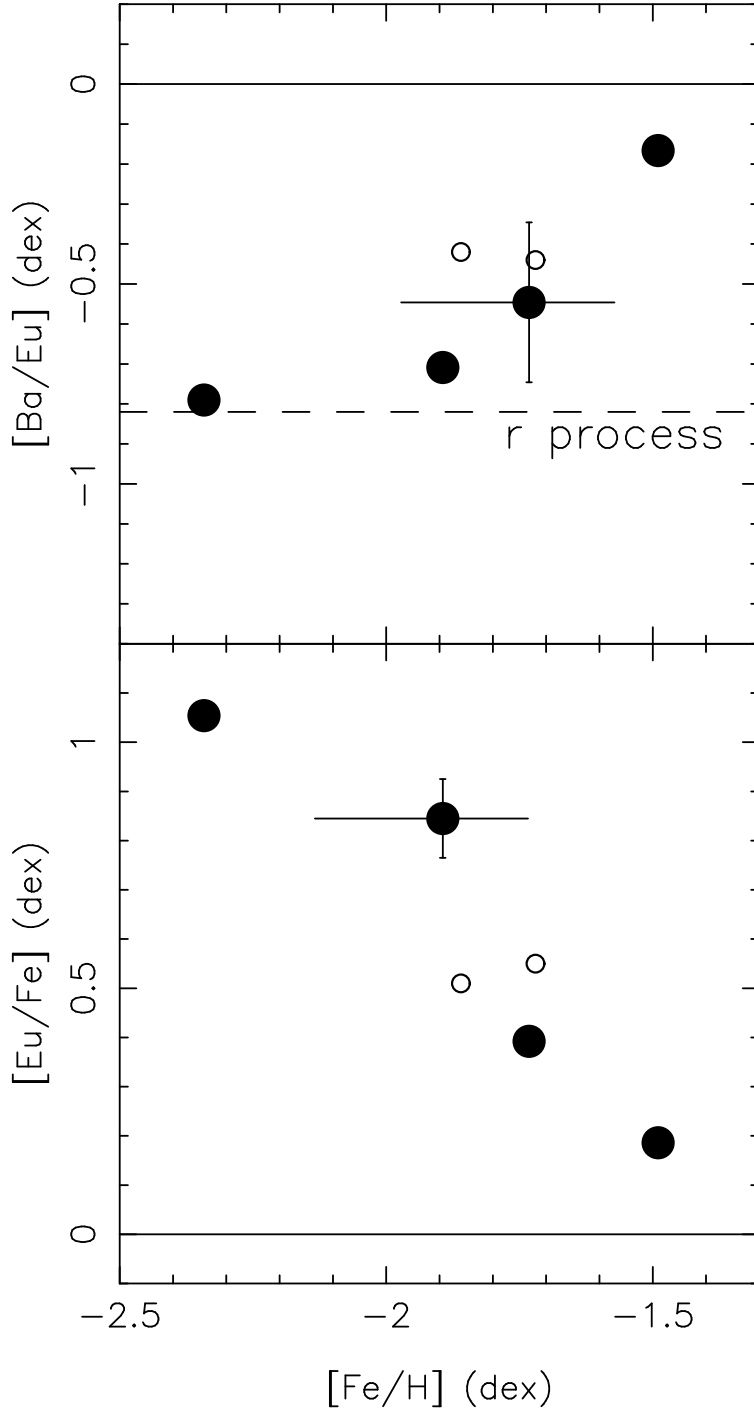


Fig. 18.— $[Ba/Eu]$ (upper panel) and $[Eu/Fe]$ (lower panel) vs $[Fe/H]$ is shown for the four giants our Draco sample and the two from Shetrone, Côté & Sargent (2001) with detected Eu. The Solar ratio is the solid horizontal line, while the dashed horizontal line is the r -process ratio from Simmerer et al (2004). Typical uncertainties are shown for one Draco star.

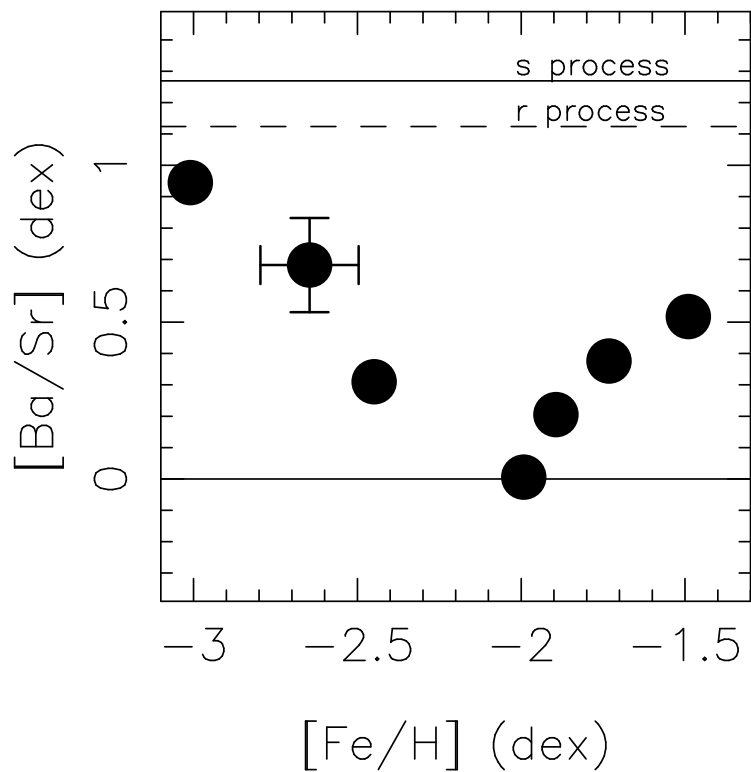


Fig. 19.— $[\text{Ba}/\text{Sr}]$ is shown as a function of $[\text{Fe}/\text{H}]$ for our Draco sample. The Solar ratio is the lower solid horizontal line. The pure s and pure r -process ratios from Simmerer et al (2004) are indicated. A typical error bar is shown for one star.

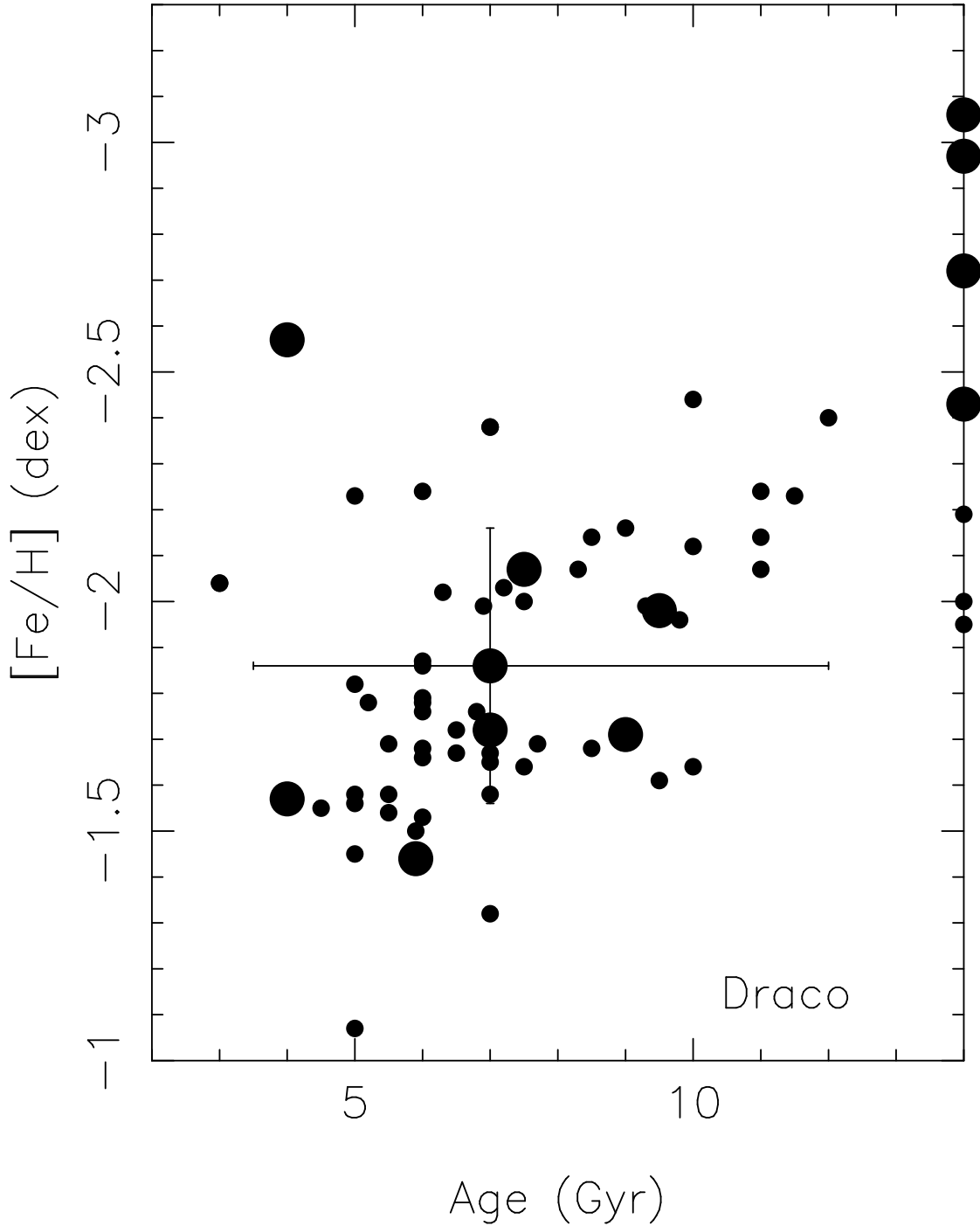


Fig. 20.— The age of each giant with $M_i < -2.0$ mag known to be a member of Draco from Table 2.9 of Winnick (2003). The Dartmouth isochrones (Dotter *et al.* 2008) were used with $[\text{Fe}/\text{H}]$ set to $[\text{Ca}/\text{H}]$ as derived by Winnick (2003) or are from HIRES spectra (large filled circles). Typical error bars are shown for a single star.

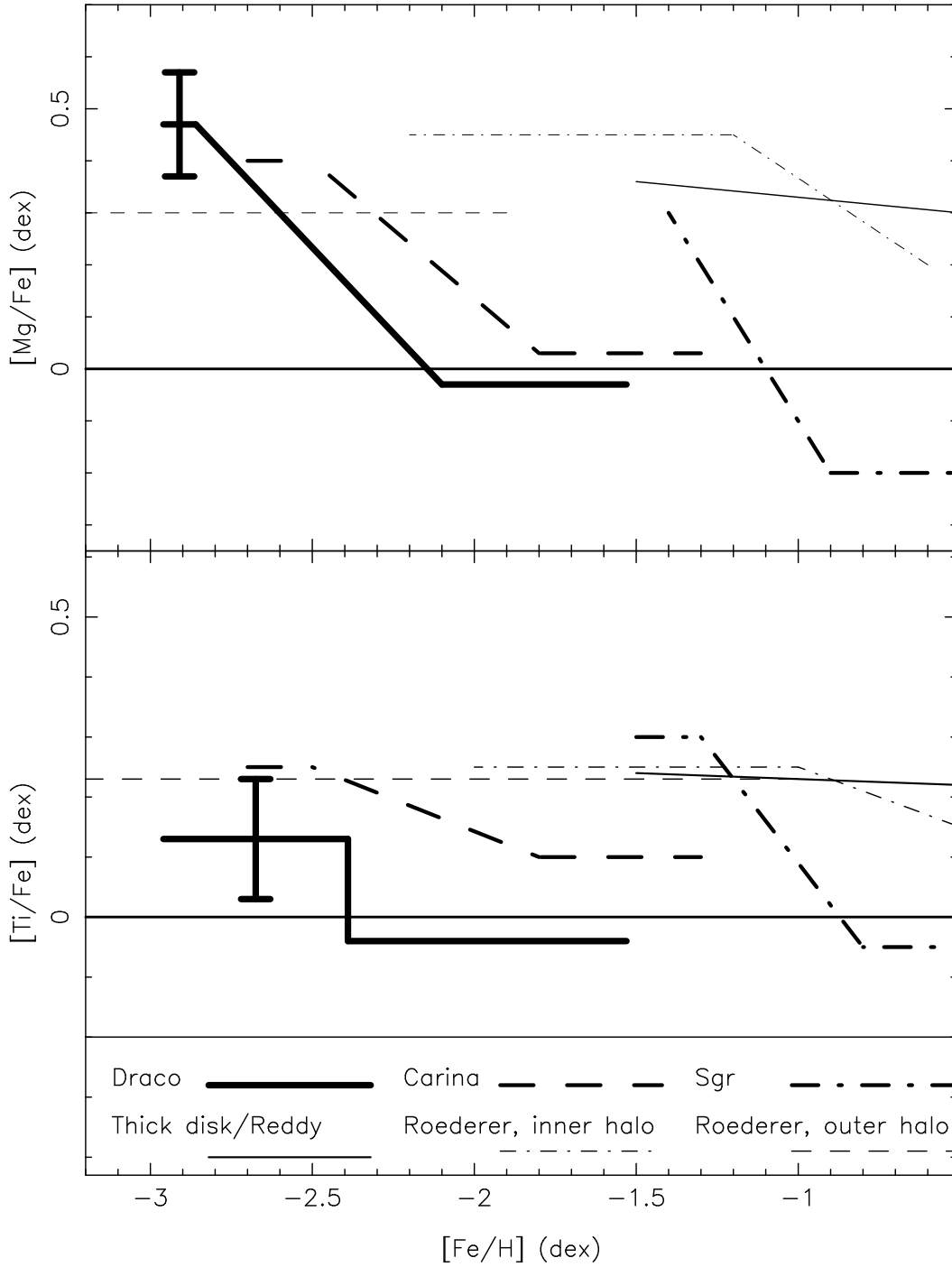


Fig. 21.— The toy model fit for $[Mg/Fe]$ vs $[Fe/H]$ (top panel) and for $[Ti/Fe]$ (bottom panel) for the sample of 14 Draco giants is shown together with that for the Sgr (Monaco et al 2005; Sbordone et al 2007) and Carina (Koch et al 2008a) dSph galaxies. Fits for Galactic components to data from Roederer (2008) and from Reddy, Lambert & Allende Prieto (2006) are shown as well. Typical errors in abundance ratios for the average of two stars are shown.

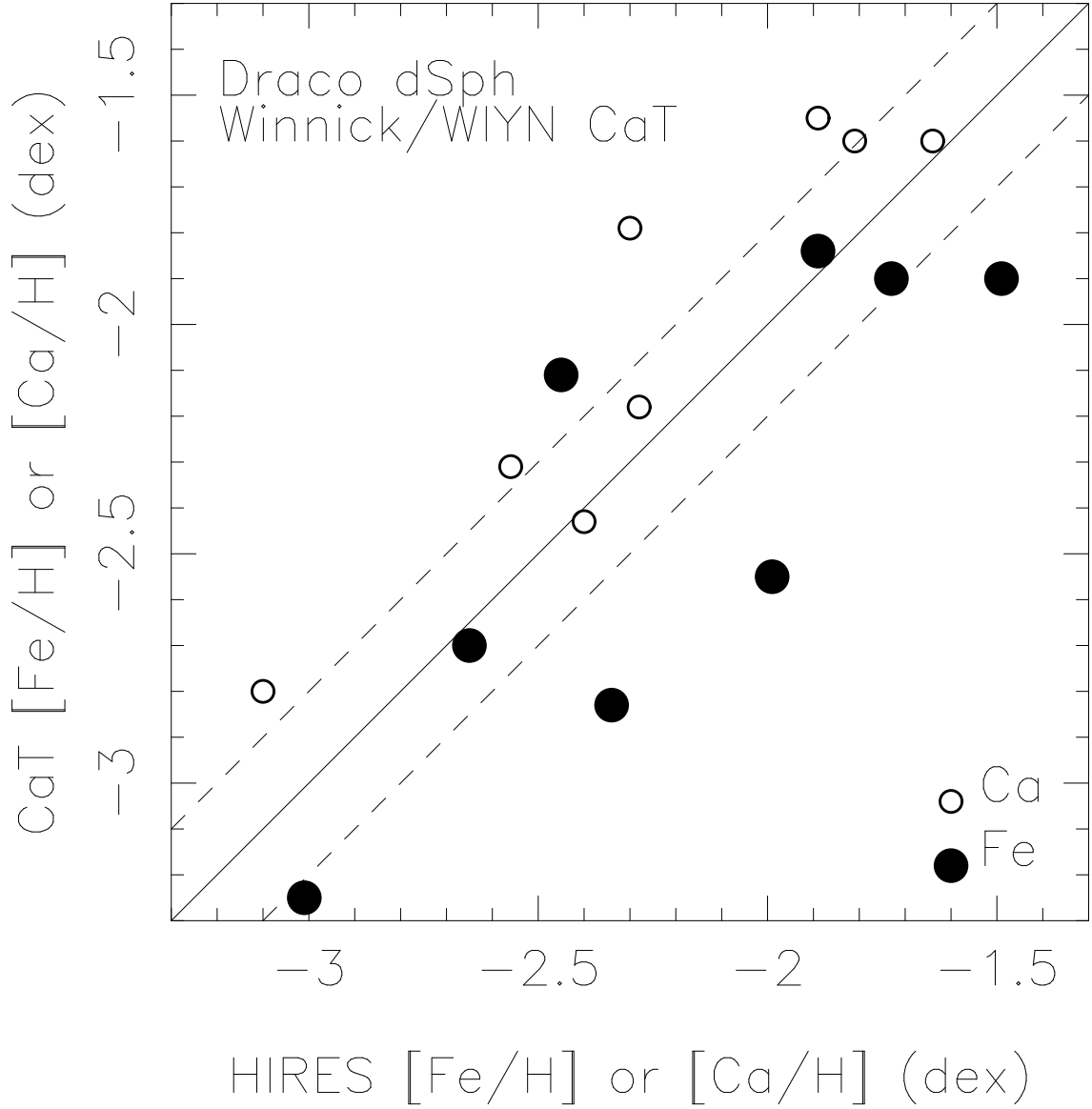


Fig. 22.— The $[\text{Fe}/\text{H}]$ (filled circles) and $[\text{Ca}/\text{H}]$ values derived from indices of the strength of the infrared Ca triplet by Winnick (2003) are compared to the results of our high-resolution detailed abundance analyses for our sample of 8 RGB stars in the Draco dSph galaxy. The solid line represents equality, while the dashed lines show offsets between the two determinations of ± 0.2 dex.